ISSN: 2764-5886
e-ISSN: 2764-622X

Volume 6· Nº 3 · September 2023

Journal of Bioengineering, Technologies and Health

An Official Publication of
SENAI CIMATEC

ISSN: 2764-5886 / e-ISSN 2764-622X

Volume 6 • Number 3 • September 2023

JOURNAL OF BIOENGINEERING TECHNOLOGIES AND HEALTH

An Official Publication of SENAI CIMATEC

PUBLISHED BY SENAI CIMATEC

Sistema FIEB | SENAI CIMATEC
PELO FUTURO DA INOVAÇÃO

September 2023
Printed in Brazil

JOURNAL OF BIOENGINEERING, TECHNOLOGIES AND HEALTH

An Official Publication of SENAI CIMATEC

JOURNAL OF BIOENGINEERING AND TECHNOLOGY APPLIED TO HEALTH

Volume 6 • Number 3 *September 2023*

SUMMARY

Original Articles

Systematic Review / Review Articles

The Journal of Bioengineering, Technologies and Health (JBTH) is an official publication of the SENAI CIMATEC (Serviço Nacional de Aprendizagem Industrial - Centro Integrado de Manufatura e Tecnologia). It is published quarterly (March - June - September - December) in English by SENAI CIMATEC – Avenida Orlando Gomes, 1845, Piatã, Zip Code: 41650-010, Salvador-Bahia-Brazil; phone: (55 71) 3879-5501. The editorial offices are at SENAI CIMATEC.

Editorial Office

Correspondence concerning subscriptions, advertisements, claims for missing issues, changes of address, and communications to the editors should be addressed to the Deputy Editor, Dr. Roberto Badaró, SENAI CIMATEC (Journal of Bioengineering, Technologies and Health – JBTH) – Avenida Orlando Gomes, 1845, Piatã, Zip code: 41650-010, Salvador-Bahia-Brazil; phone: (55 71) 3879-5501; or sent by e-mail: jbth@fieb.org.br / jbth.cimatec@gmail.com.

Permissions

The permissions should be asked to the Ediot in Chief of the Journal of Bioengineering, Technologies and Health and SENAI CIMATEC. All rights reserved. Except as authorized in the accompanying statement, no part of the JBTH may be reproduced in any form or by any electronic or mechanic means, including information storage and

Postmaster

Send address changes to JBTH, Avenida Orlando Gomes, 1845, Piatã, Zip Code: 41650-010, Salvador-Bahia-Brazil.

Information by JBTH-SENAI CIMATEC

Address: Avenida Orlando Gomes, 1845, Piatã, Zip Code: 41650-010, Salvador-Bahia-Brazil
Home-page: www.jbth.com.br
E-mail: jbth@fieb.org.br / jbth.cimatec@gmail.com
Phone: (55 71) 3879-5501 / 3879-5500 / 3879-9500

DOI:10.34178
ISSN: 2764-5886 / e-ISSN 2764-622X

COVER: Caulerpa cylindracea (*C. racemosa*) by Marta Terry L. https://www.flickr.com/photos/143000094@N07/29838339578# Accessed on September 30, 2023. CC BY-NC-ND 2.0 DEED.

Aphasia Rehabilitation: Decision Support Model

Claudia Simões Pinto da Cunha Lima[1*], Jeferson Andris Lima Lopes[2], Victor Mascarenhas de Andrade Souza[3], Sarah Leite Barros da Silva[4], Ingrid Winkler[5], Valter de Senna[6]

[1]SENAI CIMATEC University Center, MCTI; Salvador, Bahia; [2]Technical School of Brasília; Brasília, Distrito Federal; [3]Department of Neurology, São Rafael Hospital; Salvador, Bahia; [4]Neurological Rehabilitation Sector, CEPRED; Salvador, Bahia; [5]GETEC, SENAI CIMATEC University Center; Salvador, Bahia; [6]MCTI, SENAI CIMATEC University Center; Salvador, Bahia, Brazil

Aphasia impacts functional communication, daily activities, and social relationships. Aphasia is treated with traditional therapeutic methods, which involve repeating language tests and observing the progress of their responses. Technology is being used to investigate the activities of the brain. However, some of these technologies are very robust, have high costs for implementation, and require a team of specialized professionals to handle them. This paper aims to develop an aphasia screening model to support the conventional therapy used by speech-language pathologists in rehabilitation centers. The model was created in the first instance to test the instruments and procedures, focusing on the brain activation of aphasic participants through the criteria of lesion location (affected hemisphere) and hemiparesis (right or left side). Furthermore, secondly, to support conventional therapy in the rehabilitation process of the aphasic. The model used electroencephalography (EEG) as a non-invasive instrument and object naming task as a linguistic test, described in the adult language paradigm proposed in 2017 by the American Society for Functional Neuroradiology. We tested the method with 11 aphasic participants diagnosed with post-stroke aphasia in rehabilitation. We conclude that the results can support the health professional's decision in conventional therapy to adjust the conduct of language stimulation with a personalized and monitored approach throughout the rehabilitation process.

Keywords: Aphasia. Electroencephalography. Biomedical Signal Monitoring. Language Rehabilitation.

Introduction

Aphasia is a condition resulting from a lesion in the brain, commonly in the left hemisphere. It is considered "one of the most common neurological changes after focal lesion acquired in the Central Nervous System (CNS), in areas responsible for comprehensive and/or expressive language, oral and/or written" [1].

The aphasias' classification is based on the patient's performance, which is evaluated through tests to verify the fluency of speech, the ability to understand orders, the capacity to name objects, and the ability to repeat words [2]. Table 1 shows the types of aphasia, and the test parameters with their impacts.

Received on 20 June 2023; revised 18August 2023.
Address for correspondence: Claudia Simões Pinto da Cunha Lima. SENAI CIMATEC University Center. Av. Orlando Gomes, 1845 - Piatã, Salvador – Bahia, Brazil. E-mail: claudia.lima@fieb.org.br.

J Bioeng. Tech. Health 2023;6(3):199-207

The aphasia assessment process involves language examination instruments and should address "different language levels and components, among them comprehension and expression" [3]. These language assessment instruments, used by neuropsychologists and speech-language pathologists for diagnosing aphasia, are also used as a treatment strategy.

Language assessment and rehabilitation involves analyzing the ability to name, repeat, comprehend, read, and write [4]. The definition of the battery of tests will depend on the theoretical approach used by the therapist. Not having a single approach hinders the sharing of data, which is essential for research integrity and scientific transparency. Therefore, members of the American Society for Functional Neuroradiology from many institutions have created a standard language paradigm that balances ease of application and clinical utility.

Beside this background, this study aimed to develop an aphasia tracing model to support the conventional therapy used by speech-language pathologists in rehabilitation centers.

Table 1. Types of aphasia.

Aphasia	Fluency	Comprehension	Nomination	Repetition
Broca	Non fluent	Normal	Disturbed	Disturbed
Wernickle	Fluent	Disturbed	Disturbed	Disturbed
Conduction	Fluent	Normal	+/- Disturbed	Disturbed
Anomic	Fluent	Normal	Disturbed	Normal
Transcordial Motor	Non fluent	Normal	Disturbed	Normal
Transcordial Sensorial	Fluent	Disturbed	Disturbed	Normal
Transcordial Mixed	Non fluent	Disturbed	Disturbed	Normal
Global	Non fluent	Disturbed	Disturbed	Disturbed

Our approach to supporting the rehabilitation process for aphasics is based on tracking electrophysiological stimuli, a method that can aid personalized, monitored rehabilitation.

The present research was approved by the Ethics Committee on Human Research of the Integrated Manufacturing and Technology Campus (CIMATEC) - Senai/ Bahia (CAAE: 29622120.2.0000.9287) and approved by the Health Secretariat of the State of Bahia - SESAB (CAAE: 29622120.2.3001.0052) with the Center for Prevention and Rehabilitation of People with Disabilities - CEPRED, as a co-participant center.

Materials and Methods

This is an exploratory study [5] that used the Descriptors in Health Sciences/Medical Subject Headings (DeCS/MeSH) and the platform Virtual Health Library (VHL) to find the decision model to be used [6].

We used the model EEG, an electrophysiological monitoring method based on brain electrical activity, and incorporates Fourier analysis, which has several scientific applications, among them signal processing with the separation of data into frequency intervals and brain regions.

The model was created to evaluate the instruments and procedures, focusing on brain activation in aphasic participants through the criteria of lesion location (affected hemisphere) and hemiparesis (right or left side).

Population and Sample

The study population was made up of participants diagnosed with post-stroke aphasia, according to their medical records, that were undergoing rehabilitation treatment and were recruited by the speech therapy team in the adult neurological rehabilitation sector of CEPRED in the city of Salvador, Bahia, Brazil, following the inclusion and exclusion criteria.

The sample comprised eleven aphasic participants (8 women, and 3 men). The average age of all the participants was 54 ± 7 years. Of these participants, 10 had brain damage in the left hemisphere, and one had right hemisphere damage, all with hemiparesis (difficulty moving half of the body) (Table 2). None of the participants had hearing impairment.

Inclusion Criteria

- Participants of both genders,
- Over 18 years
- Diagnosed with post-stroke aphasia, and standard or normal-corrected vision.

Exclusion Criteria

- Participants with mental disorders identified by a healthcare professional were not invited to the study.
- Participants with unstable cardiovascular disease or other serious illnesses that

Table 2. Participants descriptions.

ID	Gender	Age	Hemiparesis	Hemisphere affected	Type of Aphasia
P01	Female	53	Right	Left	Broca
P02	Female	51	Right	Left	Broca
P03	Female	53	Right	Left	Anomic
P04	Female	45	Right	Left	Transcortical motor
P05	Female	63	Right	Left	Broca
P06	Female	45	Right	Left	Transcortical motor
P07	Male	58	Right	Left	Broca
P08	Male	63	Right	Left	Broca
P09	Female	59	Right	Left	Broca
P10	Female	45	Left	Right	Global
P11	Male	60	Right	Left	Global

ID: Identification; P: participant.

prevented them from performing the tasks were also not part of the research.

Non-Invasive Method

We used electroencephalography (EEG) as a non-invasive and accessible method, a device with 16 channels, with electrodes placed according to the international 10-20 positioning system for electroencephalographic analysis. We choose this device (Figure 1) because it is wireless, designed for human brain research, and already validated by other researchs [7-11].

We used 16 electrodes for the analysis of this study: 4 electrodes positioned in the frontal lobe, 2 in the left hemisphere (F7, F3), and 2 electrodes in the right hemisphere (F4, F8) in the five frequency ranges: Theta (4-8 Hertz), Alpha (8-12 Hertz), Low Beta (12-16 Hertz), High Beta (16-25 Hertz) and Gamma (25-45 Hertz).

Figure 1. Emotiv Epoc+.

Test Task: Object Naming

In this task, natural objects are presented on the video monitor. For each object on the screen, the participant must think of its name (Figure 2). At the end of the sequence of objects, there is a segment with six symbols, which not be named. Thus, we have 36 stimuli objects and 36 control symbols. The object naming task activates the frontal region more strongly than the temporal region [4].

The language paradigm chosen was proposed by the American Society for Functional Neuroradiology and is used as the standard language paradigm because it strikes a balance between ease of application and clinical utility [4]. These factors were essential for the present study.

Tools

We used the software EmotivPro 3.3.0.433 to check the connection of all the electrodes, which should appear in the interface with a green

Figure 2. Object naming task.

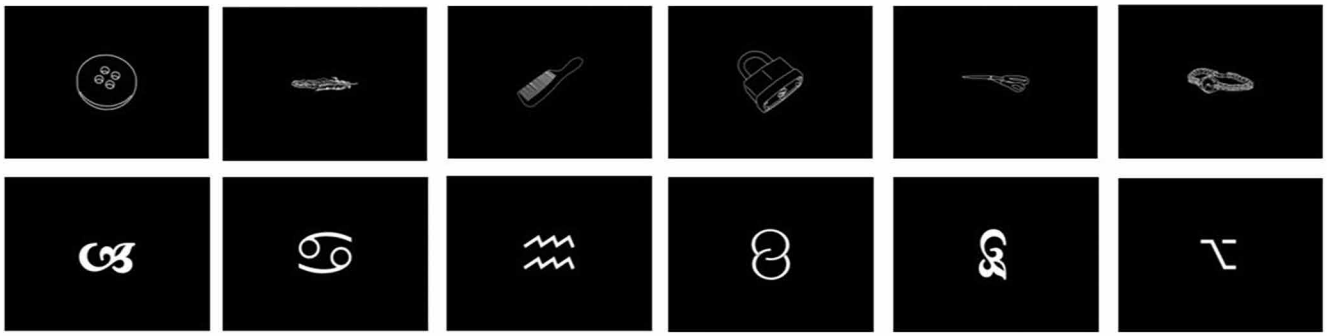

color (Figure 3), showing the connection. If any electrode is not green, the researchers must adjust by removing strands of hair under the electrode or rehydrating it with saline solution. The collection only begins after the green connection of all the electrodes.

We used Matlab to process the data, version 9.12 (R2022a), where we work with calculus, matrices, signal processing, filtering, and graph construction.

Decision Support Model

The model presented in Figure 4 was created to evaluate the instruments and procedures, focusing on brain activation in aphasic participants using the criteria of lesion location (affected hemisphere) and hemiparesis (right or left side). In the second instance, speech pathologists support the decision of rehabilitation procedures in a personalized way.

Figure 3. Interface showing good electrode connection.

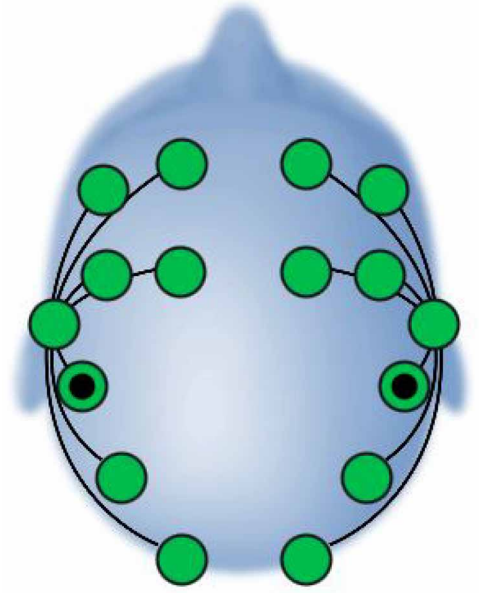

After positioning the device on the participant's head and verifying the connection of all the electrodes, data collection begins with the EEG protocol, with the subject's eyes open and closed for 40 seconds. Once the protocol is finished, the "1" key is pressed to identify the exact beginning of the task. Each participant generated a data file exported from the EEG platform (EMOTIPRO) in CSV (Comma-separated values) format and imported it into Matlab.

We convert the signal to microvolts(uV) and process the signal with different techniques, starting with removing the DC level from the signal to avoid signal distortion. The asymmetric response to the fault is called DC Offset and is a natural phenomenon of the electrical system, applying a filter and decomposing the signal using the Fourier transform.

We created an algorithm to fragment the signal into "windows", making it possible to analyze the stimulus and control intervals. We used the calculation of the RMS value of the signal in each window (the practical value, also known as the RMS value from Root Mean Square).

We developed algorithms to generate the results in a graphical format. We normalized the power per electrode (F7, F3, F4, and F8), generated graphs with the frequency bands for each aphasic participant alone, and graphed the participants' average. We calculated the mean and median

Figure 4. Decision support model.

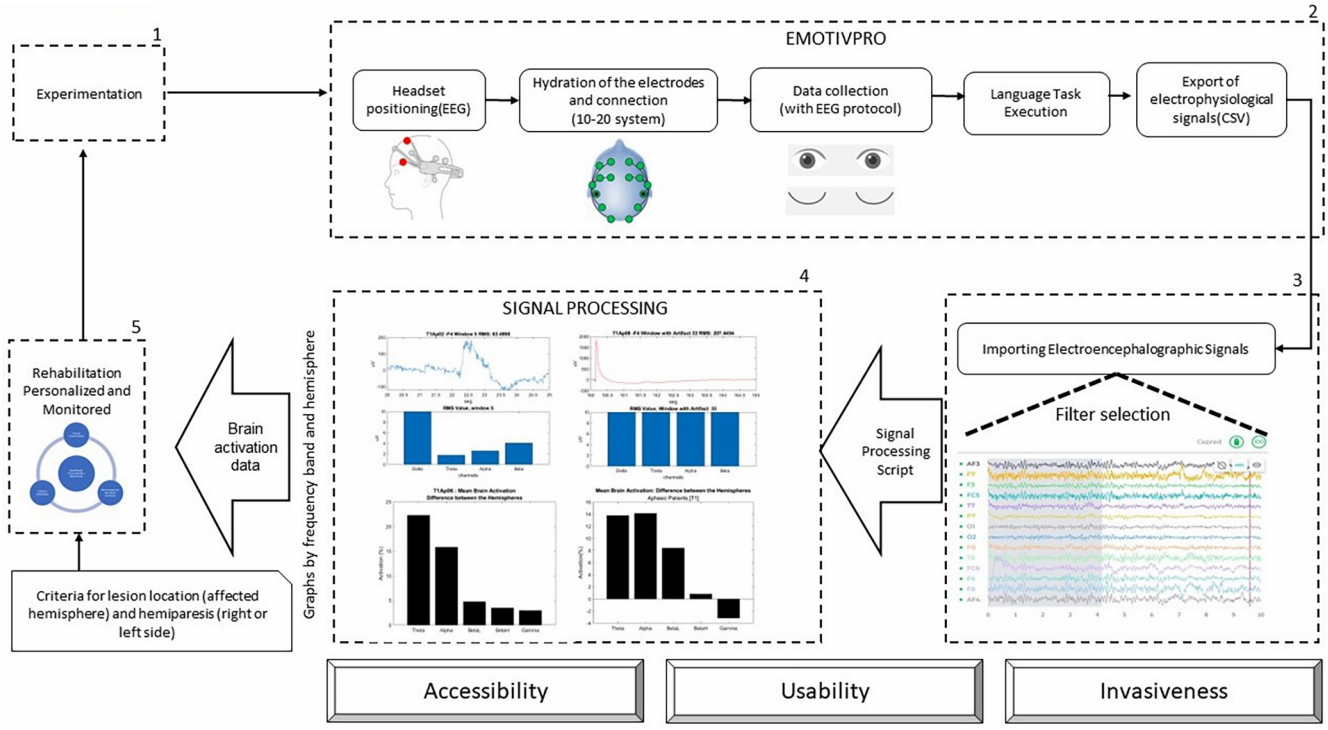

power in each frequency band for each of the four electrodes, generating graphs for each aphasic participant. Moreover, finally, we calculated the difference in brain activation between the left and right hemispheres, plotting the graphs. We used lesion location and hemiparesis criteria to infer the language-dominant hemisphere's location. With the generated graphs, the healthcare professional can analyze the brain activation during the execution of the task.

Figure 5 shows how the continuous monitoring of brain signals can support conventional therapy in the rehabilitation process of aphasic patients. Based on the analysis of the graphics generated by the decision support model (Figure 4), the speech therapists may decide to adjust or maintain the language stimulation conducted in the following appointments and throughout the rehabilitation.

Results and Discussion

In our analysis, we did not include the data from participants (P10 and P11) with global aphasia because both failed to meet the guidelines of the research protocol, frequently diverted the focus of attention to looking at their hands, to objects in the room, and verbalized a few words. Thus, we considered only aphasics with preserved comprehension, with nine participants in the final sample.

In Figure 6, we observed that for all four participants (b, c, d, e), greater electrical activation was identified in the right hemisphere (bars up) than in the left hemisphere (bars down) at all wave frequencies (Theta, Alpha, Beta, BetaH, Gamma).

In the participant P2 (Figure 6b), for example, a 35% greater increase in activation of the right side of the brain, which is the non-language dominant hemisphere, is observed on average. The value on the y-axis shows the difference in the percentage of electrical activation between the brain's two hemispheres.

Participant P01 and Participant P09 (Figure 6a and Figure 6f) also showed increased electrical activation on the right side of the brain, with a single frequency (Theta and Gamma, respectively) with

Figure 5. Personalized and monitored rehabilitation.

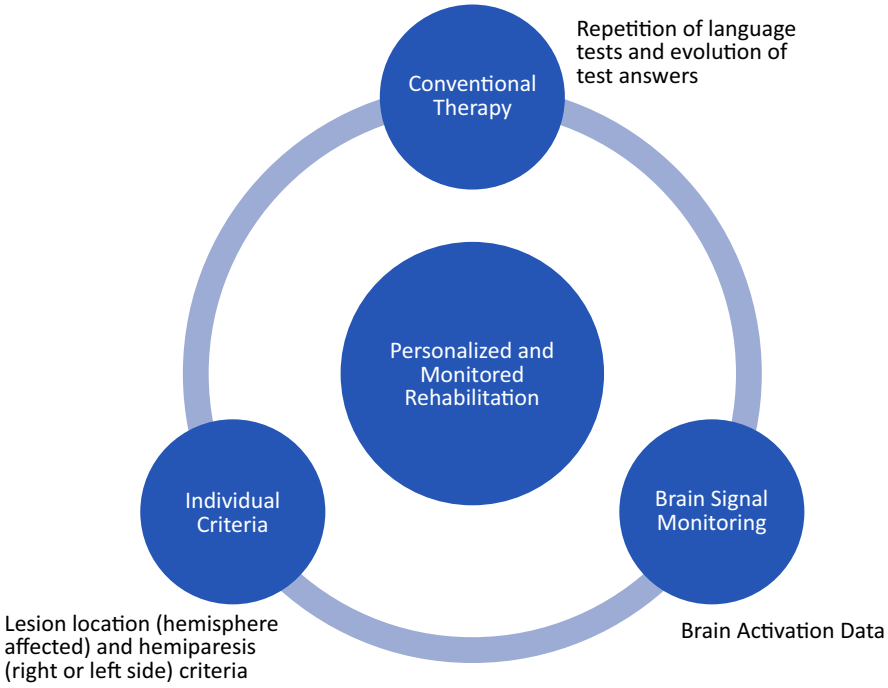

higher electrical activity in the left hemisphere, although with values close to zero.

Thus, an increase in electrical activity was evidenced during task execution in the right hemisphere, which in this sample refers to the non-dominant hemisphere of language. This result may reveal language migration to the contralateral hemisphere.

In Figure 7, we observed that participant P06 (Figure 7g), had greater electrical activation in the right side of the brain, at the frequencies Theta, Alpha, and Beta L, and participant P07 (Figure 7h) had greater electrical activation in the right hemisphere at Theta and Alpha, and at the latter frequency with a value very close to zero.

Figure 8 shows that a single participant had greater electrical activation in the left hemisphere (bars down) at all wave frequencies.

Our study evidenced that four participants showed increased electrical activation in the language non-dominant hemisphere at all brainwave frequencies (Figure 6, b,c,d,e), and 2 participants with a single frequency with increased activation in the left hemisphere (Figure 6, a,f). It also evidenced one participant (Figure 7g) with increased electrical activation in the right hemisphere at Theta, Alpha, and BetaL frequencies and one participant (Figure 7h) with increased electrical activation in the right hemisphere at Theta, Alpha, and the latter near zero frequencies. Finally, it evidenced a single participant (Figure 8) with all frequencies with increased electrical activation in the left hemisphere of language.

Conclusion

In our sample, 6 out of 9 participants showed increased electrical activation in the non-language dominant hemisphere. This fact may reveal a migration of language counter-lateral processing. In this group, 2 out of 9 aphasics had increased activation in both hemispheres at different wave frequencies. Finally, 1 in 9 participants had all frequencies increased in the left hemisphere, the injured side of the brain.

The decision support model proposed in this study tested the applicability of the EEG and the

Figure 6. Difference in electrical activation between hemispheres.

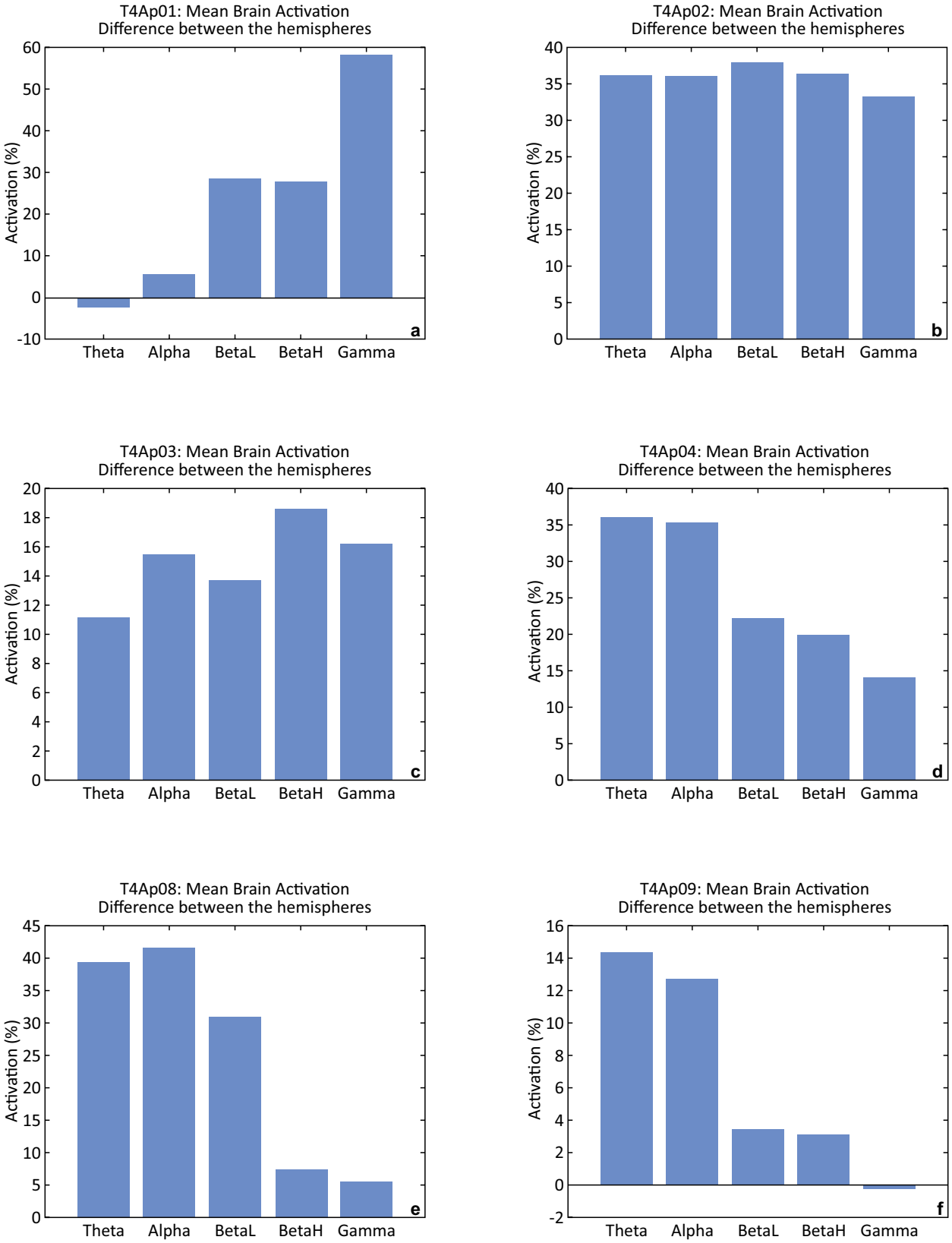

Figure 7. Difference in electrical activation between hemispheres.

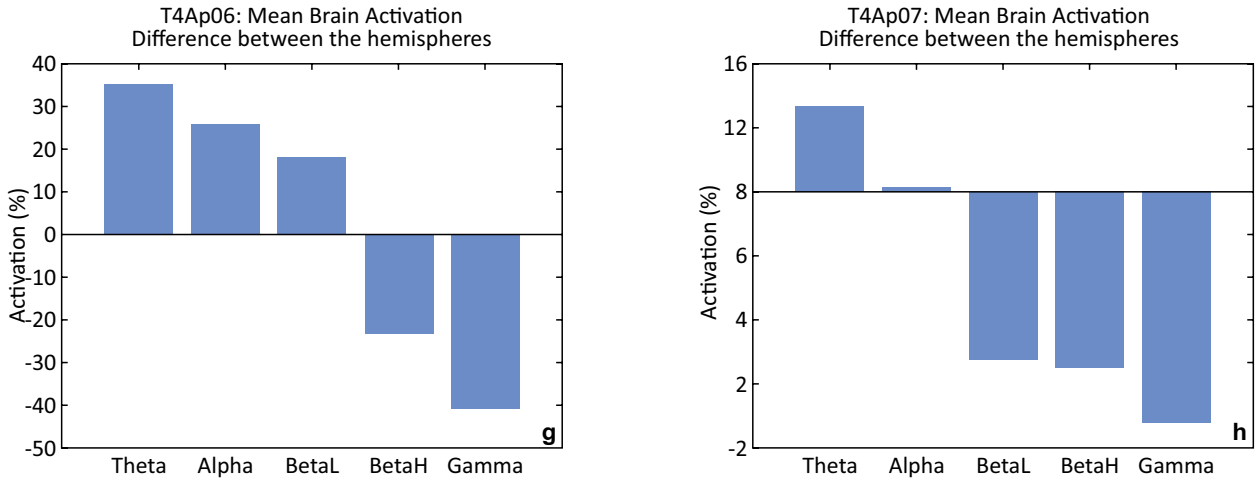

study method and had some positive implications, such as the possibility of graphical visualization of which areas are more active in the brain, especially if there is an activation in non-language dominant areas, which may indicate improvement in the participant's rehabilitation, including provoking greater involvement of the aphasic.

The adoption of the proposed model may serve as support for conventional language therapy in deciding the therapeutic approach and to promote personalized and monitored rehabilitation.

Figure 8. Aphasic participants (AP05) have greater activation in the left hemisphere.

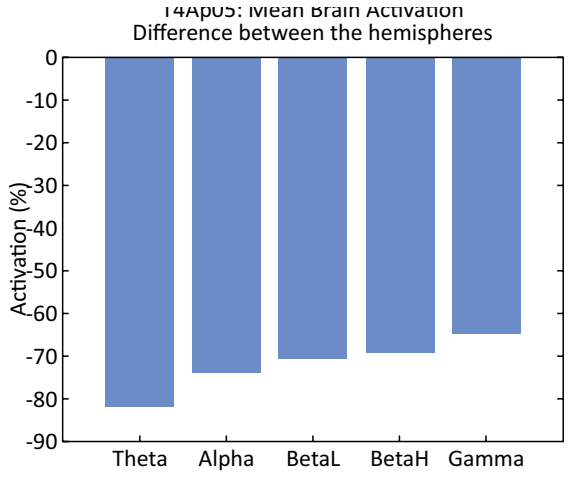

Acknowledgment

We thank the Fundação de Amparo à Pesquisa do Estado da Bahia (FAPESB), process 0195/2019, for supporting this research project; to the Center for Prevention and Rehabilitation of People with Disabilities (CEPRED) for the availability of the health team to work collaboratively in this research, and to the National Council for Scientific and Technological Development (CNPq), Proc. 308783/2020-4.

References

1. Kunst LR et al. Effectiveness of speech therapy in a case of expressive aphasia due to stroke. CEFAC Journal 2013;15(1712-1717.
2. Mineiro A et al. Revisiting aphasias in PALPA-P. Health Notebooks, 2008:135-145.
3. Pagliarin KC et al. Instruments for language assessment following a left brain damage/Instrumentos para avaliacao da linguagem pos-lesao cerebrovascular esquerda. Revista CEFAC: Atualizaçãoo Científica em Fonoaudiologia e Educacao 2013;15(2):444-455.
4. Black DF et al. American Society of Functional Neuroradiology–recommended RMF paradigm algorithms for presurgical language assessment. American Journal of Neuroradiology 2017;38(10):E65-E73.
5. Gil C. Como Elaborar Projetos de Pesquisa. 4.ed - 9. Reimpr. Atlas: São Paulo, 2007.
6. VHL. Virtual Health Library. Available at: <https://bvsalud.org/>. Accessed on: February 25, 2023.

7. Badcock NA et al. Validation of the Emotiv EPOC® EEG gaming system for measuring research quality auditory ERPs. Peer J 2013;1:e38.
8. Yu JH, Sim K-B. Classification of color imagination using Emotiv EPOC and event-related potential in electroencephalogram. Optik 2016;127(20):9711-9718
9. Kotowski K et al. Validation of Emotiv EPOC+ for extracting ERP correlates of emotional face processing. Biocybernetics and Biomedical Engineering 2018;38(4):773-781.
10. Fouad IA. A robust and reliable online P300-based BCI system using Emotiv EPOC+ headset. Journal of Medical Engineering & Technology 2021;45(2):94-114.
11. Melek M, Manshouri N, Kayikçoglu T. Low-cost brain-computer interface using the emotiv epoc headset based on rotating vanes. Traitement du Signal 2020;37(5).

Cell Acquisition Method Validation by Flow Cytometry for MCTI CIMATEC HDT RNA Vaccine Immunogenicity Evaluation Against SARS-CoV-2

Elen Azevedo da Costa[1*], Carlos Augusto Oliveira Júnior[1], Alana Costa de Oliveira[2], Emanuelle de Souza Santos[2], Milena Botelho Pereira Soares[2], Bruna Aparecida Souza Machado[2]

[1]Technological and Industrial Development – DTI-B; [2]SENAI CIMATEC University Center; Salvador, Bahia, Brazil

The COVID-19 pandemic highlighted the importance of developing and improving techniques that can help diagnose and evaluate the disease's immunological response. Standardizing methods is necessary to ensure the confidence and reproducibility of the results. Therefore, the objective of this work was to carry out a concurrent validation to compare the reference methods for acquiring data used in the evaluation of the immunogenicity of the Vaccine. RNA MCTI CIMATEC HDT, performed by flow cytometry. From the analysis of the cellular profile through the evaluation of cell size and complexity and expression of immunophenotypic markers, no significant differences were found, demonstrating that the methodology used in the BD FacsMelody cytometer at SENAI/ CIMATEC is suitable for obtaining the results.

Keywords: Flow Cytometry. Validation. COVID-19.

Introduction

According to the World Health Organization, the coronavirus pandemic caused by SARS-CoV-2 was responsible for the deaths of more than six million people around the world [1]. Under these circumstances, there was a significant investment in developing diagnostic tests capable of detecting possible infection by the virus and an escalation in the production of vaccines that would reduce the risk of complications and the mortality rate [2,3].

Several techniques can be used to quantify immunological responses to vaccines, including flow cytometry, which consists of quantifying cells marked with antibodies coupled to a specific fluorochrome for a marker of interest [4]. During this pandemic, this technique gained more space, exerting a strong influence on published data [5]. This fact demonstrates the need to ensure that operational procedures can guarantee data robustness and reproducibility. The preparation and storage of samples, the calibration of equipment, and the standardization and optimization of the protocols used help to improve processes, ensuring better performance of functions and contributing to more excellent reliability of the data generated.

Therefore, this work aimed to validate the reference methods for data acquisition used in the immunogenicity assessment carried out by flow cytometry of the MCTI CIMATEC HDT RNA Vaccine.

Materials and Methods

A concurrent validation was carried out, which refers to a combination of retrospective and prospective validation applied in the case of a process similar to another previously validated.

Blood samples were collected and subjected to the density gradient separation technique (Ficoll-Hypaque, Histopaque/Sigma-Aldrich) to obtain peripheral blood mononuclear cells (PBMC) through centrifugation, which were subsequently cryopreserved until the use. The cells were cultivated in 96-well plates under the following conditions:

1. Only with RPMI-1640 culture medium (Gibco®- Thermo Fisher Scientific);
2. Stimulated with phytohemagglutinin (PHA - Phytohemagglutinin) as positive control at concentrations of 5 µg/mL and 10 µg/mL;
3. With Spike, a SARS-COV-2-specific protein, at a concentration of 2.5 µg/mL.

Received on 7 March 2023; revised 20 May 2023.

Address for correspondence: Elen Azevedo da Costa. Av. Orlando Gomes, 1845 - Piata, Salvador - BA, 41650-010. E-mail: elen.costa@fbter.org.br.

J Bioeng. Tech. Health 2023;6(3):208-210

The cells were incubated in the culture oven for 24h at 37°C and 5% CO_2, and four hours before the end, monensin and brefeldin were added to all wells. We used surface marker antibodies to perform cell labeling (CD3 - APC-H7, CD4 - Krome Orange, CD8 - PerCP-Cy 5.5, CD107a - FITC, CD69 - BV786, CD137 - PE, CD40 - PE-Cy7, CD19 - FITC, CD30 - BV421). Cell permeabilization was performed to label intracellular antibodies (IL-2 - BV421, TNF-α - BV750, IFN-γ - PE-Cy7, IL-5 - PE, IL-13 - APC, Granzyme B - Alexa Fluor 647) and then fixing. Several washing steps were performed, and the cells were subsequently maintained in 1X PBS until acquisition on the cytometers.

As an evaluation criterion, analyses carried out on the BD LSRFortessa flow cytometer from FIOCRUZ-Ba were used, comparing those carried out by the BD FACSMelody cytometer from SENAI/CIMATEC, evaluating the cellular profile (size and granularity) as well as the frequency of expression of immunophenotypic markers. The acceptable variation is ± 5% as a criterion for accepting values.

Results and Discussion

During the coronavirus pandemic, the need to develop and improve techniques to assist in the rapid and accurate diagnosis of immunological responses to vaccination became even more evident. The standardization of experiments is necessary to eliminate the possibility of variables that could compromise the results, making the technique reproducible and reliable [6]. In addition, validating a process or equipment certifies that the result found is what was expected [7].

Based on the results found in the analysis of the cellular profile through the evaluation of cellular size and complexity and expression of immunophenotypic markers from the data acquired on the two cytometers LSFortessa from FIOCRUZ-Ba and the BD FacsMelody from SENAI/CIMATEC, it was verified that there are no significant differences between the data, thus indicating that the methodology used to acquire data on the SENAI/CIMATEC BD FacsMelody cytometer is suitable and can continue to obtain the results (Figure 1).

Establishing a standard operating procedure for sample preparation and data acquisition improves results by ensuring that possible discrepancies are not due to erroneous procedures that could cause deviations in results [7,8]. In this way, validation provides robustness and effectiveness of the results generated, ensuring the quality of the process.

Final Considerations

This study provided that the method used to acquire data on the SENAI/CIMATEC BD FacsMelody cytometer can continue to be carried out since, in the validation process, it was considered suitable, the previously validated method.

Acknowledgments

We thank the National Council for Scientific and Technological Development (CNPQ) for the grant granted and the support of the ISI-SAS team, particularly the Cytometry team.

References

1. WHO – World Health Organization. Coronavirus disease (COVID-19) pandemic. Disponível em: https://www.who.int/emergencies/diseases/novel-coronavirus-2019. Accessed on March 22, 2023.
2. Pardi N, Hogan MJ, Weissman D. Recent advances in mRNA vaccine technology. Current Opinion in Immunology 2020;65:14–20.
3. Edwards AM, Baric RS, Saphire EO, Ulmer JB. Stopping pandemics before they start: Lessons learned from SARS-CoV-2. Science 2022;(80)375:1133–1139.
4. Cossarizza A et al. Guidelines for the use of flow cytometry and cell sorting in immunological studies (second edition). Eur J Immunol 2019;49:1457–1973.
5. del Molino del Barrio I, Hayday TS, Laing AG, Hayday AC, Rosa F. COVID-19: Using high-throughput flow cytometry to dissect clinical heterogeneity. Cytometry Part A 2021. doi:10.1002/cyto.a.24516.
6. Kalina T. Reproducibility of flow cytometry through standardization: Opportunities and challenges. Cytometry Part A 2020;97:137–147.

Figure 1. Analysis of the cellular profile on the LSRFortessa (FIOCRUZ-Ba) and BD FACSMelody (SENAI/CIMATEC) cytometers.

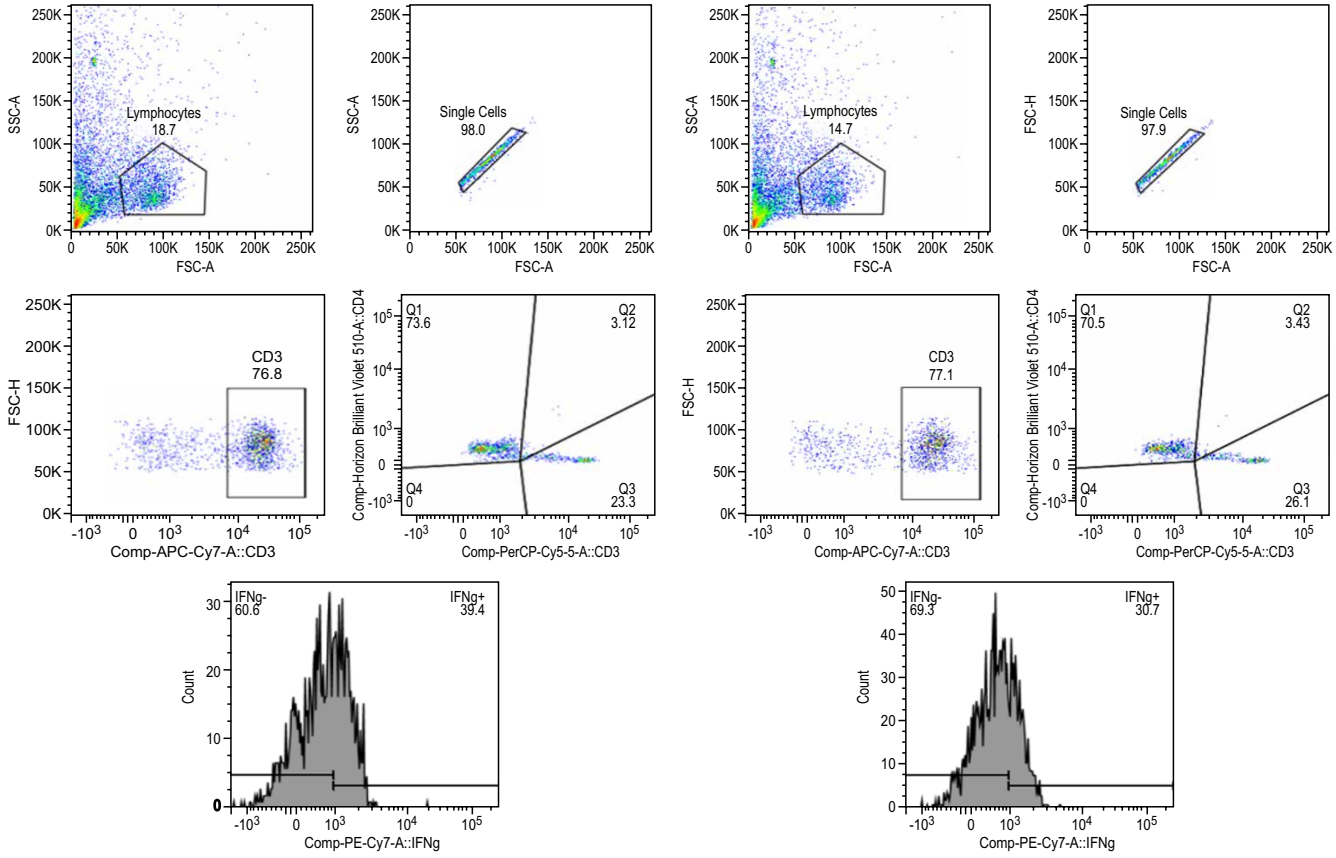

7. Brasil. Agência Nacional de Vigilância Sanitária (ANVISA). Resolução - RDC no 210, de 04 de agosto de 2003. Dispõe sobre o Regulamento técnico das boas práticas para a fabricação de medicamentos. (2003). Disponível em: http://189.28.128.100/dab/docs/legislacao/resolucao210_04_08_03.pdf. Accessed on March 24, 2023.
8. Kaur G, Rana AC, Bala R, Seth N. An overview: the role of process validation in pharmaceutical industry. IRJP 2012.

Technology Transfer in Vaccine Production: Implementation of Physical-Chemical Quality Control and Sodium Hydroxide Purity Analysis

Camila Carane Bitencourt Brito[1*], Rodrigo Souza Conceição[2], Bruna Aparecida Souza Machado[2]
[1]CNPQ Scholarship Holder; [2]SENAI CIMATEC University Center; Salvador, Bahia, Brazil

The transfer of technology for vaccine production is crucial to ensuring the fight against infectious diseases on a global scale. Thus, among the various requirements for this production to be carried out safely, the implementation of quality control stands out, which involves everything from acquiring raw materials and qualifying suppliers to carrying out microbiological and physical-chemical tests. The objective of this work was to demonstrate the purity test used in the quality control of sodium hydroxide, one of the inputs acquired for the production of the RNA MCTI CIMATEC HDT vaccine. The limit of carbonates present in the sample under study was determined as described in the official compendium, obtaining results compatible with current specifications.
Keywords: Sodium Hydroxide. Quality. Vaccine.

Introduction

The development of vaccines is one of the objectives of medicine, considering it as a strategy for reducing the global incidence of infectious diseases [1]. Vaccine innovation requires expertise, which initially includes demand from society, investment in research, intellectual property, and production, as well as the need to guarantee quality and compliance with regulatory standards [1]. From this perspective, technology transfer is one of the fastest ways to achieve the technology necessary for vaccine production [2]. In this sense, HDT BioCorp, in partnership with SENAI-CIMATEC and the Ministry of Health, developed the RNA MCTI CIMATEC HDT vaccine, which is under investigation for COVID-19 and in the process of technology transfer to Brazil.

In this context, many steps must be followed to carry out this process, guaranteeing the product's safety. Among them, the physical-chemical quality control of raw materials and the finished product is a primary requirement, recommended by RDC 658/2022 on good drug manufacturing practices [3]. This stage includes the literature review and development of all tests for the sample of interest to prove the raw material's compliance with current quality specifications. The present work aimed to implement quality tests, as purity test for the quantification of carbonates.

Received on 28 May 2023; revised 15 July 2023.
Address for correspondence: Camila Carane Bitencourt Brito. Avenida Orlando Gomes, 1845, Piatã. Zipcode: 57930-000. Salvador, Bahia, Brazil. E-mail: camila.brito@fbter.org.br.

J Bioeng. Tech. Health 2023;6(3):211-213

Materials and Methods

The analyses were occurred at the Pharmaceutical Formulations Laboratory of SENAI-CIMATEC, and the tests were carried out in the sodium hydroxide monograph, IF224-00, of the Brazilian Pharmacopoeia 6th edition [4].

Sample Description

We analyzed the appearance and color of the sample with 1mg of sodium hydroxide (exodo®) added to a test tube

pH Determination

A 0.01% (w/v) aqueous solution was prepared to determine the pH. The sample was diluted with carbon dioxide-free water. The pH reading used the FP20 Five Easy Plus Mettler Toledo® pH meter.

Carbonate Limit

The solutions used in the test were prepared as described below:

Hydrochloric Acid M SV

The volumetric solution (VS) was prepared by slowly adding 85mL of hydrochloric acid to carbon dioxide-free water to obtain 1,000 mL of aqueous solution. The solution was standardized in duplicate, and each sample of 1.5g of anhydrous sodium carbonate was subjected to drying in an oven at 120°C for 1 hour. 100 mL of water and two drops of methyl red indicator solution (SI) were added. Hydrochloric acid M SV was slowly added from a burette until a faint pink color. The solution was heated, and when boiling began, the solution was removed from heating and cooled to room temperature to continue the titration. This sequence of operations was repeated until heating no longer affected the pink color. The molarity calculation was carried out considering that every 52.99 mg of sodium carbonate (Na_2CO_3) equals 1 mL of M hydrochloric acid.

Methyl Red SI

The indicator solution was prepared from a mixture of 0.1g of methyl red, 1.85 mL of 0.2 M sodium hydroxide and 5 mL of 90% (v/v) ethyl alcohol. The solution was heated at 40°C for 15 minutes. After solubilization, the volume was up to 250 mL with 50% (v/v) ethyl alcohol. For the sensitivity test of the indicator solution, 0.1 mL of SI methyl red, 100 mL of carbon dioxide-free water, and 0.05 mL of 0.02 M hydrochloric acid were used, and the addition of 0.1 mL of 0.02 M sodium hydroxide changed the color to yellow.

Phenolphthalein SI

The indicator solution was prepared by dissolving 0.1 g in 100 mL of 80% (v/v) ethyl alcohol. For the sensitivity test, a solution of 0.1 ml of SI phenolphthalein was prepared in 1000 mLof carbon dioxide-free water, and a change in color from colorless to pink was observed after adding 0.2 mL of 0.02M sodium hydroxide.

SI Methyl Orange

The indicator solution was prepared by dissolving 0.1 g of methyl orange in 100 mL of 20% (v/v) ethyl alcohol. For the sensitivity test, 0.1 mL of indicator solution was used with 100 mL of carbon dioxide-free water, and a change from yellow to red color was observed after adding 1 mL of 0.1 M hydrochloric acid.

Procedure for Determining Carbonate Limits

The purity test was carried out in two stages, as described below:

1st stage: 2 g of the sample was dissolved in 80 mL of carbon dioxide-free water. Immediately afterward, 0.3ml of SI phenolphthalein was added, and titration was carried out with hydrochloric acid M SV until the color changed.

2nd stage: 0.3 mL of SI methyl orange solution was added, and the titration was carried out again with hydrochloric acid M SV until the color changed.

The calculations were carried out considering that each mL of hydrochloric acid M SV used in step 2 of the titration is equivalent to 0.1060 g of Na_2CO_3, and each mL of hydrochloric acid M SV used in the total titration (steps 1 and 2) is equivalent to 40 mg of the total base, in the form of NaOH. The experiments were carried out in duplicate, and the average of the analyses was used to calculate the percentage of carbonate.

Results and Discussion

Sodium hydroxide appeared as a white crystalline mass in the shape of spheres. The sample solution presented pH 11, which describes a primary medium following current specifications.

Carbonate Limit

Sodium hydroxide (NaOH) is classified as a base and can easily react with an acidic oxide

such as carbon dioxide [5] (CO_2), forming sodium carbonate (Na_2CO_3) and water (H_2O), according to the equation described below:

$$2\ NaOH(s) + CO_2(g) \rightarrow Na_2CO_3(s) + H_2O(l)$$
(Equation 1)

Therefore, we need to verify the occurrence of this reaction and whether the carbonate content is within the limits established by legislation to guarantee the quality of the sample used in the vaccine production stages.

Quantification was based on acid-base volumetry with the addition of phenolphthalein and methyl orange indicator solutions, proceeding in two stages, with previously standardized hydrochloric acid being used as a titrating agent. In the 1st stage of titrating sodium hydroxide with hydrochloric acid (Equation 2), the turning point was observed after adding 49.5 mL of HCl, evidenced by the change from pink to colorless. In the 2nd stage of the titration, with the addition of methyl orange, an orange-yellow color was observed with a turning point after titration of 0.1mL of HCl.

For the first titration stage, the sodium hydroxide is completely neutralized (Equation 2). In the second stage, with methyl orange, the carbonate present in the sample is neutralized (Equation 3), as shown below:

$$NaOH(s) + HCl(l) \rightarrow NaCl(s) + H2O(l)$$
(Equation 2)
$$Na_2CO_3(s) + HCl(l) \rightarrow NaHCO_3(s) + NaCl(s)$$
(Equation 3)

The acceptance limit for carbonates is a maximum of 2.0%, and the percentage obtained in the analysis was 0.4% (±0.019), showing that the sample complies with the specifications for the purity test described.

Final Considerations

The present work described the purity test for the physical-chemical quality control of sodium hydroxide and demonstrated compliance with current specifications. The analyses are part of implementing physical-chemical quality control of the LION formulation, an adjuvant for the RNA MCTI CIMATEC HDT vaccine, and are in the process of technology transfer. New assays are under development and will be carried out to complete the quality analysis of the sample of interest.

Acknowledgments

We thank to CNPQ for financing the project and SENAI-CIMATEC for the structure for developing the analyses.

References

1. Van de Burgwal LHM et al. Towards improved process efficiency in vaccine innovation: The vaccine innovation cycle as a validated, conceptual stage-gate model. Vaccine 2018.
2. Hamidi A et al. Lessons learned during the development and transfer of technology related to a new Hib conjúgate vaccine to emerging vaccine manufactures. Vaccine 2014.
3. Brasil. Ministério da Saúde. Agência Nacional de Vigilância Sanitária (ANVISA). Resolução da Diretoria Colegiada - RDC nº 658, de 30 de março de 2022. Dispõe sobre as Diretrizes Gerais de Boas Práticas de Fabricação de medicamentos. Diário Oficial da União. Brasília.2022.
4. Agência Nacional de Vigilância Sanitária (ANVISA). Farmacopeia Brasileira, 6th ed. 2019.
5. Mello LC et al. Metodologia experimental para reações gás-líquido. Quimica Nova 2016

3D Bioprinting and Characterization of Bioinks with Different Concentrations of Hyaluronic Acid Methacrylate (AHMA)

Caio Athayde de Oliva[1*], Arthur João Reis Lima Rodovalho[2], Leonardo Santana Ramos Oliveira[3], Lucca Ribeiro Alves[3], Willams Teles Barbosa[2], Ana Paula Bispo Gonçalves[4], Jaqueline Leite Vieira[4], Paulo Romano Cruz Correia[2], Milena Botelho Pereira Soares[4], Josiane Dantas Viana Barbosa[2]

[1]Graduating in Mechanical Engineering; Scientific Initiation - CNPQ; [2]SENAI CIMATEC University Center; [3]Bahiana School of Medicine and Public Health; [4]Gonçalo Moniz Institute, Oswaldo Cruz Foundation, FIOCRUZ; Salvador, Bahia, Brazil

The 3D Bioprinting technique for tissue engineering has been constantly developed and generating different results due to the range of applicability of the technique. It is necessary to study and analyze matrices to use this technology, as an example of hydrogels, which are viable for use in conjunction with cells to create the bioink used in bioprinting, verifying their physicochemical properties, cellular reviews, and properties mechanics for the desired application. Based on this, this work aims to analyze these properties, focusing on the hyaluronic acid (HA) matrix in different concentrations during the manufacture of bioink for 3D bioprinting for future application in tissue engineering.

Keywords: Hyaluronic Acid. Bioprinting. Bioink. Tissue Engineering.

Introduction

In tissue engineering, a technique that has been gaining prominence with its recent advances and several studies is the implementation of 3D bioprinting [1]. This technology allows variation of parameters for the most diverse applications in health and regeneration and tissue mimicry with the help of hydrogels capable of simulating a viable environment for cells that can differentiate into living tissue. This technique generates products that must undergo chemical, mechanical, and biological studies and analyses to verify various aspects to find out whether the application of a certain hydrogel with cells (called bioink) is compatible with the tissue that is desired to be regenerated or mimic so that both the correct parameters and the correct raw material are used to produce the hydrogel and bioink [2].

In tissue engineering, a technique that has been gaining prominence with its recent advances and several studies is the implementation of 3D bioprinting [1]. This technology allows variation in the production parameters of scaffolds, structures used for cell growth, and the most diverse applications in health and regenerative medicine. The molds produced using this technique aim to mimic tissues, using thermoplastic biopolymers and hydrogels capable of simulating the cells' natural environment so that they can later even differentiate into tissue similar to that *in vivo*. The materials used to synthesize the products of this technique must undergo physical-chemical, mechanical, and biological studies and analyses to verify various aspects to know whether the application of a given biomaterial is compatible with the tissue desired to regenerate or mimic. Furthermore, in the case of hydrogels used for printing together with cells (bioinks), a rigorous adjustment of parameters is necessary so that, in the end, a viable scaffold is obtained [2].

Hyaluronic acid (HA) has been widely studied due to its viscoelasticity, ease of gelation, and biological properties for various applications in biomedicine[3]. This study aimed to produce scaffolds with different concentrations of HA by 3D bioprinting to evaluate the printability of these hydrogels, analyzing their physicochemical, mechanical, and biological properties, verifying

Received on 22 June 2023; revised 18 August 2023.

Address for correspondence: Caio Athayde de Oliva. Rua Castro Neves, Edf Diana 394, Apt 1101 - Matatu. Zipcode: 40255-020 Salvador, Bahia, Brazil. E-mail: olivathayde.jr@gmail.com.

J Bioeng. Tech. Health 2023;6(3):214-217

how the concentration of HA interferes with these properties and their capacity to produce scaffolds with viable cells for application in future tissue engineering studies.

Materials and Methods

The method of this work was divided into four stages: preparation of the hydrogel, preparation of the bioink, printing of the scaffolds by 3D bioprinting, and finally, the characterization of the biomaterials.

The hydrogel was prepared using HA dissolved in ultrapure water under constant stirring until complete dissolution. Then, methacrylate was added to the solution, and its pH was adjusted to 8 by dripping a 5 M NaOH solution. With the pH adjusted, the solution was left in a shaker, shaken overnight at 4ºC, and removed for washing with ethyl alcohol, using a centrifuge to remove the unreacted methacrylate from the solution. After washing, the precipitate formed was frozen at -80ºC for at least 2 hours and then taken to a freeze dryer for 10 hours to complete the production of HA methacrylate (AHMA).

The lyophilized AHMA was weighed to different concentrations (1.5, 3; 4.5, and 6% w/v) and dissolved in Phosphate-Buffered Saline (PBS) in a sterile environment inside a syringe to create a compatible and viable environment for cells to prepare the bioink. Subsequently, these were suspended in Dulbecco's Modified Eagle Medium (DMEM) mixed with the hydrogels, giving rise to bioinks. 0.05% of the photoinitiator Lithium phenyl-2,4,6-trimethylbenzoylphosphinate (LAP) was used for each bioink concentration and was then taken to bioprinting to obtain the scaffolds.

The printer used in this study was the Octopus from 3D Biotechnology Solutions (3DBS) company. Cylindrical scaffolds measuring 13 mm in diameter, 4 mm in height, and 80% filled were printed. These were printed on Petri dishes and sterile 6-well plates through a 0.7 mm needle and exposed to UV light for 5 minutes for photocuring. After the end of UV light exposure, the scaffolds were subjected to mechanical compression rheological and biological testing.

For mechanical analysis, the behavior of the stress x strain curve of each scaffold at different concentrations was analyzed using a Brookfield CT3 texturometer to evaluate how increasing the concentration of AHMA could change this parameter. This test used a 1000g load cell and 0.01 mm/s speed. The rheological analysis was carried out using a Haake Rheotest rheometer (Medingen 2.1) to check the viscosity of the bioink with the variation in its concentration using the Ostwald-de Waele model. For biological analysis, 5x104 cells/mL GFP murine stem cells were analyzed by microscopy 10 days after printing.

Results and Discussion

Figure 1 shows the stress x strain curve obtained by the compression test for each printed scaffold. The increase in tension required to rupture the scaffold is notable with the increase in concentration of each AHMA made. Therefore, the 6% AHMA concentration was the one that presented the highest stress value due to the increased HA content in the formulation. These curves are characterized by a linear elastic and plastic region caused by an increase in tension without a significant increase in deformation.

Figure 2 shows the viscosity x shear rate curves of the different formulations studied. It is noted that the higher the concentration, the more viscous the hydrogel tends to become, maintaining its shear rate similar for all concentrations.

Figure 3 shows the cells (light points) distributed in the bioink, demonstrating its viability for concentrations of 1.5 to 6% as bioinks for application in 3D bioprinting.

Final Considerations

The results generated were favorable for future studies on the viability and applicability of AHMA in tissue engineering due to the increase in compressive strength and cell viability at higher concentrations, as shown in the results. From

Figure 1. Stress x strain curves of scaffolds with different concentrations of AHMA.

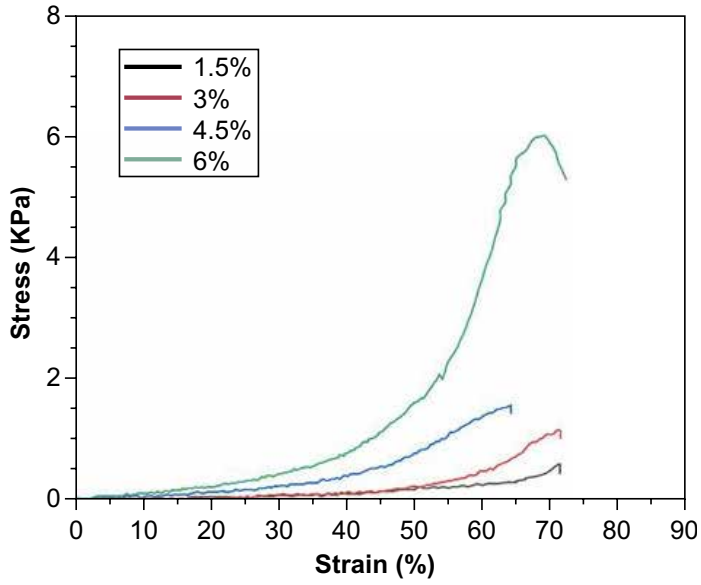

Figure 2. Viscosity x shear rate curves of hydrogels with different concentrations of AHMA.

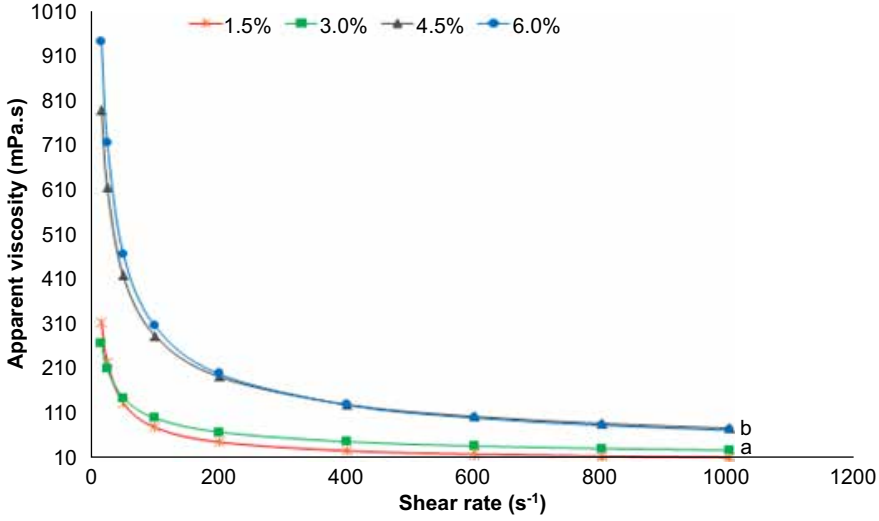

Figure 3. Visualization of L929 within AHMA at concentrations 1.5% (a), 3% (b), 4.5% (c) and 6% (d).

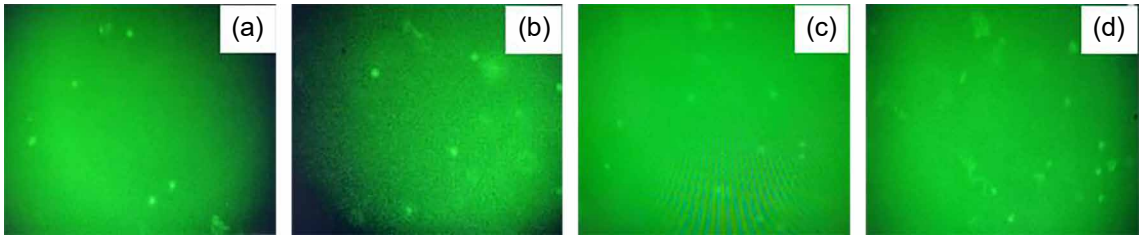

this, it is possible to extend the level of the study further, increasing both the number of days for the biological test and the concentration to find a viability limit that increases mechanical properties but only makes cell growth feasible within bioink.

Acknowledgments

The authors thank CNPq, CAPES, and FIOCRUZ for the scholarship opportunity. To SENAI CIMATEC to provide the infrastructure. Moreover, the team for their help in carrying out this work.

References

1. Choi G, Cha HJ. Recent advances in the development of nature-derived photocrosslinkable biomaterials for 3D printing in tissue engineering. Biomaterials Research 2019.
2. Ding Y, Zhang X, Mi C, Qi X, Zhou J, Wei D. Recent advances in hyaluronic acid-based hydrogels for 3D bioprinting in tissue engineering applications. Smart Materials in Medicine 2023;4:59-68.
3. Hachet E, Berghe HVD, Bayma E et al. Design of biomimetic cell-interactive substrates using hyaluronic acid hydrogels with tunable mechanical properties. Biomacromolecules 2012.

Study on the Technical and Economic Viability of a Polygeneration Energy System Applied to a Hospital Unit in Bahia's Countryside, Brazil

Pedro Freire de Carvalho Paes Cardoso[1*], Turan Dias Oliveira[1], Alex Álisson Bandeira Santos[1]
[1]SENAI CIMATEC University Center; Salvador, Bahia, Brazil

The present study aims to propose a polygeneration system model, integrating multiple forms of energy generation, such as photovoltaic systems, heat pumps, and other existing storage models to be used in a small-sized hospital unit in Bahia's countryside. A polygeneration system was developed through a basic Project of the individual components and their integration as a unified system. The COP value, energy saving, and macro investment predictions were calculated, and financial indicators such as payback time, VPL, and TIR were determined. The results showed that the proposed system can supply the hospital's energy demands and be considered a stimulating investment.
Keywords: Polygeneration. Heat Pump. Photovoltaic System. Hospital.

Introduction

The world has been going through a renewal in how energy is generated and managed, all the way to its utilization. The concept of sustainability goes through the primary idea of green consumption, also paying attention to generating energy and energetic efficiency, configuration, and transformation of the existing systems. According to the data from ANEEL [1], approximately 14.8% of national energy production is compromised from generation to consumption availability.

Espírito Santo and colleagues [2] state that the efficient use of natural resources and energy generation decentralization through polygeneration can contribute to primary energy saving and the planet's health.

Many studies on polygeneration have been developed around the world. For instance, Pina and colleagues [3] developed a polygeneration analysis destined for a hospital unit located in Campinas (Brazil), composed of a photovoltaic system, photothermic system, biomass generator, and natural gas associated with thermal storage units and net connection. Calise and colleagues [4] approach a polygeneration system analysis, also destined for a hospital, using a natural gas-powered engine, heat exchangers, an absorption chiller, a cooling tower, and other components. Other polygeneration systems were developed and studied in the literature [5, 6].

Photovoltaic systems are a more promising electric energy generation alternative because they provide sustainable energy at an attractive energy-saving cost. According to data from ABSOLAR [7], in the last 12 years, the capacity of installed photovoltaic generators in Brazil has increased from approximately 8 MW to over 32 MW till June 2023.

Heat pumps are another application for a generator system that has increased in the number of researches for using and commercializing. According to Fischer and colleagues [8], heat pumps are already a well-known technology. They play a more and more critical role in Europe for cooling and heating buildings due to their capacity to increase energetic flexibility, integrate other systems, reduce CO_2 emissions, and improve efficiency.

A polygeneration system was proposed and studied in Chiang Mai, Thailand, by Kong and colleagues [9]. The model proved that combining systems enables a more significant individual performance generation for the thermic and photovoltaic systems and the heat pump.

Received on 20 June 2023; revised 21 August 2023.
Address for correspondence: Pedro Freire de Carvalho Paes Cardoso. Avenida Orlando Gomes, Piatã, Salvador, Bahia, Brazil. Zipcode: 41650-010. E-mail: pedropcadoso06@gmail.com.

J Bioeng. Tech. Health 2023;6(3):218-223

The present study introduces as its primary focus the proposition for a polygeneration energy system for hospital units, including photovoltaic systems and heat pumps, among other generation and storage systems already known. It intends to prove its technical and economic viability for a small-sized hospital unit in Bahia's countryside.

Materials and Methods

The polygeneration system analysis began with the consumption unit selection and knowing its energy demands. In the work of Melo and colleagues [10], a polygeneration system study, data from a hospital in Buritirama, Bahia (-10,72N, -43,65L) were available. The hospital is considered small-sized, with an approximate area of 783 m², with 15 bed rests and one birth room, operating 24 hours a day, with 17 collaborators and an average of 15 patients daily.

The hospital's energy load comes from electric and thermal hot water and air conditioning. Regarding the electric energy consumption for the hospital, there is an average of 6,857.83kWh/month, with approximately 10.62% for electric showers, 45.45% for air-conditioning, and 43.92% for other equipment and lighting.

Thermal loads have peak power calculated for February of 31.66 kW and a maximum monthly load of 11,102.85 kWh/month for air-conditioning units and 713.00 kWh/month for electric showers. Electric showers drive the hospital's hot water demand, considering COP equals 1. Cooling demand comes from air-conditioning units, with a COP value of 3. The electric energy is provided by the concessionary electric net [10].

After the energetic demand determination, the macrostructure for the polygeneration system was defined for analysis. The proposed system presents a photovoltaic system and uses the concessionary electrical network for feeding the electric energy, an air-water heat pump for generating hot water, an absorption chiller for cold water, and accumulation tanks for cold and hot water. The polygeneration model is presented in Figure 1.

The polygeneration system was dimensioned starting from the thermal demands. Data from storage tanks and absorption chillers by Melo and colleagues [10] were used. The accumulation tanks have a 6% performance, a 1700 kW capacity for hot water, and 400 kW for cold water. The chosen absorption chiller is the EAW Wegracal 50, with a 71kW entrance power rating of 54kW, COP of 0.81, hot water entry temperature of 71oC to 86oC, and cold water exit of 9ºC.

The heat pump was empirically dimensioned to supply the hot water thermal demands for consumption and the absorption chiller's need to provide the cold water demand.

For calculating the heat pump, the current peak of monthly cooling demand was 11,102.85 kWh, the chiller performance with COP was equal to 0.81, and the accumulation tanks had a 6% loss. As for the hot shower water, the peak demand considered was 713.00 kWh and a 6% loss from the accumulation tank. So, we calculated a pump generation demand of 15,340.66 kWh/month and a power of 21.31 kW. After analyzing the market's disponibilities, two heat pumps were selected: LG model HM121M.U33. The primary data from the heat pump are in Table 1.

Table 1. Primary data - Heat pump system LG HM121M.

Heat pump maker	**LG**
Module model	HM121M
Number of heat pumps selected	2
COP warming range (variation to entry/exit temperatures)	2.9 to 4.9
Thermal rated capacity - warming (kW)	12
Thermal rated capacity - cooling (kW)	14
COP cooling range (variation to entry/exit temperatures)	2.7 to 4.6
Domestic hot water temperature range (ºC)	15 an 80
Compressor type	Scroll

Figure 1. Polygeneration system model.

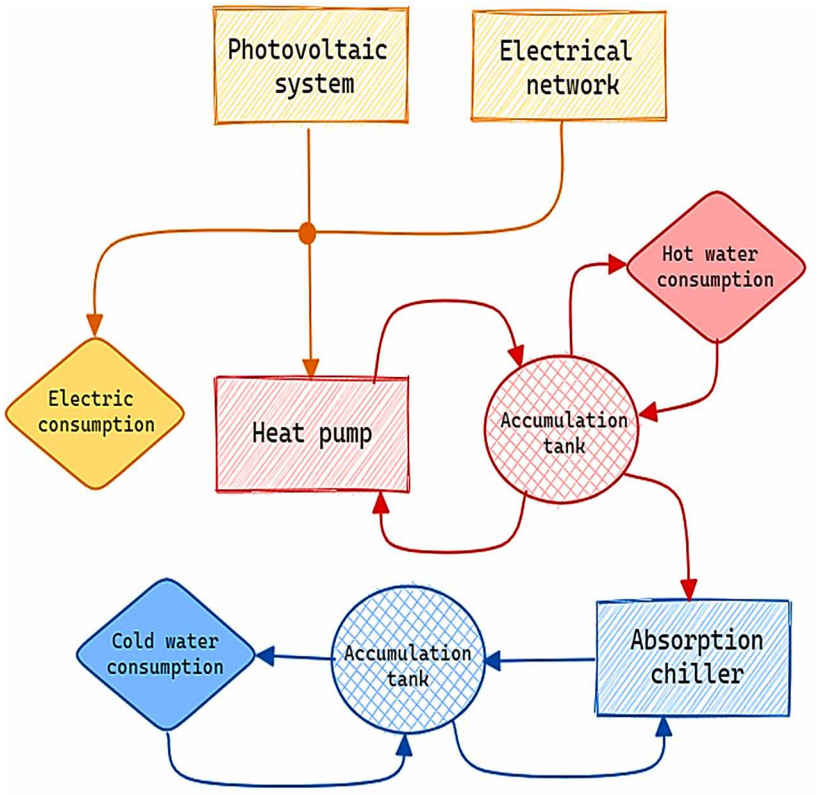

After calculating the heat pump, the consumption adjustments were made due to its installation's predicted increase in efficiency. The hospital is situated in a high-temperature region with few variations, so the COP was considered as 4 for the heat pump. Therefore, comparing the pump's COP of 4 to a COP of 1 for the electric showers and COP of 3 for the air-conditioning units [10], considering the absorption chiller's performance losses, the electric energy consumption reduction calculated was approximately 11.22%.

From the results found in electric energy consumption, an on-grid photovoltaic system was dimensioned to supply the hospital's mean consumption. The system was empirically dimensioned by Excel sheets and generation and performance calculation guidance from the literature [11,12]. The system's dimensioning considered solar irradiation from the zone according to solarimetric data from CRESESB of 5.99 kWh/m², day [13], total system performance of 0.8 [11, 12]. Table 2 describes the photovoltaic generator.

After dimensionalizing the system, equipment market prices were consulted for photovoltaic and heat pumps [14,15]. The photovoltaic system projected has a foreseen value of R$ 91,312.63, and the two heat pumps have a total value of R$ 69,139.80. Based on the initial investment cost and calculating the economy of annual electric energy by the polygeneration system, the payback time and the value of VPL and TIR were calculated. For the energy economy calculus, the study considered the Brazilian law 14.300 for regulating the distributed generated energy and energy taxes indicated by ANEEL [16] for the place in concern. The annual loss predicted in performance was also considered for the modules, the country's inflation, and the energy inflation projected based on last year's average.

Table 2. Primary data – projected Photovoltaic System.

Electric energy average consumption. (kWh/day)	200.18
Average HSP (CRESESB) - (kWh/day)	5.99
Assumed performance	0.80
Theoretic power of the photovoltaic generator	41.77
Module power (kWp)	0.55
Minimum number of modules	76
Total power of Photovoltaic Inverters (kW)	37.5
Total power with the modules (kWp) - updated	41.8
Number of modules	76

Results and Discussion

According to developed calculations, the proposed system can supply the current hospital demand for electric, hot, and cold thermal energy from the macro module of polygeneration.

The heat pump was dimensioned to meet the maximum thermal load of the electric showers, although it has a COP value of 4 times the estimated COP for electric showers. It enables supplying the thermal load demanded and projected but with an electric energy consumption of only 25% of that electric showers consume.

The heat pump can elevate the water temperature to 80ºC, which is compatible with the operating range of the absorption chiller. The assumed absorption chiller power of 50 kW is also superior to the hospital's thermal peak of 31.66 kW in February, which indicates the possibility of meeting the peak power with a relative operating slack. The total COP calculated for the cold thermal set was 3.24, considering the series connection of the heat pump, the absorption chiller, and the accumulation tanks. The set COP is approximately 8% bigger than the current air-conditioning units' COP.

By calculating the predicted energy generation for the photovoltaic system throughout the year, according to the solar irradiation variability during the year, a mean generation of 6097.51 kWh/month was determined, which is larger than the mean has foreseen hospital consumption of 6088.67 kWh/month with the polygeneration system. That indicates that the system can supply to the maximum its energetic compensation through the distributed generation, bringing the hospital an investment financial return. The hospital can operate with a concessionary network during low solar generation hours. Figure 2 below shows the generation consumption curves over the year.

An investment return curve was calculated for the leading equipment through the foreseen energy economy for the year and considered the annual inflation adjustments, energy inflation, TUSD - FIO B tax charging adjustments, and performance loss from the photovoltaic modules predicted by the supplier. The payback time found was 3.14, and the financial gain after 25 years was R$ 2,258,438.92. Taking the average of last year's inflation, the VPL value calculated was R$ 1,173,312.52, and the TIR was 33.75%. Figure 3 shows the returning income of the two main analyzed components.

Conclusion

The present study aimed to project a polygeneration system model for a hospital unit. According to the available parameters and developed calculations, the system can meet the hospital's energetic demands - electric, warm, and cold heat. The system presented promising results for energetic efficiency value and a reliability degree superior to the current energetic structure in the hospital. After analyzing the central polygeneration system's cost, it was possible to identify that the project is viable and thrilling regarding financial investment, with significant payback time, VPL, and TIR values.

Figure 2. Generation curve and monthly consumption.

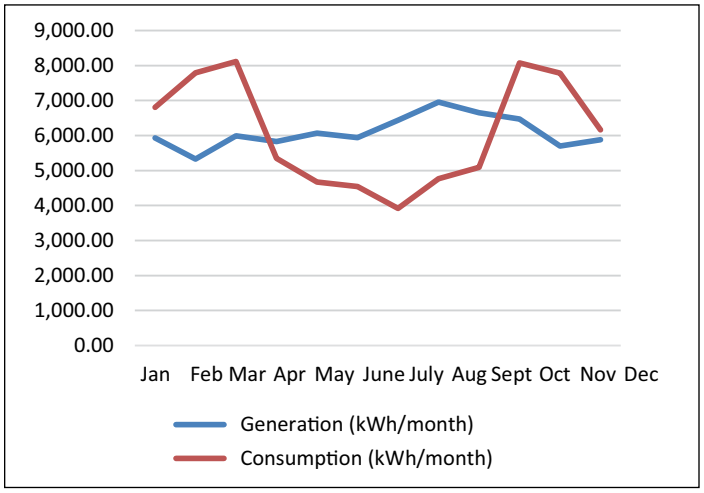

Figure 3. Financial return curve.

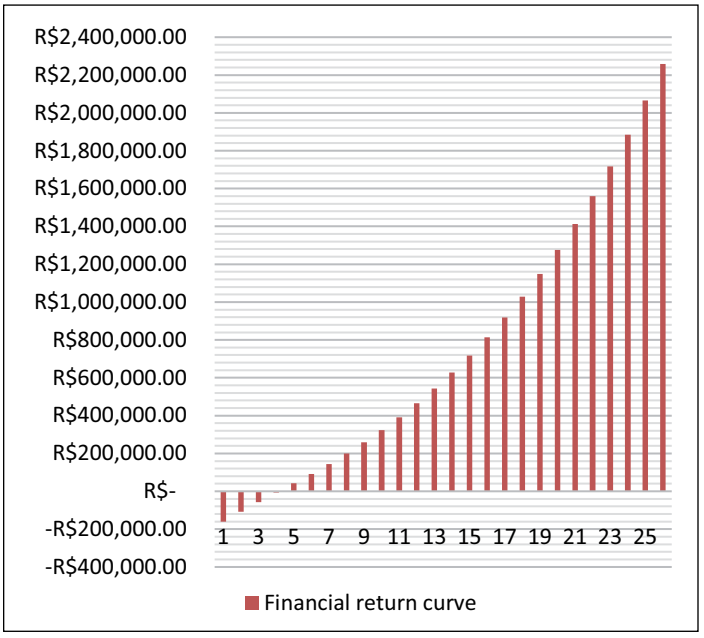

References

1. ANEEL. Relatório - Perdas de Energia Elétrica na Distribuição. Available at: <https://antigo.aneel.gov.br/documents/654800/18766993/Relat%C3%B3rio+Perdas+de+Energia_+Edi%C3%A7%C3%A3o+1-2021.pdf/143904c4-3e1d-a4d6-c6f0-94af77bac02a> Acessed on: July 31, 2023.
2. Espírito Santo DB. An energy and exergy analysis of a high-efficiency engine trigeneration system for a hospital: A case study methodology based on annual energy demand profiles. Energy and Buildings 2014;76:185-198.
3. Pina EA et al. Opportunities for the integration of solar thermal heat, photovoltaics and biomass in a Brazilian hospital. International Solar Energy Society, EuroSun 2018.
4. Calise F et al. Dynamic Simulation and optimum operation strategy of a trigeneration system serving a hospital. American Journal of Engineering and Applied Sciences 2016;9:854-867.
5. Silva HCN et al. Modeling and simulation of cogeneration systems for buildings on a university campus in

Northeast Brazil – A case study. Energy Conversion and Management 2019;186:334-348.
6. Malagueta DC et al. Análise paramétrica de uma planta CSP-ISCC de trigeração para um hospital em Bom Jesus da Lapa. V Congresso Brasileiro de Energia Solar, Recife, Brasil, 2014.
7. Absolar. Energia Solar Fotovoltaica no Brasil – Infográfico ABSOLAR; Available at: <https://www.absolar.org.br/mercado/infografico/>. Acessed on: August 1st, 2023.
8. Fischer D et al. On heat pumps in smart grids: A review. Renewable and Sustainable Energy Reviews 2017;70:342-357.
9. Kong R et al. Performance and economic evaluation of a photovoltaic/thermal (PV/T) - cascade heat pump for combined cooling, heat and power in tropical climate area. Journal of Energy Storage 2020;30(101507).
10. Melo DSC et al. Simulação de um sistema solar combinado em um hospital localizado no semiárido do nordeste brasileiro. Revista Desafios 2023;1(1).
11. Ziller R et al. Sistemas fotovoltaicos conectados à rede elétrica. Oficina de Textos 2012.
12. Pinho JT et al. Manual de engenharia para sistemas fotovoltaicos. CEPEL – CRESESB, 2014.
13. Cresesb. Potencial Solar – SunData v 3.0; Available at: <http://www.cresesb.cepel.br/index.php?section=sundata&>. Acessed on August 1st, 2023.
14. LG. Therma V R32 Monobloco LG. Available at: <https://www.rolearmais.pt/uploads/product_documents/Folheto_THERMA_V_R32_Monobloco_v3_a.pdf>. Acessed on August 1st, 2023.
15. Altus Equipamentos. Simulação de orçamento de sistema fotovoltaico para unidade hospitalar. Available: https://www.altusequipamentos.com.br/Acessed on: August 15, 2023.
16. ANEEL. Base de Dados das Tarifas das Distribuidoras de Energia Elétrica. Available at: <https://portalrelatorios.aneel.gov.br/luznatarifa/basestarifas#!>. Acessed on: August 15, 2023.

Biomass from Beached Algae of the Genus *Caulerpa* to Obtain the Alkaloid Caulerpin

Tiago Tosta Alves Cruz[1*], Jailson Bittencourt de Andrade[1], Sabrina Teixeira Martinez[1]
[1]SENAI CIMATEC University Center; Salvador, Bahia, Brazil

Caulerpin is a molecule that has several biological activities that are extremely important and sought after in the pharmaceutical market. It is found in algae of the genus *Caulerpa*, mainly in the species *Caulerpa racemosa*. This species of algae can be found beached in the sand along the Baía de Todos os Santos (Salvador, Bahia, Brazil). This project aims to study the use of the biomass of these marginalized algae. We extracted and analyzed the algae collected alive to evaluate the presence of caulerpin and then continue the research and processing of data with beached algae. The results showed that caulerpin was identified in all extractions. Therefore, the method for extracting and analyzing caulerpin was optimized and could be used in beached algae later.
Keywords: *Caulerpa racemosa*. Marginalized algae. Biomass. Extraction.

Introduction

Bioprospecting in the seas and oceans has been paramount for the global pharmaceutical market in recent decades [1]. The marine environment constitutes an immense biodiversity of algae rich in biologically active compounds, which makes them increasingly sought after for different purposes [2]. In the context of marine natural products with pharmacological properties, caulerpin is a molecule that stands out [3].

Caulerpin is a bisindole alkaloid with an orange-red color and molecular formula $C_{24}H_{18}O_4N_2$ [3]. This molecule has several biological activities, among which antitumor, antinociceptive, anti-inflammatory, antioxidant, antifungal, and antiviral activities stand out [4]. It is found in macroalgae of the genus Caulerpa, especially in *Caulerpa racemosa*, commonly found on the Brazilian coast [5].

In addition to being located on rocky structures and even associated with other algae in the sea, *Caulerpa racemosa* can also be found on the sand due to a natural process in which tidal activity eventually causes some algae to detach from the surface, in which they are fixed, taking them to the beach [6]. Although there may be degradation of the natural product in question caused by the time the algae is in the sand, many molecules do not change, among which we can consider the alkaloids, substances often produced as a form of defense during the marginalization of algae [7]. In this sense, investing in algae biomass as natural resources for chemical innovation is imperative, especially regarding the pharmaceutical industry, such as a highly sustainable alternative that values what is considered dysfunctional [8].

Therefore, the present work aims to investigate the possibility of using biomass and adding value by obtaining caulerpin, a natural product with diverse biological activities, in algae located in the genus *Caulerpa*, through the extraction and identification of the caulerpin alkaloid in species *Caulerpa racemosa*.

Materials and Methods

The methodological stage of the project took place at the Applied Chemistry Research Laboratory (LIPAQ), where experiments were carried out with algae of the species *Caulerpa racemosa*. The live algae were collected from the coral reef via free diving at a depth of 2 meters in Baía de Todos os Santos, Salvador, Bahia, Brazil, and transported in a thermal box to the laboratory, where they were sorted, freeze-dried and crushed with sanitized scissors.

Received on 20 May 2023; revised 17 August 2023.
Address for correspondence: Tiago Tosta Alves Cruz. Av. Rua Viviane Vieira Pedreira, 21, Ipitanga, Lauto de Freitas - BA, Brazil. Zipcode: 41.706-710. E-mail: tiago.tosta@aln.senaicimatec.edu.br.

J Bioeng. Tech. Health 2023;6(3):224-226

Next, the ultrasound extraction process was carried out, adapted from Cantarino and colleagues [9]. This method was chosen because the extraction uses just a few milligrams of sample. The extraction was carried out in micro extractor flasks, where 10 mg, 30 mg, and 60 mg of crushed algae were weighed, and then 500 µL of ethyl acetate was added. Micro extractor bottles containing algae and solvents were placed in the ultrasound bath for 25 minutes. Then, 10 mg of silica was added to each extractor as a cleanup step. The extracts were filtered into the bottles with a filter in their structure, thus obtaining samples analyzed on a gas chromatograph coupled to mass spectrometry (Figure 1).

After extraction, confirmation of the obtainment of the caulerpin alkaloid from the macroalga *Caulerpa racemosa* was carried out using a gas chromatograph coupled to a Shimatzu mass spectrometer (GCMS-QP2020 SE) equipped with an OAC-20i automatic sampler and a DB-5 column (30 m × 0.25 mm ID, 0.25 µm film, Agilent, Waldbronn, Germany). The chromatographic conditions were: after 1 minute at 220 °C the temperature was increased by 5 °C min^{-1} to 300°C and maintained at 300°C for 20 minutes. A 1 µL sample aliquot was injected in splitless mode at 290°C. High-purity helium (99.999%, White Martins, Brazil) was used as carrier gas at a column flow rate of 1.40 mL min^{-1}. The mass spectrometer was operated in electron ionization mode (EI, 70 eV). The ion source and transfer line temperature were maintained at 250 ◦C and 280 ◦C, respectively. Identification was performed by comparing the retention time and fragmentation pattern with the caulerpin pattern (Figure 2).

Results and Discussion

Initially, the extraction process took place with algae that were not beached to ensure that the caulerpin would be obtained. That being said, in all extractive processes from different masses of algae (10 mg, 30 mg, and 60 mg), it was possible to observe in the total ion chromatogram the peak referring to caulerpin, confirmed by comparing the retention time and the spectrum of masses with the standard and literature data [10]. Among the three extractions, the method starting with 10 mg of algae was chosen to continue the analysis as it uses the smallest sample (Figure 2).

In the mass spectrum, it is possible to observe the molecular ion peak as the base peak of the spectrum at m/z 398. The fragments referring to successive losses of methanol (MeOH) and carbon monoxide (CO) at m/z 366 (M - MeOH), m/z 338 (366 – CO), m/z 306 (338 – MeOH), and m/z 278 (306 - CO), referring to successive breakdowns of the caulerpin molecule [10].

Once the obtainment of caulerpin has been confirmed and the extraction process has been optimized, the methodology must be applied to

Figure 1. Microextraction of the algae *Caulerpa racemosa*.

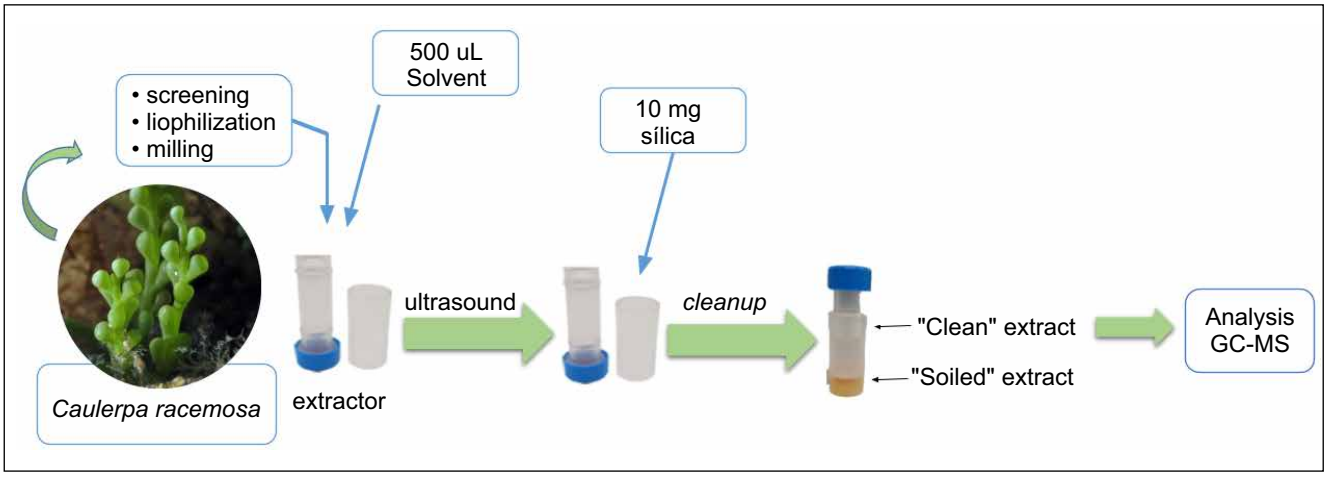

Figure 2. Total ion chromatogram and mass spectrum of caulerpin.

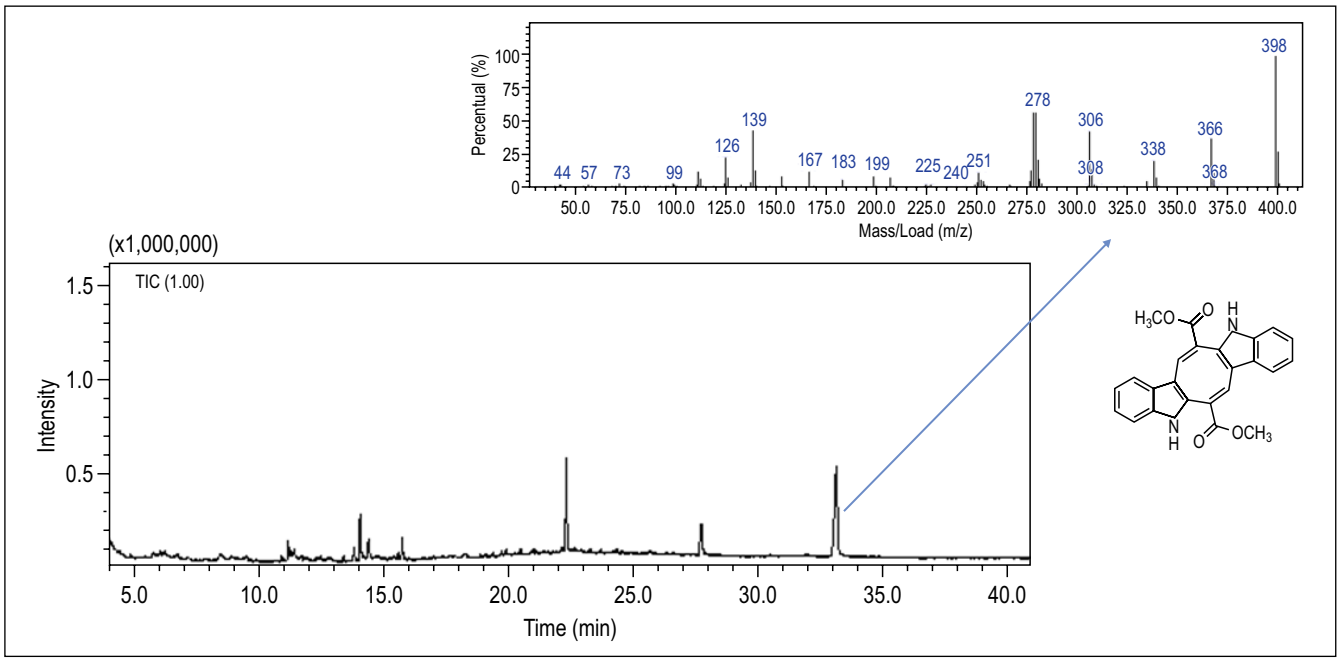

beached algae found along the Baía de Todos os Santos.

Final Considerations

From the analysis of the results obtained, it was possible to conclude that the methodology for extraction and analysis of caulerpin was optimized. This fact occurred by visualizing the total ion chromatogram and the mass spectrum generated. The molecule was identified in the three extractions carried out, each with different masses of algae (10 mg, 30 mg, and 60 mg), which were carried out quickly.

In this way, the project can be continued using the extraction methodology from beached algae and then research the use of the biomass of these algae.

References

1. Felício R et al. Bioprospecção a partir dos oceanos: conectando a descoberta de novos fármacos aos produtos naturais marinhos. Ciência e Cultura 2012;64:39-42.
2. De Alencar DB. Bioprospecção e atividade biológica de produtos naturais das algas marinhas vermelhas Pterocladiella capillacea e Osmundaria obtusiloba. Tese da Universidade Federal do Ceará, 2016.
3. Castro GMFA. Preparação de derivados da caulerpina e avaliação dos seus efeitos citotóxicos e microbiológicos. Tese da Universidade Federal da Paraíba, 2017.
4. Sousa JCF. Semi-síntese de novos derivados da caulerpina e avaliação da atividade leishmanicida do ácido caulerpínico. Tese da Universidade Federal da Paraíba, 2016.
5. Tavares DS. Theoretical study by PM6 of ions complexes type [M (1, 10-fen) 2 L] 2+ with biologic activity potential, where L= caulerpina. Resumo da 34a Reunião Anual da Sociedade Brasileira de Química, Florianópolis 2011.
6. Nova LLMV et al. Utilização de "Algas Arribadas" como alternativa para adubação orgânica em cultivo de moringa (*Moringa oleifera* Lam.). Revista Ouricuri 2014;4:68-81.
7. Harb TB et al. An overview of beach-cast seaweeds: Potential and opportunities for the valorization of underused waste biomass. Algal Research 2022;62:102643-102661.
8. Galembeck F et al. Aproveitamento sustentável de biomassa e de recursos naturais na inovação química. Química Nova 2009;32:571-581.
9. Cantarino SJ et al. Microwave irradiation is a suitable method for caulerpin extraction from the green algae *Caulerpa racemosa* (Chlorophyta, Caulerpaceae). Natural Product Research 2022;36:2149-2153.
10. Aguilar-Santos G. Caulperpin, a new red pigment from green algae of the genus Caulerpa. Journal of the Chemical Society C: Organic 1970:842-843.

Comparison of Primary Energy Consumption Between Additive Manufacturing Processes and CNC Machining Applied to Components in the Oil and Gas Sector

Joyce Mara Brito Maia[1*], Samuel Alex Sipert Miranda[1], Rodrigo Santiago Coelho[1]
[1]SENAI CIMATEC University Center; Salvador, Bahia,Brazil

This work elucidates the environmental impact on the production of components in the oil and gas sector by analyzing two different production routes. To this end, a life cycle assessment of the CNC machining process and additive manufacturing (AM) was carried out using Multi Jet Fusion (MJF) technology. Life cycle inventories were prepared for both processes, using the Open LCA software and information from the Ecoinvent database to develop the life cycle, with Cumulative Energy Demand (CED) being considered as the impact method. From the analysis, it was found that the machining process presented an energy demand of 7177 MJ. In contrast, the MJF presented 3214 MJ, less than half of the primary energy required to produce one unit of the studied component, thus indicating that manufacturing by MJF presents greater environmental sustainability than the conventional machining process.
Keywords: Oil and Gas. Machining. Additive Manufacturing. Environmental Impacts.

Introduction

The rise of Industry 4.0 and the technological development in the production sector awakened productivity linked to sustainability. This factor changed the way of analyzing the performance of the production system. Before, factors such as cost, time, quality, and flexibility were considered. However, robust global trends such as climate change have changed how performance is analyzed by including sustainability in all phases of the decision-making process.

Over the years, research into technologies that enable production with significant gains, reduced material used, improved customization, and reduced product availability time on the market has increased [1]. Thus, additive manufacturing (AM) emerged in this scenario, subsequently being considered an ally in reducing environmental impacts by generating less waste of raw materials and fewer emissions than other more traditional processes.

Received on 12 May 2022; revised 18 August 2023.
Address for correspondence: Joyce Mara Brito Maia. Av Professor Theocrito Batista 1260, CD Solaris 1, Casa 17,Caji, Lauro de Freitas; Bahia,Brazil. Zipcode: 42.721-890. E-mail:joyce.maia@aln.senaicimatec.edu.br.

J Bioeng. Tech. Health 2023;6(3):227-229

For the most part, components in specific sectors, mainly oil and gas, are manufactured using conventional processes, such as machining, forging, or casting, and are often manufactured outside the country, which generates more significant costs and impacts due to imports. The choice for conventional processes is due to the reliability and maturity of the processes since most of these components are high risk. The oil and gas industry's adoption of AM makes a significant contribution to the supply chain, as manufacturing using this process can be done with little human supervision, more quickly, and using geometries considered complex [2]. Furthermore, it is possible to contribute to reducing environmental impacts during the component production process.

However, analysis of how much the replacement of conventional processes with AM applied to the oil and gas sector contributes to reducing or generating environmental impacts still needs to be explored. As a result, this work aims to investigate the environmental sustainability of AM when applied to the oil and gas sector in the production of a camera housing used in underwater robots, with specific objectives: identifying process parameters and data, carrying out assessment life cycle considering the conventional process and AM and analyzing the results found for the investigated impact method.

Materials and Methods

The work method was based on the life cycle assessment of a camera housing used on underwater robotic platforms for the oil and gas sector.

The component was produced in conventional manufacturing using the CNC machining process and in AM using Multi Jet Fusion (MJF) technology. When manufactured by machining, Al alloy 6061 was used, weighing 6.15 kg in the end and requiring 62 screws for assembly, while when produced by MJF polyamide 12 (PA 12) was used, weighing 1.82 kg in the end and requiring just 4 screws for assembly. All processing data specific to machining and AM were identified for the life cycle assessment. The cradle-to-gate range was used, considering the impacts generated from the raw material's production to the component's final production, excluding usage impacts. The life cycle inventories were modified considering the use of 28 kg of Al alloy, 0.08 kg of oil, and energy consumption of 183.2 kWh for machining a camera housing unit, while for MA by MJF. It was achieved using 4.1 kg of virgin PA 12, 16.3 kg of recycled PA 12, 0.13 kg of fusing agent, 0.09 kg of detailing agent, and an energy consumption of 73.1 kWh. The Open LCA software was used with data extracted from the Ecoinvent database, and the Cumulative Energy Demand impact method (CED) was used for the life cycle impact assessment (LCIA) to construct inventories and calculate life cycle impacts, so it is possible to obtain information on the primary energy demand linked to production.

Results and Discussion

The results obtained for the CED impact method show a lower need for energy demand on the part of the AM using the MJF technology, with 7177 MJ being the energy demand of the CNC machining process and 3214 MJ the energy demand of the MJF (Figure 1). Some Studies indicate that material and energy consumption represent the most significant consumption among the processes in the component production system, which are the biggest generators of environmental impact [3].

The CED method is an indicator used as a parameter of energy efficiency and monitoring for the environmental impacts of processes. It compares the demand for primary energy when applying an LCA study [4]. Based on the result of the graph, it is clear that the technology of MJF has a lower CED impact than machining due to its more energy-efficient production process and lower material waste.

When checking the energy demand of machining, it is possible to identify aluminum production as the most significant contributor to environmental impacts, which can be justified by the fact that even though the Brazilian energy matrix is based mainly on hydroelectric plants, the aluminum alloy used is of origin primary, not presenting a reduction

Figure 1. CED category result for CNC and MJF machining.

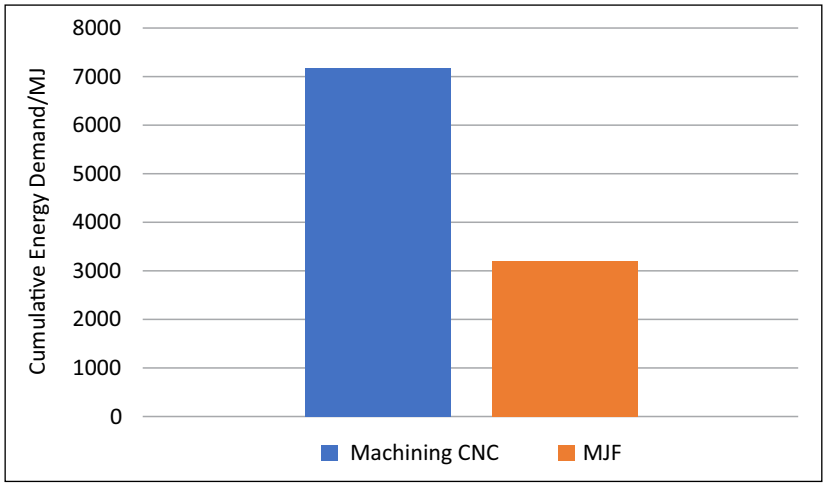

in impacts due to the recycled portion. Figure 2 shows the percentages inherent to the production of the functional unit through machining in (a) and through MJF in (b).

On the other hand, the energy demand of the PA 12 production process, the most significant contributor to the impacts of CED by MJF, is not even more significant because its proportion of use involves 80% of reused powder, dissipating the environmental impact generated by the production of the material -cousin. The energy demand for the production of PA 12 may have a high contribution due to the powder production process having the possibility of involving precipitation or direct polymerization [5]. However, even with this factor, the energy demand of MJF for the production of the camera housing has a lower value than half of that used in CNC machining.

Final Considerations

The use of AM technologies by some sectors can generate several application advantages and, in some cases, reduce environmental impacts compared to specific processes used for years. Thinking about the greater adoption of AM by the oil and gas sector and alignment with impact reduction initiatives and frameworks with companies that care about the sustainability of their processes and activities, this study analyzed the demand for primary energy for a manufactured component by machining and by MA using MJF technology. AM, using MJF technology, generated lower impacts than CNC machining when analyzing the CED method, indicating that MJF technology is a more environmentally sustainable option than machining regarding accumulated energy demand.

Acknowledgments

We thank to the National Petroleum Agency for the scholarship and financial assistance.

References

1. Almeida AM. Principais barreiras para a implementação para a manufatura aditiva no Brasil. 2019. 83 f. Dissertação (Mestrado) - Curso de Mestrado em Engenharia de Produção, Universidade Nove de Julho - Uninove, São Paulo, 2019.
2. Wooldridge M et. al. Applications of metal additive manufacturing in the oil and gas industry. Offshore Technology Conference, 4th May. 2020.
3. Peng T et al. Sustainability of additive manufacturing: an overview on its energy demand and environmental impact. Additive Manufacturing 2018;21:694-704.
4. Guanais ALR, Cohim EB, Medeiros DL. Avaliação energética de um sistema integrado de abastecimento de água. Engenharia Sanitária Ambiental 2017;22(6):1187-1196.
5. Sschmid M et al. Influence of the origin of polyamide 12 powder on the laser sintering process and laser sintered parts. Applied Sciences 2017;5:1-15.

Figure 2. Percentage of participation in manufacturing processes for the CED category:(a) Participations in machining and (b) Participations in MJF.

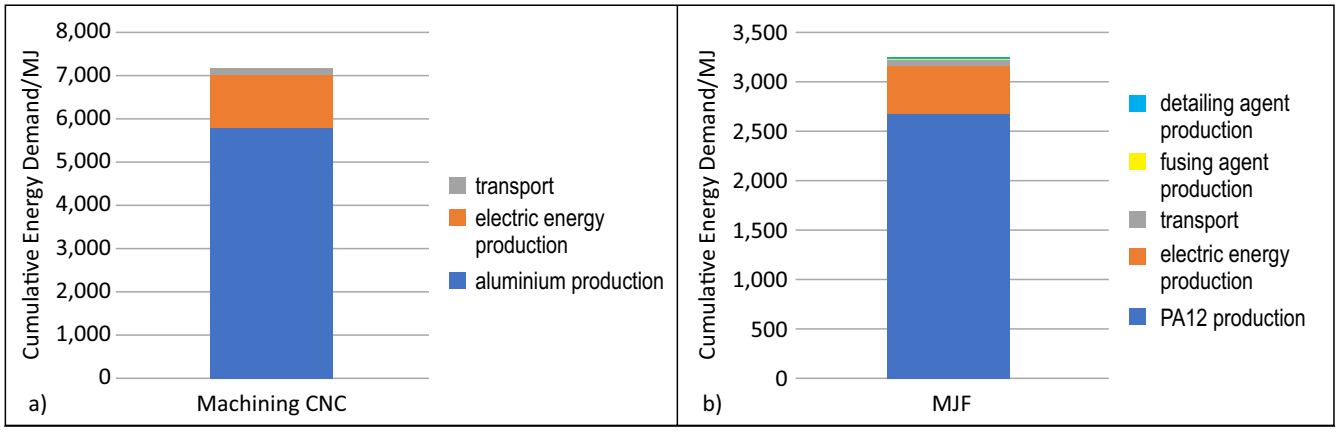

Cloud Computing Application for Digital Integration Between an Advanced Manufacturing Plant and a Model 4.0 Factory

João Vitor Mendes Pinto dos Santos[1*], Thamiles Rodrigues de Melo[2]
[1]SENAI CIMATEC University Center; Salvador, Bahia, Brazil

Industry 4.0 is a global digitalization goal for today's industries, and cloud computing is a solution that enables ubiquitous and convenient access to infrastructure, platforms, and services. Together with fog and edge computing, it leverages the advantages of manufacturing systems integration. This research proposes a cloud architecture to integrate an advanced manufacturing plant and a SENAI CIMATEC model factory. Before implementing this architecture, assessing whether the environment is adaptable is necessary. For this, fundamentals such as the TOE structure (Technology-Organization-Environment Framework) and the SEM model (Structural Equation Modeling) are used, which evaluate the degree of adherence for the application. As a methodological procedure for the research, a database is being modeled to serve the information flow between the systems. Therefore, adapting the environment to cloud computing is crucial to the success of digital system integration and process automation and optimization advances.
Keywords: Cloud Computing. Industry 4.0. Structural Equation Modeling. Database.

Introduction

The integration of manufacturing systems in Industry 4.0 has been widely adopted in different industrial sectors. It allows the connection of various production systems, including equipment, computational tools, and data management systems, to work more efficiently and effectively, aiming to improve productivity, reduce costs, and increase flexibility and agility in the production process [1]. For this integration, cloud computing is one of the technological pillars of Industry 4.0 that enables remote access to data from different processes. This computing paradigm enables ubiquitous, convenient, on-demand access to a shared network of configurable infrastructure, platforms, and service resources [2].

However, challenges are emerging, such as reducing latency between the cloud and production equipment. To solve this problem, new paradigms, such as fog computing and edge computing, have emerged. Fog computing is an extension of cloud computing to the edge network, providing services around devices close to the user, such as routers, instead of sending information to the cloud. In turn, edge computing provides services close to the data source to meet critical requirements in agile connectivity and intelligent applications [2].

In this context of system integration on a didactic scale, there is the advanced manufacturing plant (PMA), an automated production line that uses several cyber-physical systems to produce pneumatic actuators, generating a large amount of data about the production process. On the other hand, the model factory produces pistons from these actuators, but it does not have an automated system, relying only on a process management system.

This research aims to digitally integrate the systems of the advanced manufacturing plant and the model factory, following a customer-supplier proposal, to enable greater ease in the ordering process, agility in production, and traceability of ordered parts.

Theoretical Foundation

The TOE (Technology-Organization-Environment Framework) framework is a conceptual framework used to analyze the adoption of technologies in an organization. The SEM

Received on 15 May 2023; revised 10 August 2023.
Address for correspondence: João Vitor Mendes Pinto dos Santos. Avenida Orlando Gomes, 1845, Piatã. Salvador, Bahia, Brazil. Zipcode: 41650-010. E-mail: joao.v.m.p.santos@ieee.org.

J Bioeng. Tech. Health 2023;6(3):230-233

(Structural Equation Modeling) model is a statistical technique used to model the loading factor that represents the relevance of relationships between exogenous observable variables; i.e., variables external to the model represent its inputs. On the other hand, latent variables are endogenous variables that are not directly observed but are determined within the model and use observable variables as indicators. The following variables can be considered when applying the TOE framework with SEM models for adopting cloud computing: technological, organizational, and environmental (Figure 1). The the relationships between these variables and identifying those that have the greatest impact on the adoption of cloud computing services are possible by using the TOE framework in conjunction with the SEM model [3].

Kandil and colleagues [4] identified the best criteria for analyzing the adaptability of cloud computing by applying the SEM model. During the investigation, the authors reviewed several articles on adopting TOE focusing on cloud computing and selected the following variables as research instruments (Figure 2)

Among them, there are the following:

- Relative advantage, complexity, compatibility security, and trust in the context of technology;
- Management support, technological readiness and maturity, and performance issues in the context of the organization;
- Competitive pressure, telecommunications infrastructure, internet service provider, business partner support and business partner pressure in the environment.

Materials and Methods

After analyzing the TOE structure, digital integration between the advanced manufacturing plant and the model factory is proposed through a cloud architecture, which could be SaaS (software as a service), IaaS (infrastructure as a service), or PaaS (platform as a service) depending on the type of connection desired between the systems. A cloud database will be built synchronized with local data from both production systems to achieve this point. Based on the customer-supplier proposal presented in Figure 3, the operator of the model factory, as a customer, will be able to send requisitions and orders in the cloud, which will be processed and approved by the operator of the advanced manufacturing plant to start production there as a supplier. This way, optimizing the ordering and production process, guaranteeing the traceability

Figure 1. TOE framework for cloud computing adoption.

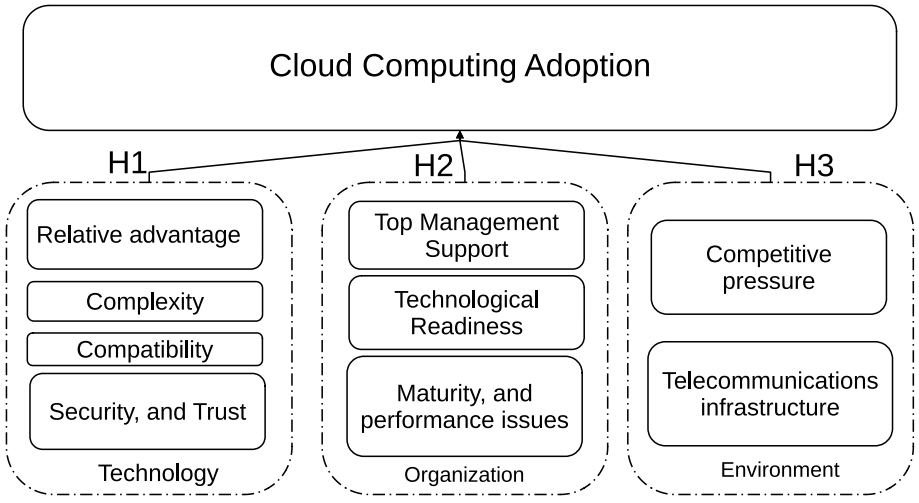

Figure 2. Example of an SEM model applied to the TOE criteria (technology).

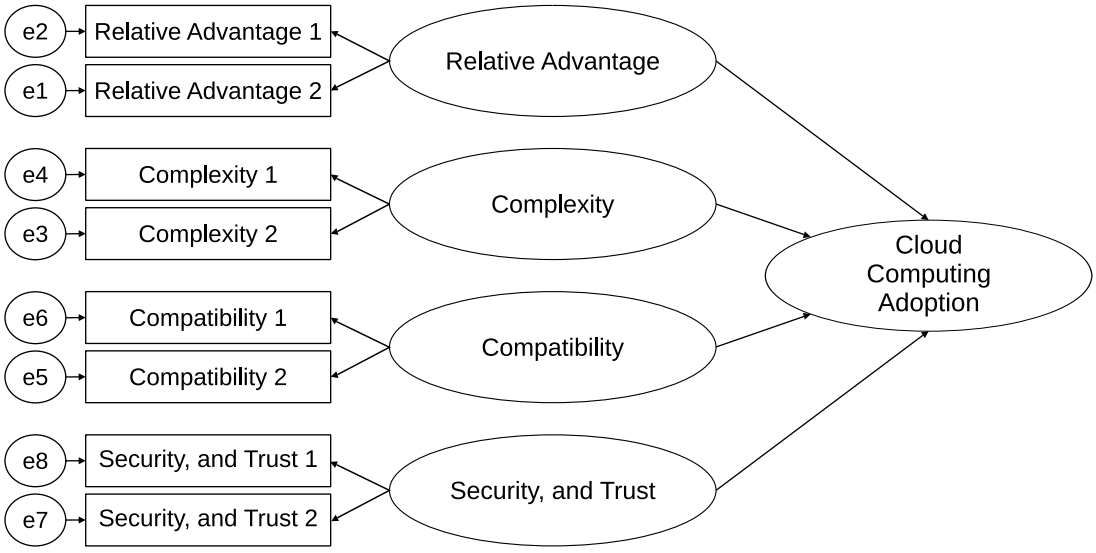

Figure 3. Proposal for integration between the model factory and PMA in the context of cloud computing.

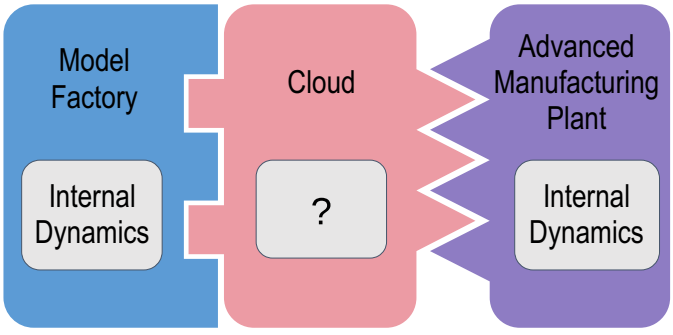

of ordered parts, and increasing production agility will be possible.

The construction of a database follows a sequence of steps inspired by the work of Date [5]. The first step is the analysis of the system requirements, where all the database's needs are identified. In the second stage, the conceptual project is carried out, where concepts and entities and their relationships are defined. In the third stage, the logical project is created, transforming the conceptual project into tables and columns of a relational data model. Finally, the database is implemented in the last step, creating the tables and columns defined in the logical project. This way, a database will be modeled that covers the entire data flow between the advanced manufacturing plant and the model factory (Figure 4).

Final Considerations

The following steps of this project consist of advancing the TOE framework to numerically evaluate the adaptability of cloud computing for data integration between the advanced manufacturing plant and the model factory. Data will be collected, and the best way to obtain the SEM model will be assessed through ordinary least squares or generalized least squares estimation. A cloud architecture will be set up based on a requirements survey to carry out integration between the parties to verify what type of service will be needed and which computational tools will be most appropriate. Finally, the cloud service will be implemented, following the defined architecture, to enable digital connection between production systems.

Figure 4. PMA and model factory data flow diagram.

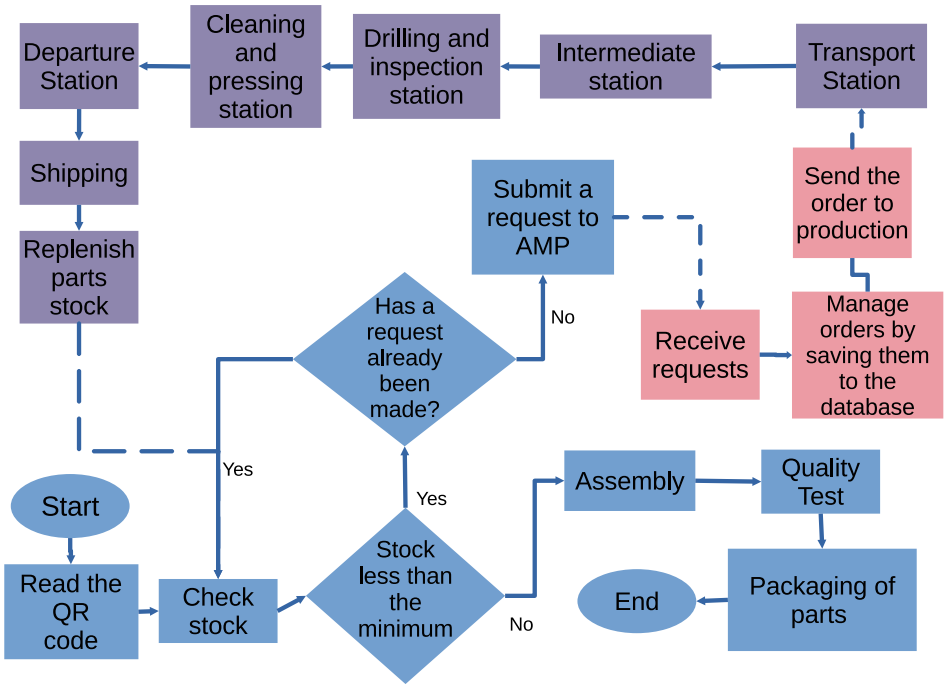

Acknowledgments

The authors thank the Fundação de Amparo à Pesquisa do Estado da Bahia (FAPESB) for the financial support in carrying out this research.

References

1. Paz ACM, Loos MJ. A importância da computação em nuvem para a indústria 4.0. Revista Gestão Industrial v. 2000;16(2).
2. Qi Q,Tao F. A smart manufacturing service system based on edge computing, fog computing, and cloud computing. IEEE Access 2019;7:86769–86777.
3. McKinnie M, Cloud Computing. TOE adoption factors by service model in manufacturing. Dissertation, Georgia State University, 2016. Doi: https://doi.org/10.57709/8571911.
4. Kandil AMNA, Ragheb M, Ragab A, Farouk M. TOE model on cloud computing adoption in Egypt. The Business & Management Review 2018;9(4):113–123.
5. Date CJ. Introdução a sistemas de bancos de dados. [s.l.] Elsevier Brasil, 2004.

Application of Generative Autoencoders in the Detection of Anomalies in Hypercompressors

Zoroastro Fernandes Filho[1*], Alex Álisson Bandeira Santos[1]
[1]SENAI CIMATEC University Center; Salvador Bahia Brazil

Hypercompressors are essential assets that compress high-flow-rates of ethylene to pressures between 100~350 MPa in the LDPE industry. They are sources of essential risks and costs. This work proposes an unsupervised and univariate monitoring method for detecting anomalies in hypercompressors through data collected from an online monitoring system in an actual installation. A variational autoencoder learns the process of generating shapelets associated with vibrational patterns. A combination of matrix profile algorithms automatically selects the training data set. A *β*-VAE composed of MLP layers is trained and applied on the input space so that a voting operation and a box-cox transformation on the absolute residual errors between the inputs and outputs lead to the upper outlier detection threshold, obtained by the Tukey fence method. The model detected suspicious vibration patterns classified a priori as potential anomalies.
Keywords: Hypercompressors. Matrixprofile. *β*-VAE. Anomalies.

Introduction

The polymerization of low-density polyethylene (LDPE) is processed on an industrial scale under temperatures of 200 to 300 °C and pressures of 100 to 350 MPa, achieved through the compression of ethylene by special reciprocating compressors (hypercompressors, occasionally also called secondary compressors). Modern LDPE mega plants are equipped by hypercompressors with capacities of up to 400 kNm³ and 33,000 kW [1]. Due to the flammability and high pressures involved, potential risks are inherent in this process, and thus, these machines are sources of essential risks and costs for the LDPE industry. The development of anomaly detection methods based on monitoring data is essential.

According to Park and colleagues [2], a large amount of data, and appropriate sampling rates, becomes mandatory for an acceptable mathematical model of a hypercompressor. There are some examples of conventional reciprocating compressors in the literature, but it is rare for hypercompressors [3,4]. The principal component analysis (PCA) is widely used among the techniques available for creating models. Considering LDPE plants, according to Park and colleagues [2], some researchers have developed fault detection models based on PCA to predict dangerous thermal decomposition reactions due to sudden compression or excess peroxide injection that occur in autoclave reactors of LDPE plants [5,6]. However, the theoretical assumption of the classical PCA transformation, assuming linearity and projecting the data into a low-dimensional latent space, may need to fit better with the nonlinear nature of vibrations typically monitored in reciprocating compressors in general. We propose the application of a variational autoencoder (VAE) to overcome this limitation.

According to Sivalingam and colleagues [7], while a classical autoencoder (AE [8]) learns to make predictions from some observations, the variational autoencoder (VAE [9]) learns to simulate the data generation process. An essential effect of VAE is the possibility of revealing a potential understanding of the inherent causal relationships of the input data entangled in the latent space, providing a better generalization of the data and not only considering time-variant or invariant data. In this way, VAE allow its application in monitoring

Received on 19 March 2023; revised 24 May 2023.
Address for correspondence: Zoroastro Fernandes Filho. Avenida Orlando Gomes, 1845, Piatã. Salvador, Bahia, Brazil. Zipcode: 41650-010. E-mail: zorofernandes@hotmail.com.

stationary or non-stationary processes, typically displayed in monitoring hypercompressors.

The data used in this work consists of 36 vibration variables (for each hypercompressors cylinder) and the motor's electrical current. A set of operating data considered "non-suspicious" was automatically selected by a method composed of an algorithms combination based on matrixprofile (MP) [10] and MP snippet [11]. Then, a β-VAE [13] was trained, and the latent space obtained by the encoder and the residual error about the encoder inputs led to the threshold of outliers, discriminating "suspicious" vibratory patterns from "normal" ones through a box-cox transformation combined with the "Tukey fence" method [14]. The extracted suspicious patterns were classified as potential anomalous cylinder vibration shapelets [15]. Data sampling (~ six continuous months) was performed every minute, starting from an online vibration monitoring system in an actual installation.

Materials and Methods

Process Description

Figure 1 describes the LDPE production process (autoclave reactor) in a simplified way. Before bagging the pellets, LDPE is produced in three stages: Compression, Reaction, and Extrusion. First, the ethylene is compressed sequentially by the two compressors (primary and secondary), reaching the reaction pressure. In the reactors, in addition to ethylene, a reaction initiator is also injected, up to a maximum of 350 MPa, and thus the polymerization reaction is initiated. Ethylene gas is the primary raw material. The compression section requires most of the energy of the production process, and the hyper compressor is the leading equipment in the chain described here.

Sensor Location and Compression Cycle

An accelerometer measures the impacts occurring in the intermediate body, those resulting from the inertia of the parts, and the loads arising from the effort to compress the gas ([Figure 2 (side view of a hyper compressor cylinder)].

With each rotation of the shaft (360°), starting from the Top Dead Center (TDC), the compression cycle is divided into four stages: 1) 0° to 25° – re-expansion, followed by the opening of the suction valve, 2) 25° to 180° – suction, followed by closing the suction valve, 3) 18° to 290° – compression, followed by opening the discharge valve and 4) 290° to 360° – expansion, followed by closing the discharge valve.

Figure 1. LDPE: Gas flowchart.

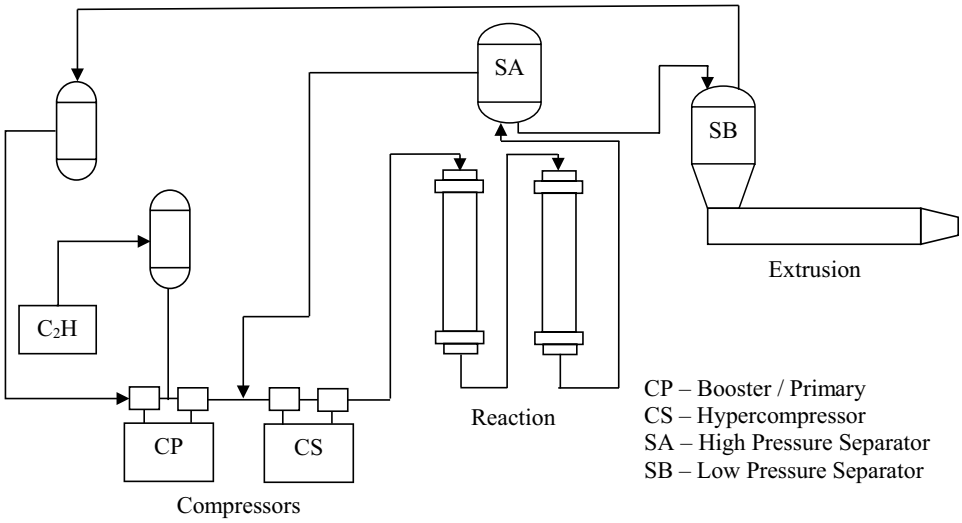

Figure 2. Hypercompressor – Accelerometer location.

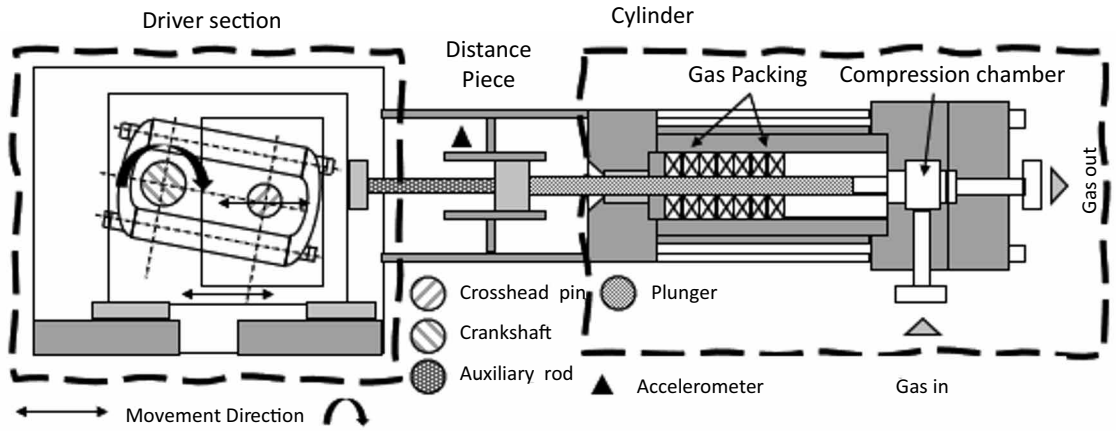

Each shaft rotation triggers a phase sensor, which is not shown in the Figure.

Dynamic Patterns (shapelets)

Vibration (acceleration) data is available in the Root Mean Square (RMS) metric and collected at sampling rates of the order of 20 kHz. The RMS values are measured and calculated in segments, following time intervals relative to each 1/36th crankshaft rotation every minute. Each measured segment is stored in a database. Thus, typical vibration patterns at each shaft turn, composed of 36 segments (shapelets), emerge as objects of investigation (Figure 3). The numbering of the segments in the figure corresponds to the angular movement of the crankshaft shaft, which corresponds to 10-degree angles.

Each segment is monitored as a univariate time series in the collected data. The shaft rotation speed is approximately 200 RPM. The compressor has eight cylinders and two stages, four in each, labeled 1-1A, 1-1B, 1-2A, 1-2B for the 1st stage, and 2-1A, 2-1B, 2-2A and 2-2B for the 2nd stage (Figure 4).

Monitored Variables and Database

In this work, the data from the monitored segments were rearranged sequentially and displayed into a univariate time series (Figure 5). The 36 time series for each cylinder were converted into a single univariate time series, referred to as RMS_Avg. The conversion provides information about the evolution of vibration patterns over time. Consequently, the final length of RMS_Avg is a multiple of 36. Data from all cylinders were used.

Table 1 shows the variables (in univariate form) monitored for 6 months.

Figure 3. Typical vibration with each turn of the shaft.

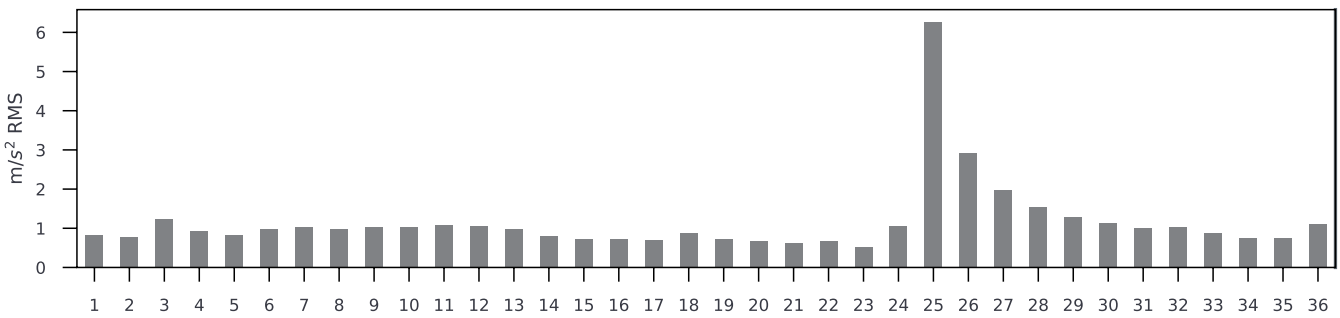

Figure 4. Physical position of the cylinders.

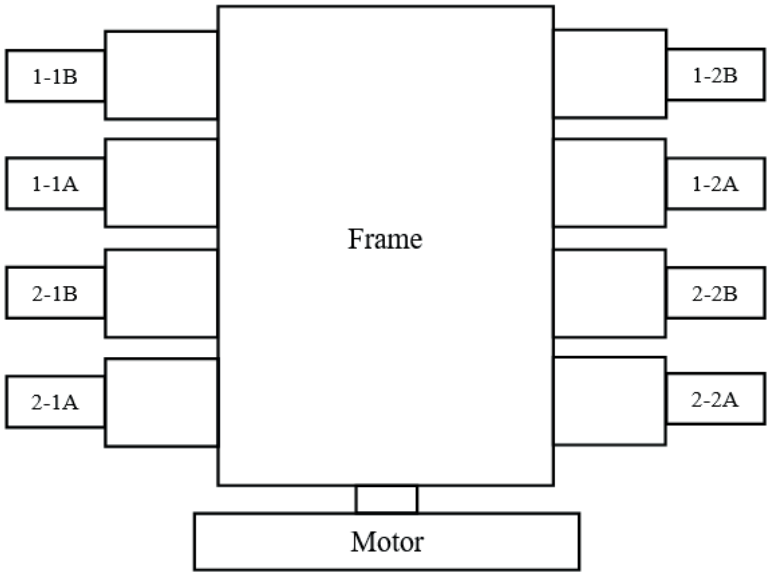

Training and Testing Data

In extensive collections of reciprocating compressor monitoring data, the challenge arises of automatically labeling the most typical and/or representative data in various operating contexts considered "normal". We proposed the use of an algorithm based on matrixprofile (MP) [10] and MP snippet to overcome this barrier, [11]. In Imani and colleagues [11], the authors demonstrated the usefulness of the MP snippet algorithm to, at a high level, seek to answer the question "*Show me some representative/typical data...*". According to the authors, despite being trivial in many domains, surprisingly, the difficulty persists in extensive data collections, given the complexity of answering what "representative/typical data" actually means. In this work, the balance in the choice of hyperparameters of the proposed algorithm is expected to maximize the probability

Figure 5. Univariate time series (RMS_Avg).

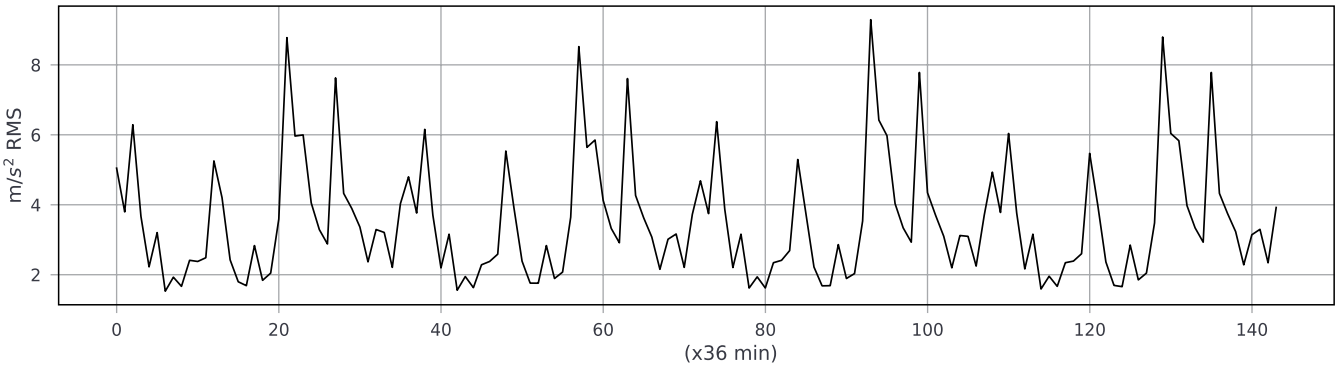

Table 1. Monitored variables.

Series	Description	Variables	Instances
RMS_Avg	Acceleration	8	32054868
Current	Electric current	1	890413

of selecting the most representative data possible for training instances.

Steps for Creating the Model

Figure 6 shows the model development steps, from cleaning the data to obtaining outliers.

Data cleaning (step 1) excludes sensor errors and removes instances with missing data and periods with vibration values above pre-defined alarms. Step 2 requires some heuristics, complementing data cleaning, excluding stop and start intervals. To this end, we selected operational periods when the motor operates above a minimum power value (electric current > 300 A), consistent with full LDPE production operational regimes.

An unusual shapelet (discord [10]) tends to have a high distance profile value (PD [10]). In the RMS_Avg series, discords are expected to be extremely rare due to the cyclic vibration patterns typical in reciprocating compressors. A "normal" shapelet (motif [10]), more common, arising in typical operational situations, tends to lower PD values. The two classes (motifs and discords) are fundamental objects in the search motors contained in MP algorithms. The idea is to use such mechanisms to select training instances.

For each cylinder, we divided the RMS_Avg series into k contiguous subseries, Figure 5, step 3, so all subseries contained only groups of 36 instances equidistant one minute apart.

In step 4 of Figure 5, the PD's, (series T') are calculated by applying the MP algorithm on each of the k separate subseries, $T = \{T_1, T_2 \dots T_k\}$, $T_i = \left\{a_1^i, a_2^i, \dots a_{p_i}^i\right\}$, $(i = 1,2,\dots k)$. The MP algorithm was applied sequentially on sections of sequential windows of length w and moving windows of length $m = 36$ on each T_i, obtaining the set of series $T_i' = \{T_1', T_2' \dots T_k'\}$, $T_i' = \left\{a'^{\,i}_{\,1}, a'^{\,i}_{\,2} \dots a'^{\,i}_{\,p}\right\}$, $(i = 1,2,\dots k)$. w and m are hyperparameters.

For step 5, the idea is to take advantage of the periodic nature of vibrational patterns and the consequent expectation of regularity (albeit relative) of these patterns in different sections of each T_i'. We applied the MP snippet algorithm on T' to reduce the probability of selecting "suspicious" shapelets as "normal". The algorithm searches each consecutive section of size w of each T_i', adopting moving windows of size m ($m = 36$), extracting its most representative shapelets. This occurrs because very sudden changes in PD values (suspicious transients) tend not to represent the fixed window considered and, therefore, not detected by the MP snippet algorithm as a training instance. The integer value Qt indicates the desired number of shapelets retrieved from each T'. The indices of the snippets retrieved in T' indicate the location of the shapelets retrieved in T. Qt is a hyperparameter.

By setting the parameter $m = 36$, we maintain the expectation that the balance between the choice of Qt and w guarantees the adequate selection of training instances. At the end of the process, $k * Qt$ indices of the T shapelets will be selected for training for each cylinder. Chart 1 shows the pseudocode described in the previous paragraphs. Data from the eight cylinders were used for training the VAE.

As an example, taking m fixed and equal to the length of the shapelets $m = 36$, the hyperparameters in Table 2 are expected to automatically select two "normal" shapelets every 30 minutes.

Intuitively, a higher value of w implies a lower probability of selecting more representative data because a smaller number of representative shapelets will be recovered for the same section of size w. The converse is accurate; however, in this case, a more significant risk is expected in selecting suspicious shapelets as more representative data because there is a greater probability of persistent suspicious values occurring, with a duration of the order of the size of the fixed window w.

A higher value of Qt implies a more significant amount of data for training; however, due to the inherent repeatability of shapelet patterns, it is expected that from a particular value of Qt onwards, an increase in the number of training instances does not necessarily imply greater capability to learn patterns..

In Figure 6, steps 6 to 10 describe the process from calculating the VAE to the threshold of outliers obtained by the Tukey fence method.

Figure 6. Steps for creating the model.

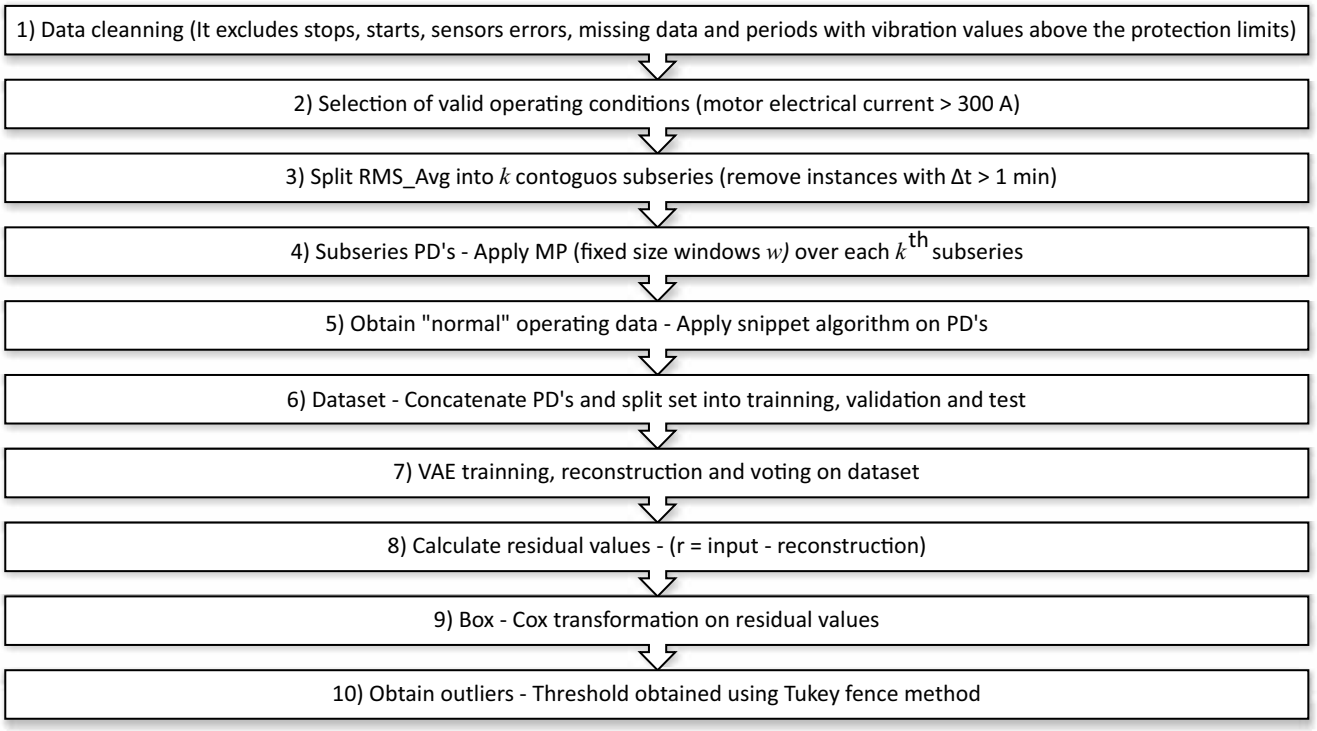

Table 2. MP hyperparameters and MP snippet.

MP				**MP snippet**					
m	36	*w*	30 min	*Qt*	2	*m*	36	*w*	30 min

<u>β-VAE and Vibration Monitoring</u>

Compressor vibration patterns are diverse, but this diversity arises from a relatively small and coherent set of mechanical properties, physical rules, construction, and operating principles. VAEs can learn representations in the latent structure of data and extract concepts based on the learned patterns.

Variations of VAEs are available in the literature. In β-VAE [13], the cost function $l(x, \hat{x})$ includes the real hyperparameter β, with $l(x, \hat{x}) = l_{rec} + \beta l_{KL}$. While the reconstruction term l_{rec} leads to the separation of points in the latent space, the second term βl_{KL} (Kulback-Leibler divergence multiplied by β) does the opposite, avoiding the learning of non-existent representations in the original data space [7]. According to the authors, β "encourages/ discourages" the disentanglement of latent variables. Table 3 shows the architecture used in β-VAE and the hyperparameters.

<u>Inference</u>

For each cylinder, we concatenate the T_i subseries and rearrange them into sequential batches of 36 units, one-time unit apart concerning the previous batch, along the entire length (size) of the concatenated subseries, obtaining a new series of sequential batches L^{obs}, of size (p_i-36, 36).

Then, the trained β-VAE reconstructed each batch contained in L^{obs}, obtaining the analogous batch series L^{rec}.

Chart 1. Pseudocode for automatic selection of VAE training instances.

	Input: $= T\ \{T_1 T_2,\ \ldots T_k\} T_i\ ,\ a\left\{ = a_1^i, a_2^i, \ldots\ a_{p_i}^i \right\}, i = 1, 2 \ldots k$
	Output: $ind\_train\_set = \{ind_1, ind_2 \ldots\ ind_n\}$, *n=1...k*Qt*
1	$ind\_train\_set = \{\}$ *// empty index set*
2	$T' = \{\}$ *// empty set of subseries*
3	***for (i=1, k, 1)*** *Do:// Scroll k (sub)subseries* T_i *calculating the PD's*
4	***for (j=1, w, w)*** *Do:// Compute the MP algorithm sequentially over* T_i *with m=36 and fixed window=*w *obtained* T_i'
5	$T_i' \leftarrow MP(ts = T_i[\,j{:}j + w + m - 1], window\_size = m)$ *// Algorithm MP according Law SM [12]*
6	$T' = T' + \{T_i'\}$ *// concatenate getting* T'
7	***for (i=1, k, 1)*** *Do:// Scroll k subseries* T_i', $T' = \{T_1', T_2', \ldots T_k'\}$
8	***for (j=1, w, w)*** *Do: // Compute the algorithm MP snippet sequentially over* T_i' *with m=36, quantity of snippets = Qt and fixed window=*w
9	$train\_set_i \leftarrow\ MP\_discover\_snippet(ts = T_i'[j{:}j + w], window = m, num\_snippets = Qt)$ *// set of selected instances of the j-th section of* T_i'. *Algorithm* $MP\_discover\_snippet$ *Law SM [12]*
10	$ind\_train\_set_i \leftarrow train\_set_i.indices$ *// retrieve the indexes of selected instances on j-th section of* T_i'
11	***for (i=1...k)*** *Do: // Concatenate the indexes retrieved from the selected instances*
12	$ind\_train\_set = ind\_train\_set + \{ind\_train\_set_i\}$

Table 3. β-VAE architecture.

Scaler	MinMax
Architecture	MLP
Optimizer	Adam
Training + validation data	(36495, 36)
Test data	(1921, 36)
Input + encoder layers	(Dense + BatchNormalization) (36, 27, 18, 18, 9)
Loss function	LeakyRelu
Latent space	1
Decoder + output layers	(Dense + BatchNormalization) (9, 18, 18, 27, 36)
Regularizer	1E-11
Epochs	80
Batch size	1
β	0.0001

A new series containing the residual values $r = abs(L^{obs} - L^{rec})$ was computed. The lst indices of the best residuals ($lst = argmin(r)$ define, by voting, the choice of the best inference over L^{rec}.

Chart 2 presents the pseudocode. As additional information, the VAE training and test sets were transformed according to steps 6 and 7, aiming to more comprehensive learning of the shapelet generation process.

Results and Discussion

Table 4 shows the MAE and MSE metrics reconstructions obtained in our study.

Figure 7a shows an example of an anomaly detected in cylinder 2-2B. The filled area (in red) highlights the difference between the observed and reconstructed values. Figure 7b shows the histogram and the detection threshold calculated on the transformed residuals (box-cox transformation) over T. The decision threshold is shown in the vertical red line ("Tukey fences", k=3) - values higher than the threshold are considered "suspicious". The anomaly detection rate reached 0.0142% across the entire dataset.

Figure 7c shows four shapelets reconstructed from equidistant values of the latent space [-3.748, -0.416, 2.915, 6.247] within the quantile interval [q0.0001, q0.9999]. Blue vertical lines separate the four patterns shown. This example illustrates how it is possible to understand the diversity of vibration patterns that arise from operational scenarios.

The histogram in Figure 7d shows the distribution of the latent space in 4 equally distributed compartments, also within the quantile range mentioned in item 7c.

Conclusion

This work aimed to establish a model for detecting potential vibration anomalies in hypercompressor cylinders.

The model was developed using operational data collected every minute for six months on a hypercompressor in an actual installation. The model considered 288 vibration variables, which were transformed into 8 univariate time series, each corresponding to a distinct cylinder. In parallel, another univariate time series, from the same time interval, representing the motor's electrical current used to finalize data cleaning, selecting periods in operational regime of interest.

Operation data labeled "normal" was extracted from the operation data using a combination of the MP and MP snippet algorithms.

A box-cox transformation was applied to the residual absolute errors between the values reconstructed by β-VAE and its inputs, and an outlier detection threshold was obtained by applying the Tukey fence method.

The anomaly detection rate reached 0.0142% on the selected dataset.

The research demonstrated the possibility of establishing a simplified model to detect potential vibration anomalies in a hypercompressor, allowing specialist technicians to focus their investigations on these instances and to correlate detected deviations with incipient operational and maintenance problems, improving safety and operational costs in LDPE plants.

For future studies, we proposed to carry out a qualitative assessment of the physical significance of the detected anomalous shapelets.

Table 4. Reconstruction metrics

	MAE	MSE
RMS_Avg - training + validation	0.1055	0.0805
RMS_Avg – test	0.0841	0.0316

Chart 2. Pseudocode for VAE inference.

	Input: $T = \{T_1, T_2 \dots T_k\},\ T_i = \left\{a_1^i, a_2^i, \dots\ a_{p_i}^i\right\}, i = 1, 2 \dots k$ *// Observed values* $(T = RMS\_Avg_{obs})$ *//* p_i *is the lenght of series* T_i
	Output: $T^{rec} = \{T_1^{rec}, T_2^{rec} \dots T_k^{rec}\},\ T_i = \left\{a\_r_1^i, a\_r_2^i, \dots\ a\_r_{p_i}^i\right\}, i = 1, 2 \dots k$ *// Reconstructed observed values* $(T^{rec} = RMS\_Avg_{rec})$
1	*size* $\leftarrow (\sum_1^k p_i)$ *// Sum of the length of all subseries* T_i
2	$L^{obs} \leftarrow \{\}$ *// Empty set*
4	$T \leftarrow concat(\{T_1, T_2 \dots T_k\})$ *// Concatenate the subseries* T_i *into a single series of length=size*
5	$T \leftarrow scaler.apply(T)$ *// Compute scaler used in VAE trainning over T, for reconstruction inference*
6	***for (i=0, size-36, 1)*** *Do: // Cycle through the observed values and rearrange them in batches of 36 elements*
7	$L^{obs} \leftarrow L^{obs} + T[i: i + 36]$ *// Add to the set* L^{obs}*, sequential batches of 36 elements contained in T*
8	$L^{rec} \leftarrow encoder(decoder(L^{obs}))$ *// Inference on the batches of 36 elements contained in L*
9	$L^{rec} \leftarrow reshape(L^{rec})$ *// Reshape of (size-36, 36) to ((size-36)*36,1)*
10	$L^{rec} \leftarrow scaler.inverse.apply(L^{rec})$*// Scaler inversion of the step 5*
11	$L^{rec} \leftarrow reshape(L^{rec})$ *// Reversion of reshape of the step 9*
12	***for (i = 36, size, 1)*** *Do: // Go through the entire timeseries and rearrange in batches taking diagonals to i of* L^{rec} *e* L^{obs}
13	$diag^{rec} \leftarrow L^{rec}.diagonal(i)$ *// Reconstructed values - Each new batch with 36 (distinct) inferences of the same instance*
14	$diag^{obs} \leftarrow L^{obs}.diagonal(i)$ *// Observed values - Each new batch with 36 (same) inferences of the same instance*
15	$r_i \leftarrow abs(L^{obs} - L^{rec})$ *// Compute the residuals* r_i
16	$lst \leftarrow argmin(r_i)$ *// Find the indexes of the best values by vote (lower residuals)*
17	$T^{rec} \leftarrow L^{rec}[lst]$ *// Assign the best values inferred from the lst index list*

Figure 7 . a) Example of anomaly detection, b) Histogram, outliers, and detection threshold, c) Examples learned by VAE, d) Relative frequency of shapelets occurrence.

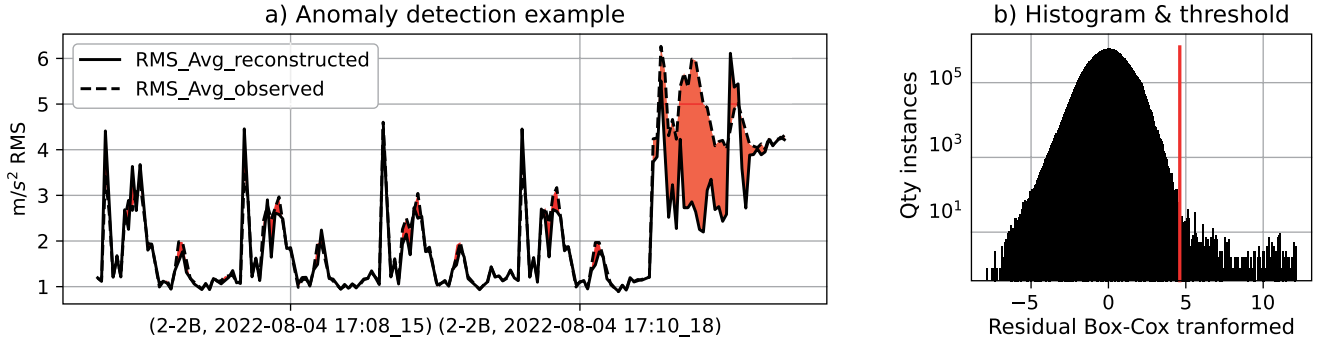

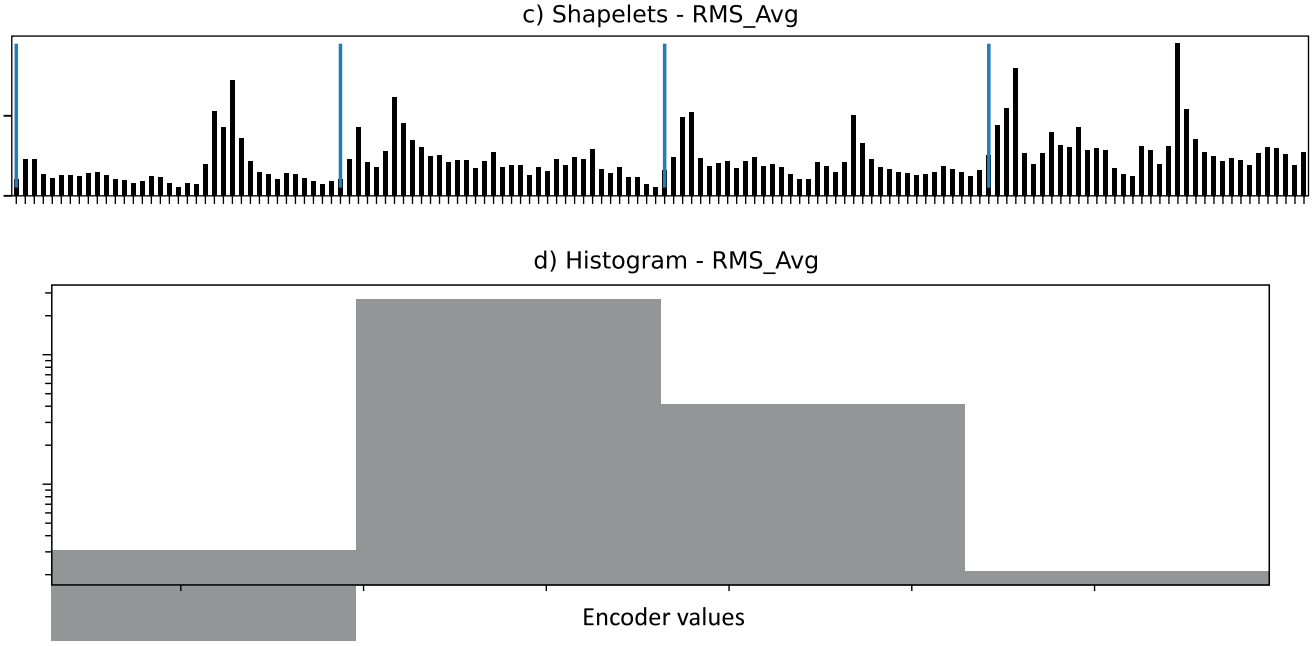

As a second option, compare the nature of the detected anomalies by varying the size of the latent space, the family and architecture of the autoencoder, and the hyperparameters of the automatic selection of the training dataset.

References

1. Compression B. Compressors-for-LDPE. https: //www.burckhardtcompression.com/, 2018. Disponivel em: https://www.burckhardtcompression.com/wp-content/uploads/2021/03/Compressors-for-LDPE_210305.pdf. Accessed on January 31, 2023
2. Park BE et al. Anomaly detection in a hyper-compressor in low-density polyethylene manufacturing processes using WPCA-based principal component control limit. Korean Journal of Chemical Engineering 2020;37:11-18.
3. Xiao S et al. Dynamic behavior analysis of reciprocating compressor with subsidence fault considering flexible piston rod. Journal of Mechanical Science and Technology 2018;32:4103-4124.
4. Xiao S et al. Dynamic analysis for a reciprocating compressor system with clearance fault. Applied Sciences 2021;11(23):11295.
5. Sivalingam G, Soni NJ, Vakil SM. Detection of decomposition for high pressure ethylene/vinyl acetate copolymerization in autoclave reactor using principal component analysis on heat balance model. The Canadian Journal of Chemical Engineering 2015;93(6):1063-1075.
6. Kumar V et al. Multivariate statistical monitoring of a high-pressure polymerization process. Polymer Reaction Engineering 2003;11(4):,1017-1052.
7. Canziani A. Generative Models - Variational Autoencoders, 2020. Disponivel em: <https://atcold.github.io/pytorch-Deep-Learning/pt/week08/08-3/>. Accessed on January 25, 2023.
8. Hinton GE, Salakhutdinoc RR. Reducing the dimensionality of data with neural networks. Science 2006;313(5786):504-507.
9. Kingma DP, WwllingM. Auto-encoding variational bayes. arXiv preprint arXiv:1312.6114, 2013.
10. Yeh CCM et al. Matrix profile I: all pairs similarity joins for time series: a unifying view that includes motifs, discords and shapelets. In: 2016 IEEE 16th International Conference on Data Mining (ICDM). IEEE 2016:1317-1322.
11. Imani S et al. Matrix profile XIII: Time series snippets: A new primitive for time series data mining. In: 2018 IEEE International Conference on Big Knowledge (ICBK). IEEE 2018:382-389.
12. Law SM. STUMPY: A powerful and scalable python library for time series data mining. Journal of Open Source Software 2019;4(39):1504.
13. Higgins I et al. beta-vae: Learning basic visual concepts with a constrained variational framework. In: International conference on learning representations, 2016.
14. Tukey JW. Exploratory data analysis. Addison-Wesely, 1977.
15. Ye L, Keogh e. Time series shapelets: a new primitive for data mining. In: Proceedings of the 15th ACM SIGKDD International Conference on Knowledge Discovery and Data Mining 2009:947-956.

Production of the Scaffold Using 3D Bioprinting Applied to the Biomedical Area: A Bibliometric Study

Ana Paula Bispo Gonçalves[1*], Willams Teles Barbosa[2], Jaqueline Leite Vieira[1], Josiane Dantas Viana Barbosa[2], Milena Botelho Pereira Soares[1,2]

[1]Oswaldo Cruz Foundation, Fiocruz; [2]SENAI CIMATEC University Center; Salvador, Bahia, Brazil

Tissue Engineering is an ascent area with clinical applications through combining cells and biomaterials to reconstitute organs and tissues using scaffolds. These are defined as porous, temporary, biodegradable three-dimensional supports used to mimic the structure of the extracellular matrix and stimulate specific cellular responses at the molecular level. Among the existing technologies for producing scaffolds, 3D bioprinting stands out as one of the most promising technologies that enable layer-by-layer deposition with precise control of the spatial arrangement of functional components. One of the most used biomaterials for the fabrication of scaffolds for application in Tissue Engineering is poly(lactic acid), PLA, a biodegradable, biocompatible, and non-toxic polyester, whose main application is in the regeneration and replacement of bone tissue. In this way, the present article aims to obtain a comprehensive view of the current scenario of PLA scaffolds obtained by 3D bioprinting for biomedical applications through bibliometric analysis. The research was conducted in the Web of Science database between August 16 and 17, 2022. The following set of keywords was used: "scaffolds" AND "PLA" AND "3D printing" AND "biomedical applications" OR "biomedical application," resulting in 2,351 publications in the last five years. The VOSviewer software was used as a bibliometric analysis tool to visualize country networks and keywords on the topic studied. Based on the results, it was possible to observe that China, India, and the USA are the countries that published the most on the subject, and Chinese institutions and authors are also responsible for a considerable part of the publication of documents. There was also an increase in publications in the last five years, reinforcing the research interest that strengthens Tissue Engineering.

Keywords: Scaffolds. PLA. 3D Printing. Biomedical Applications.

Introduction

Research indicates that people's life expectancy has increased. However, this population aging represents a relevant problem for the health system, demanding treatments related to bone tissue [1]. Tissue Engineering has received considerable attention in this context, becoming increasingly important in leading tissue development research [2]. This area includes knowledge about Engineering, Biology, and Medicine and aims to develop biomaterials to replace or repair already injured tissues or organs from scaffolds. These three-dimensional structures provide mechanical support in which cells can be grown to regenerate or construct new tissue [2]. Scaffolds also allow the association of nutrients and metabolites to the extracellular ambiance [3].

Biocompatibility, biodegradation, adequate mechanical strength, uniformly interconnected pores, and the ability to mold into different shapes or dimensions are essential requirements for materials used to manufacture scaffolds [4].

Factors such as three-dimensional structure and the interconnection of pores allow the infiltration of blood vessels from adjacent tissues to the interior of the scaffold [4]. As scaffolds are produced from biodegradable polymers, removing the implant is unnecessary, as is often the case with metallic materials, as they are expected to degrade as new tissue forms [5]. Besides, the scaffolds must also have an adequate chemical surface that favors cell adhesion, proliferation, and differentiation. Poly (lactic acid) is among the biomaterials used to manufacture scaffolds. Poly(lactic acid), PLA, is a biodegradable, biocompatible polyester and can be obtained from renewable sources [6-10]. Due to

Received on 22 June 2023; revised 28 August 2023.
Address for correspondence: Ana Paula Bispo Gonçalves. Rua Waldemar Falcão, 121, Salvador, Bahia, Brazil. Zipcode: 440296-710 . E-mail: anapaulabisgon@gmail.com.

J Bioeng. Tech. Health 2023;6(3):244-251

its mentioned characteristics, combined with good processability and mechanical properties, PLA has a significant interest in biomedical applications [11]. In Tissue Engineering, one of its main applications is in the development of scaffolds for the regeneration and replacement of bone tissue used alone or in combination with other biomaterials, such as polyglycolic acid (PGA), polycaprolactone (PCL) [12–14].

When used as scaffolds, PLA offers interconnected porous structures and ease of construction in different shapes and structures similar to the natural extracellular matrix [15,16].

The degradation of PLA is from hydrolysis, in which it releases lactic acid monomers that are not toxic. These compounds are present in the human body and are removed by natural metabolic pathways [10].

Manufacturing techniques such as additive manufacturing have emerged as new tools for manufacturing 3D scaffolds. 3D bioprinting is a method that consists of layer-by-layer deposition with precise control of the spatial arrangement of functional components with well-defined and reproducible architectures, allowing the creation of an accurate 3D model of bone tissue for a given patient [10,17].

The great interest in the possibility of the reproduction of biological tissues and organs is still driven by the growing need for personalized medicine, enabling bioprinting to establish itself in biomedical research [17]. In this context, this article proposes a bibliometric analysis of the 3D bioprinting scenario of PLA scaffolds for biomedical applications to provide a view of the scientific scenario regarding the principal countries, institutions, periodic, authors, and keywords.

Materials and Methods

Research published in scientific journals indicates that a particular topic or area of knowledge has aroused interest in the scientific community.

The activities for measuring scientific knowledge have been carried out through bibliometric techniques [18]. Bibliometrics corresponds to an information science research area whose main objective is to measure scientific production, encompassing quantitative methods adopted to analyze the most differentiated means of scientific communication [18]. Bibliometrics is also responsible for the quantitative approach and analysis of bibliographic data, such as the year of publication, countries, journals, and authors [18].

Data collection was carried out on the Web of Science platform, which corresponds to a database used enough for bibliometric analysis, as it includes extensive coverage of indexing of journals in several areas of knowledge [19]. The search was carried out on August 16 and 17, 2022. The set of keywords was used: "scaffolds" AND "PLA" AND "3D printing" AND "biomedical applications" OR "biomedical application," resulting in 2,351 publications. This research was made considering the publication date of the last five years. The data collected from each search were exported as "files delimited by tabs", including the complete record and cited references. The VOSviewer software (version 1.6.17, Leiden University, Leiden, Netherlands) was used in this work to construct and visualize bibliometric networks, enabling the extraction of information from publications and obtaining network maps related to the keywords.

The evaluation of documents obtained from the database search was divided into three phases (Figure 1). Phase 1 refers to data collection in the Web of Science, phase 2 corresponds to data visualization from documents exported to the VOSviewer software for bibliometric analysis, and phase 3 evaluates data to identify the main topics discussed in the research.

For the present study, information regarding the productivity of articles per year, countries, institutions, authors, and keywords of the subject studied will be evaluated. Table 1 summarizes the type of element analyzed and its objective.

Results and Discussion

Based on the graph of the number of publications per year (Figure 2), it is possible to observe an

Figure 1. Phases, main steps, and analyzed criteria applied in this study.

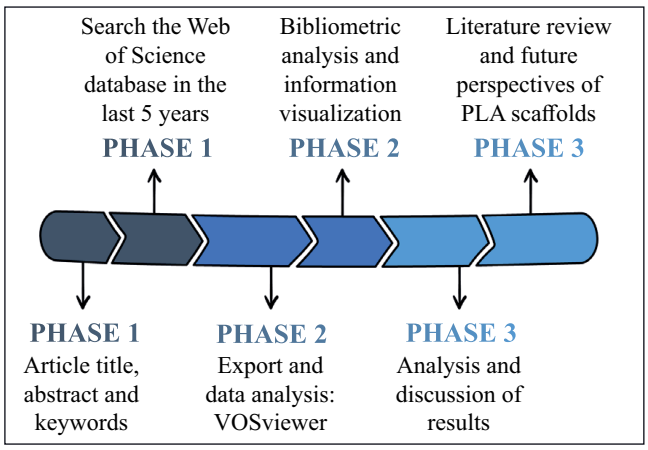

Table 1. Data evaluated in the study.

Analyzed element	Goal
Articles per year	Evaluate productivity through time
Countries	Identify the most productive and cited countries
Institutions	Identify the most productive institutions
Periodicals	Identify the most essential periodicals
Authors	Identify the authors who published the most on the topic
Keywords	Identify the most used keywords

increase in this factor in the last five years. This fact is due to the rise in research in Tissue Engineering.

Given the increase in the average life expectancy of people, the wear of tissues over the years, and trauma caused by impacts or diseases that cause tissue damage, it is necessary to use technologies to develop implant scaffolds [10].

From this perspective, scaffolds have recently received considerable attention in the scientific environment.

In 2022, the trend is for the number of publications to exceed previous years, as observed in 2018 and 2019.

The present study identified 2,711 institutions (affiliations) that published publications on the subject studied. The top ten institutions with the most published documents on PLA scaffold obtained by 3D bioprinting for biomedical applications are organized hierarchically in the TreeMap in Figure 3. Size and color represent numerical dimensions separated by institutions. The three institutions that published the most in the last five years were the Chinese Academy of Sciences, with 132 documents (5.6%); the Chinese Academic University of Sciences, with 43 documents (1.8%) and the Indian Institute of Systems, totaling 43 publications (1.8%).

Figure 4 shows the TreeMap of the top 10 periodicals that most published documents in the last 5 years with PLA scaffolds obtained by 3D bioprinting for biomedical applications. Among the three most cited periodicals are Materials Science Multidisciplinary, with 558 publications, corresponding to 23.8% of the 125 periods; Chemistry Multidisciplinary, with 328 publications (14.0%); and Nanoscience Nanotechnology, with 327 publications (13.9%).

Table 2 summarizes the types of published documents. These have been divided into three main categories. Of the 2,351 papers published, 69.4% were references to articles, 20.6% referred to review articles, and 8.9% were related to conference articles. The first type of publication

Figure 2. Number of publications per year.

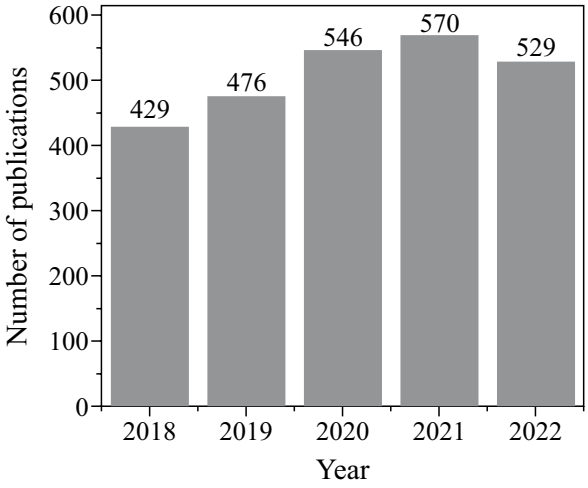

Figure 3. TreeMap is one of the top 10 institutions that published the most studies on scaffolds obtained by 3D bioprinting for biomedical applications.

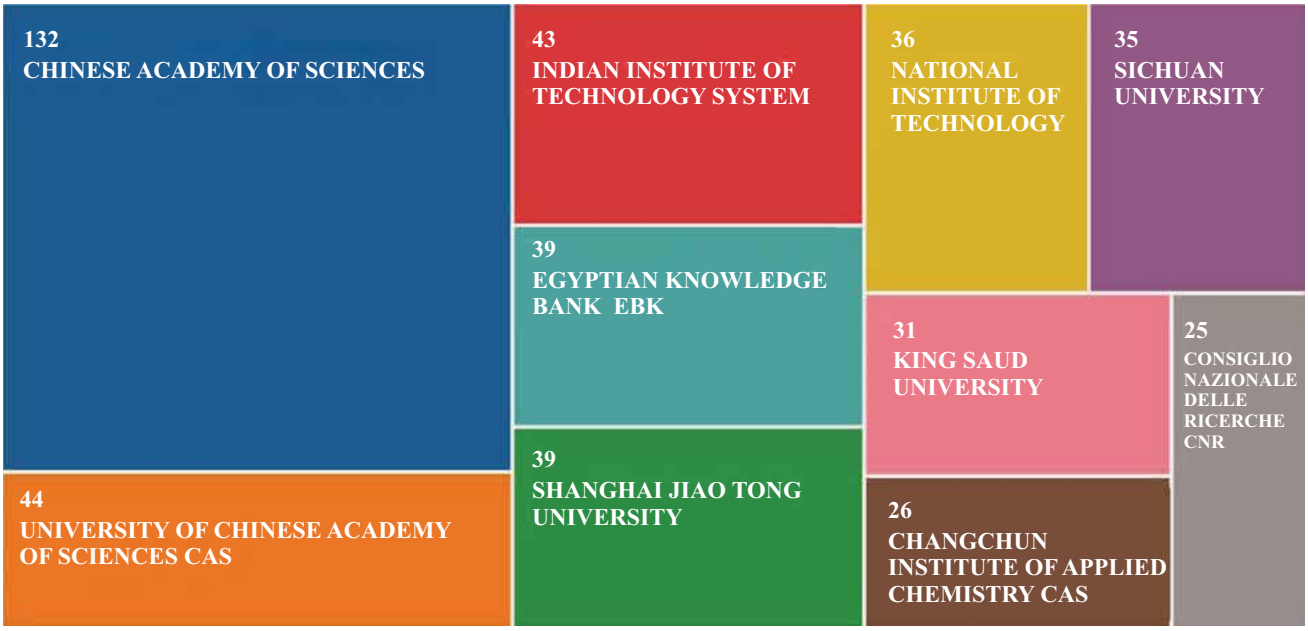

Source: Web of Science (2022).

Figure 4. TreeMap is one of the top 10 periodicals with the most published papers on PLA scaffolds obtained by 3D bioprinting for biomedical applications.

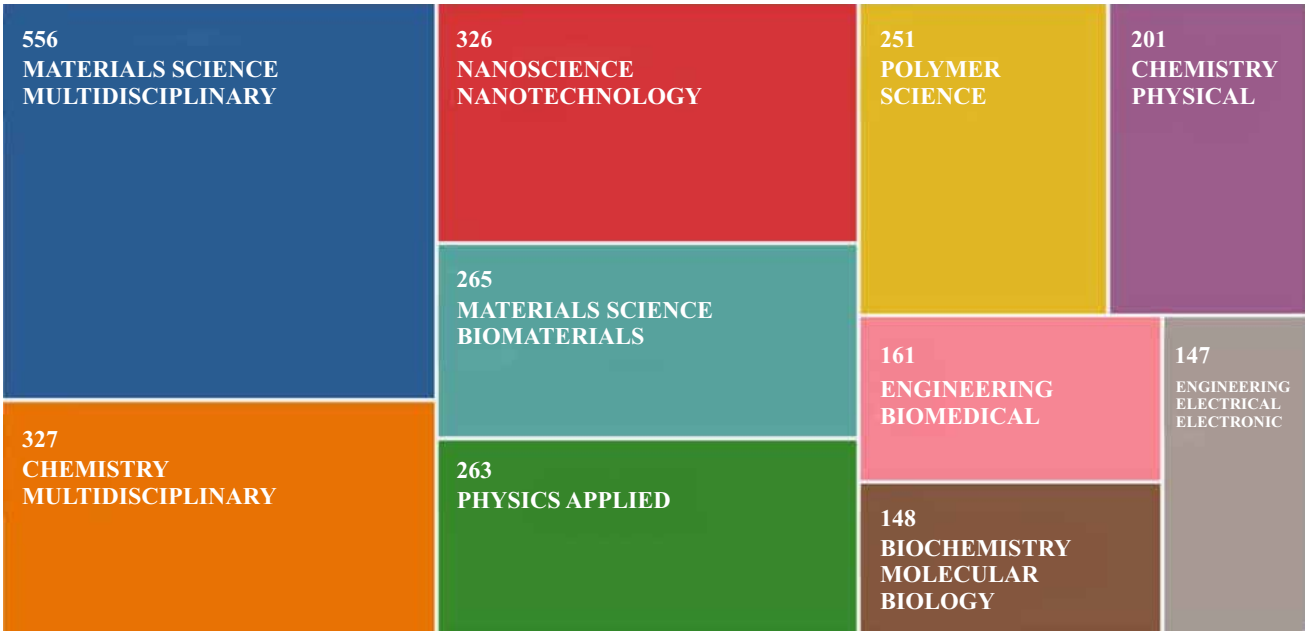

Source: Web of Science (2022).

Table 2. Types of documents referring to the production of PLA scaffolds by 3D bioprinting for biomedical applications.

Type of documents	Number of documents published
Article	1,632
Review article	486
Conference article	211

reflects the study that addresses experimentally obtained results. On the other hand, review articles contemplate a general evolutionary perspective on the topic. On the other hand, conference articles are those presented at scientific events.

Figure 5 shows the countries that most published on the subject of 3D bioprinted PLA scaffolds for biomedical applications. It was observed that China (most emphasis in the Figure) is the country with the most published documents, with 520 publications, followed by India with 200 documents, and the USA with 117 publications. Brazil appears in the eighth position with 38 published documents. These data corroborate studies by Santoni and colleagues (2021) that point out the three countries mentioned among the most relevant in research involving 3D bioprinting [17]. In this work, the authors mentioned that although China occupies second place in leadership, just a few institutions have authors with many publications on 3D bioprinting [17].

The top ten authors with the most publications are affiliated with Chinese institutions (Table 3). These data corroborate with data from publications by countries, in which China appeared as the place where most published documents on that topic, and Chinese institutions were the ones that carried out the most studies on 3D bioprinting to obtain scaffolds for biomedical applications. It should be noted that many authors participate not only as

Figure 5. Network visualization of the most productive countries regarding scaffold research for biomedical applications by 3D bioprinting.

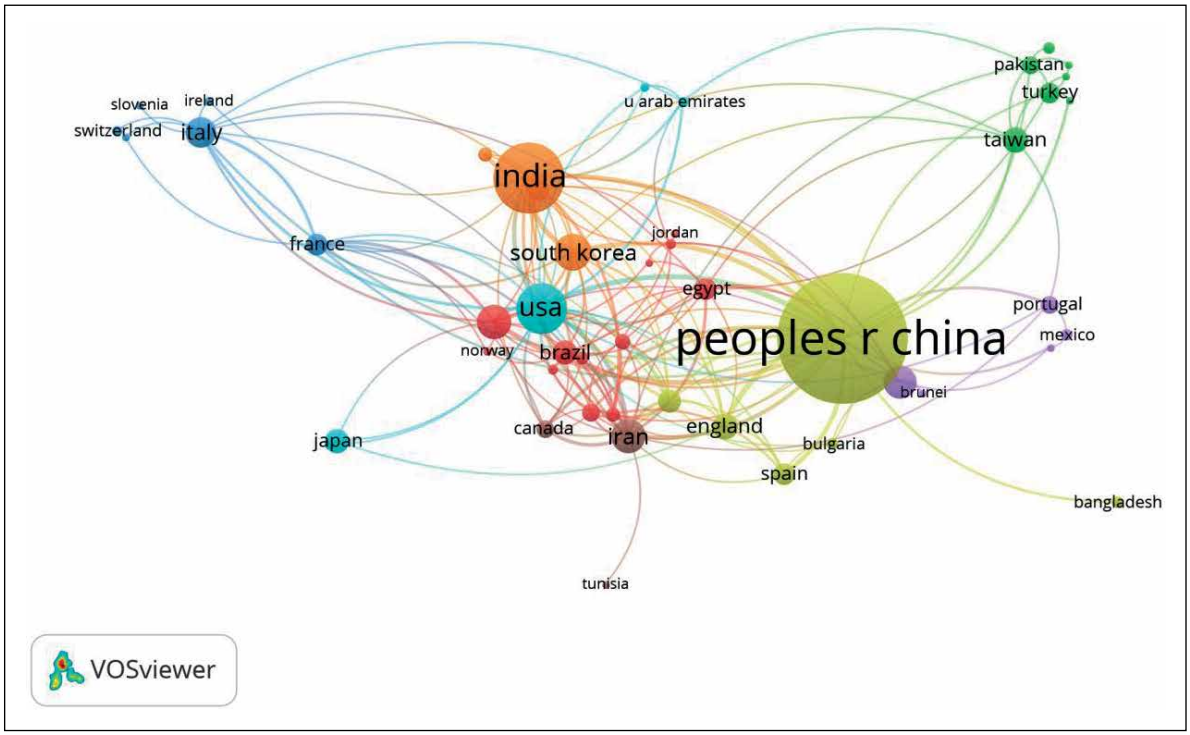

Source: VOSviewer (2022).

Table 3. Principal authors and many publications on producing PLA scaffolds by 3D bioprinting.

Authors	Number of publications	Percentage of the total number of publications (%)
Zhang Y	26	1,106
Wang Y	23	0.9878
Zhang L	21	0.893
Li J	17	0.723
Liu Y	17	0.723
Zhang H	17	0.723
Ramakrishna S	15	0.638
Wang L	15	0.638
Chen Y	14	0.595
Li Y	14	0.595

principal authors but also in studies in which they are co-authors contributing with partnerships with other institutions.

Figure 6 shows the connections between bibliometric data and the correlation between the scope of the study and the main research topics. It was necessary to evaluate each document and extract its main keywords. This analysis is relevant to determine ascent research, development, and innovation trends.

Repeated or irrelevant terms for this study were excluded. The distance between two or more circles is related to the strength of the connection between the terms represented by each one. In the image, different groups of terms are represented by different colors. The size of the circles is associated with the frequency of the appearance of the terms [20,21].

The number of clusters in each network map can change depending on the number of links. Considering the connections between keywords in each cluster, it was verified that the presence of four clusters was represented by different colors: yellow (cluster 1), blue (cluster 2), green (cluster 3), and red (cluster 4). In cluster 1, the most prominent term was "biocompatibility," with 83 occurrences and 524 connections. In cluster 2, "biomedical applications," "in-vitro," and "cells" are the most evident words. For cluster 3, "mechanical properties" was the most prominent term (81 occurrences) and was interconnected by 462 connections. The mechanical properties of the scaffolds, such as the tensile strength, should be as close as possible to the replaced tissue because if it is lower than that of the injured tissue, deformation of the implanted material may occur. Finally, in cluster 4, the most prominent term, "scaffold," is associated with applying the topic studied. One of the applications of tissue engineering is reconstructing cartilage and bone tissue cells, such as osteoblasts. So, the network map shows the connection between these keywords.

Conclusion

The present study showed an overview of the main topics related to scaffolds for biomedical applications that have been researched in the last five years. There was a trend in the growth of publications, which indicates that this topic has been attracting more and more interest.

Among the countries mentioned, China currently stands out as the country with the most publications on the subject studied, with 520 publications in the world, in addition to having the author with the highest number of publications, citations, and reference institutions for the publication of that country. The leading periodicals that publish studies on PLA scaffolds are multidisciplinary, confirming that Tissue Engineering encompasses several areas. From the analysis of the most cited keywords, it was identified that mechanical properties, biocompatibility, and biomedical applications are the main topics currently under study on scaffolds.

Acknowledgments

The authors thank Fiocruz and SENAI CIMATEC.

Figure 6. Network visualization of keywords based on total link strength.

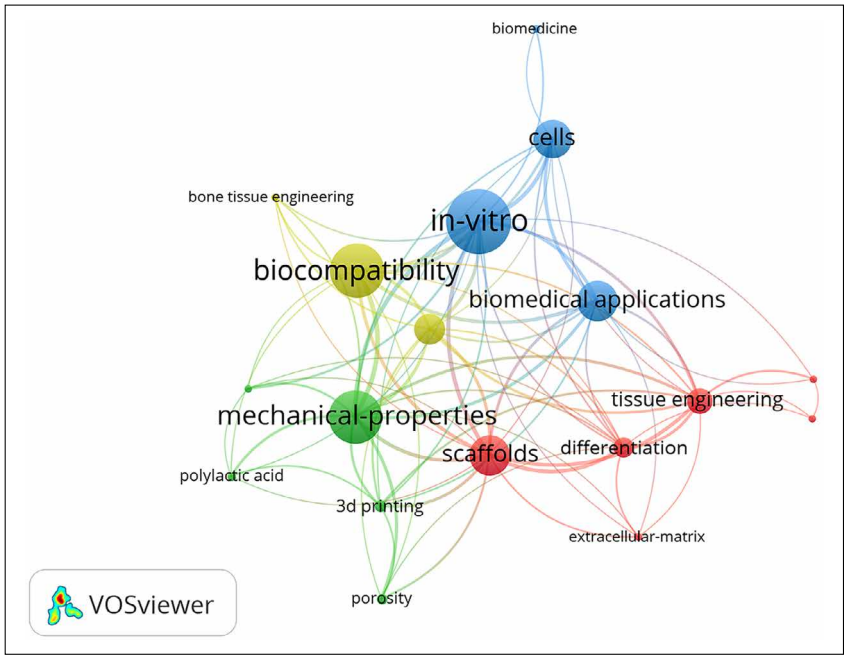

Source: VOSviewer (2022).

References

1. Musalek C, Kirchengast S. Grip strength as an indicator of health-related quality of life in old age-A Pilot Study. Int J Environ Res Public Health 2017;14:1447. https://doi.org/10.3390/ijerph14121447.
2. Saji JJ, Malindisa ST, Ntwasa M. Two-dimensional (2D) and three-dimensional (3D) cell culturing in drug discovery. Cell Cult 2019: 1–23. https://doi.org/10.5772/intechopen.81552.
3. Williams DF. Challenges with the development of biomaterials for sustainable tissue engineering. Front Bioeng Biotechnol 2019;7:127. https://doi.org/10.3389/fbioe.2019.00127.
4. Geetha RB, Muthoosamy K, Manickam S, Hilal-Alnaqbi A. Graphene-based 3D scaffolds in tissue engineering: fabrication, applications, and future scope in liver tissue engineering. Int J Nanomedicine 2019;14:5753–5783. https://doi.org/10.2147/IJN.S192779.
5. Chocholata P, Kulda V, Babuska V. Fabrication of scaffolds for bone-tissue regeneration. Materials (Basel) 2019;:568. https://doi.org/10.3390/ma12040568.
6. Donate R, Monzón M, Alemán-Domínguez ME. Additive manufacturing of PLA-based scaffolds intended for bone regeneration and strategies to improve their biological properties, E-Polymers 2020;20:571–599. https://doi.org/doi:10.1515/epoly-2020-0046.
7. Balla E, Daniilidis V, Karlioti G, Kalamas T, Stefanidou M, Bikiaris ND., Vlachopoulos A, Koumentakou I, Bikiaris DN. Poly(lactic acid): A versatile biobased polymer for the future with multifunctional properties-from monomer synthesis, polymerization techniques and molecular weight increase to PLA applications. Polymers 2021;13(11).MDPI AG. https://doi.org/10.3390/polym131118228.
8. Gregor E, Filová M, Novák J, Kronek, Chlup H, BuzgoM, Blahnová V, Lukášová V, Bartoš M, Nečas A, Hošek J. Designing of PLA scaffolds for bone tissue replacement fabricated by ordinary commercial 3D printer. J Biol Eng 2017;11:31. https://doi.org/10.1186/s13036-017-0074-3.
9. Narayanan G, Vernekar VN, Kuyinu EL, Laurencin CT. Poly (lactic acid)-based biomaterials for orthopaedic regenerative engineering. Adv Drug Deliv Rev 2016;107:247–276. https://doi.org/https://doi.org/10.1016/j.addr.2016.04.015.
10. Serra T, Mateos-Timoneda MA, Planell JA, Navarro M. 3D printed PLA-based scaffolds, Organogenesis 2013;9:239–244. https://doi.org/10.4161/org.26048.
11. Sha L, Chen Z, Chen Z, Zhang A, Yang Z, Polylactic acid based nanocomposites: Promising safe and biodegradable materials in biomedical field. Int J Polym Sci 2016; 6869154. https://doi.org/10.1155/2016/6869154.
12. Grémare A, Guduric V, Bareille R, Heroguez V, Latour S, L'heureux N, Fricain JC, Catros S, Nihouannen DL,

Characterization of printed PLA scaffolds for bone tissue engineering. J Biomed Mater Res A 2018;106:887–894. https://doi.org/10.1002/jbm.a.36289.
13. Lopes TF, Levandowski A, da Fonseca SC, Zielak JC, Leão MP. Stem cells carrier scaffolds for tissue engineering, RSBO 2017;13:98–113. https://doi.org/10.21726/rsbo.v13i2.278.
14. Sartore L, Inverardi N, Pandini S, Bignotti F, Chiellini F. PLA/PCL-based foams as scaffolds for tissue engineering applications. Mater Today Proc 2019;7:410–417. https://doi.org/https://doi.org/10.1016/j.matpr.2018.11.103.
15. Bodnárová S, Gromošová S, Hudák R, Rosocha J, Živčák J, Plšíková J, Vojtko M, Tóth T, Harvanová D, Ižariková, G, Danišovič L. 3D printed polylactid acid based porous scaffold for bone tissue engineering: an *in vitro* study. Acta Bioeng Biomech 2019;21:101–110.
16. Tamaddon M, Blunn G, Liu C. 3D printed PLA/collagen hybrid scaffolds for bone-cartilage interface tissue engineering. Eur Cells Mater 2016;32:113.
17. Santoni S, Gugliandolo SG, Sponchioni M, Moscatelli D, Colosimo BM. 3D bioprinting: current status and trends—a guide to the literature and industrial practice, Bio-Design Manuf 2022;5:14–42. https://doi.org/10.1007/s42242-021-00165-0.
18. Costa M, Oliveira D. Ciência da informação e bibliometria: mapeamento da produção científica em periódicos brasileiros na temática educação a distância. Rev do Inst Ciências Humanas e da Informação Rio Gd 2020;34:19–44.
19. Guimarães A. Modelos de inovação: análise bibliométrica da produção científica. Brazilian J Inf Sci Res Trends 2021;15:e02106.
20. Van Eck NJ, Waltman L. VOSviewer Manual 1.6.11. Manual, (version 1.6.9), 2018.
21. Ji B, Zhao Y, Vymazal J, Mander Ü, Lust R, Tang C. Mapping the field of constructed wetland-microbial fuel cell: A review and bibliometric analysis. Chemosphere 2021;262:128366. https://doi.org/10.1016/j.chemosphere.2020.128366.

Diagnostic Tests, Vaccination and SUS: Analysis of Brazilian Measures to Address the COVID-19 Pandemic

Jéssica Rebouças Silva[1,2*], Katharine Valéria Saraiva Hodel[2], Bruna Aparecida Souza Machado[2]
[1]DTI-A Scholarship, CNPq; [2]SENAI CIMATEC University Center; Salvador,Bahia,Brazil

Mass testing and vaccination are essential for controlling the COVID-19 pandemic. This study aims to evaluate the initial strategies adopted by Brazil to combat the COVID-19 pandemic. Information collected from public and government databases on the approvals and acquisition of diagnostic tests and the immunization process in several countries was analyzed. It was observed that 73% of the tests approved by Anvisa were of the rapid type, of which 92.5% were for antibody detection. However, immunization against COVID-19 started late in Brazil, with 75% of the population vaccinated faster than in the United States, United Kingdom, and Russia. Negligence in the scope of public health policies, combined with reduced testing and the troubled start of vaccination, may have contributed to the high number of cases and deaths presented at the beginning of the pandemic.
Keywords: COVID-19. Vaccine. Diagnostic Kit. SUS.

Introduction

COVID-19 is an acute respiratory disease with an inflammatory profile caused by the coronavirus SARS-CoV-2, whose clinical characteristics vary from mild to fatal [1]. The disease was identified in late 2019 in the city of Wuhan, China, and only in March 2020 was it officially declared pandemic status by the World Health Organization (WHO). Due to the intrinsic characteristics of the new coronavirus, such as high virulence and speed of propagation, the virus soon spread throughout the world, leading to 761.07 million cases and 6.88 million confirmed deaths worldwide [2,3].

Primary health measures to combat COVID-19, recommended by the WHO, are limited to combating the spread of the virus - such as hand hygiene, social distancing, and epidemiological surveillance - as well as reducing the severity of the disease - such as vaccine administration. Consequently, the world has experienced an unprecedented scientific race to develop and approve vaccines against COVID-19, in addition to diagnostic tests. As a result, there was a rapid development and availability of several *in vitro* diagnostic products for COVID-19 worldwide, as well as the availability and approval of effective vaccines in 2020. Therefore, countries such as Russia, the United Kingdom, and the United States United States began mass vaccination of the population in the first year of the pandemic [4,5].

On the other hand, Brazilian strategies to contain the spread of the pandemic were composed of a mix of political and economic interests, logistical problems, and ideological disputes, causing the country to present regional inequalities in allocating resources for the health system. Such measures affect not only the process of acquiring vaccines and diagnostic kits but also the acquisition of strategic inputs, such as syringes and needles, and vital, such as compressed oxygen, used in hospitals to support patients affected by COVID-19 or other illnesses [6,7]. Consequently, the country ended 2020 presenting the worst indicators of the pandemic, such as a high number of confirmed cases and deaths and without starting vaccinating the population.

We analyzed the measures adopted by the Brazilian government in the first year of the pandemic to combat COVID-19, the approval of diagnostic kits for COVID-19, the acquisition of vaccines, and the importance of the Unified Health System (SUS) as a catalyst for the mass vaccination process. The analysis of the conduct adopted by Brazil at the beginning of the pandemic constitutes

Received on 31 May 2023; revised 29 July 2023.
Address for correspondence: Jéssica Rebouças Silva. Rua Guilherme Pessoa Serrano, 156, Apt 104 - Bancários. João Pessoa, Paraíba. Zipcode: 58051-350. Salvador,Bahia, Brazil. E-mail: jessica.reboucas@fbter.org.br.

J Bioeng. Tech. Health 2023;6(3):252-255

a vital learning tool, which makes it possible to evaluate the effectiveness of the actions adopted, setting precedents for implementing more effective measures to combat new health crises.

Materials and Methods

Database

A systematic search was carried out in the PubMed bibliographic database, on the Anvisa website, through the access "Complete List of *In vitro* Diagnostic Products for COVID-19"; on the Our World in Data website. Data on approval and testing were collected on the Anvisa and Ministry of Health (MS) website until December 5, 2020.

Software

The data presented were prepared in GraphPad Prism v.9.00 for Windows (GraphPad Software, San Diego, California).

Results and Discussion

Approval and Acquisition of Diagnostic Kits

Carrying out diagnostic tests is crucial for controlling infectious diseases, as it allows the identification and correct management of contaminated people and their contacts [8,9]. In this context, regulatory agencies in several countries have adopted measures to speed up the processes of analysis and registration of diagnostic kits [10-12]. In Brazil, the regulatory flexibilities imposed by ANVISA, through RDC n. 348/2020, culminated in the approval of 441 *in vitro* diagnostic kits for COVID-19 in 2020, of which 83% (n = 364) were immunological tests and 17% (n = 73) were molecular tests (Figure 1a) [13]. Furthermore, it was observed that 73% (323) of the approved tests were rapid tests, of which 92.5% were for antibody detection (Figure 1b and 1c). MS data show that Brazil prioritized acquiring rapid diagnostic tests for detecting antibodies about others, since until

Figure 1. Characteristics of diagnostic tests for COVID-19 registered with ANVISA between May 18 and December 9, 2020.

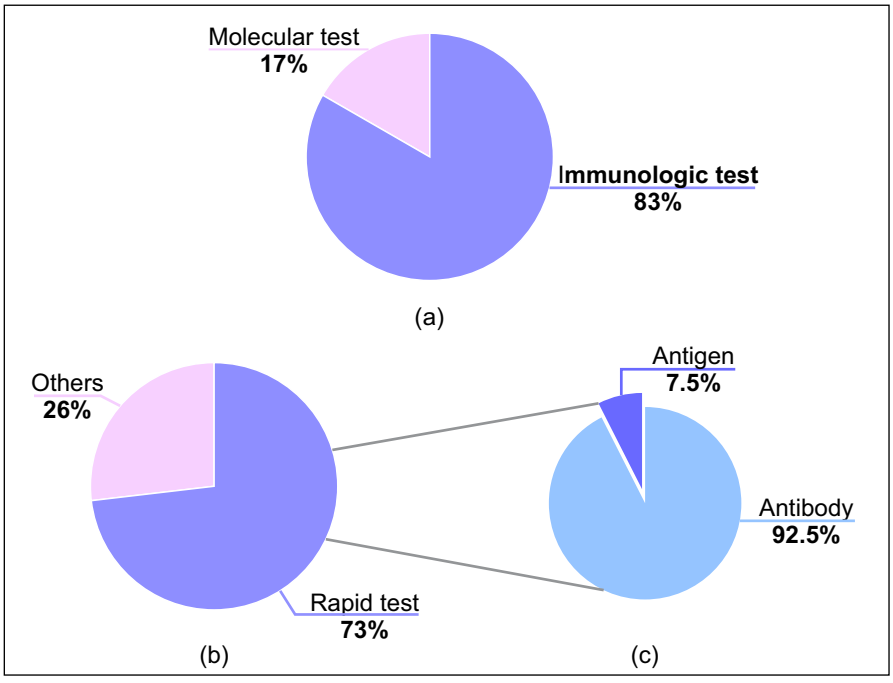

(a) percentage of serological and molecular tests; (b) percentage of rapid tests and (c) percentage of rapid tests for antigen detection and antibody detection.

December 2020, the SUS carried out around 19,507,974 tests, of which 11,409,144 were of this type.

This measure is in line with WHO recommendations, which guide the use of molecular tests and rapid antigen detection tests for diagnosis and epidemiological surveillance of COVID-19 due to the better analytical performance of these tests.

Mass Vaccination and the Role of SUS

Unlike countries like the United States and the United Kingdom, which prioritized and ensured the rapid acquisition of large quantities of vaccines, even those still under development, Brazil initially delayed and restricted the purchase of immunizations to a few suppliers. In this sense, despite negotiations for the purchase of 1.5 million doses from Pfizer/BioNtech dating back to August 2020, the Brazilian government only signed a contract with the pharmaceutical company in March 2021, even with authorization from Anvisa for a clinical trial in Brazil dating back to July 2020 [14,15]. Thus, the vaccination of the Brazilian population began late, on January 17, 2021, and was characterized by slowness, staggering of doses and heterogeneity in the acquisition and application of immunizations between Brazilian states [16].

On the other hand, the SUS and the National Immunization Program (PNI) once again showed their potential in immunizing large masses of the population, revealing that the country already had essential tools to combat COVID-19. In this sense, despite Brazil starting the immunization process late compared to the United States, United Kingdom, and Russia, the country reached 75% of the population vaccinated with the initial immunization protocol more quickly than other countries in 15 months. Currently, the country has around 82% of the population fully vaccinated, surpassing the other countries evaluated (Figure 2). Part of the scientific community defends the need to obtain coverage vaccination rate between 60-70% to achieve "herd immunity", defined as acquired mass immunity capable of protecting

Figure 2. Percentage of people fully vaccinated with the initial vaccination protocol against COVID-19 by country and time.

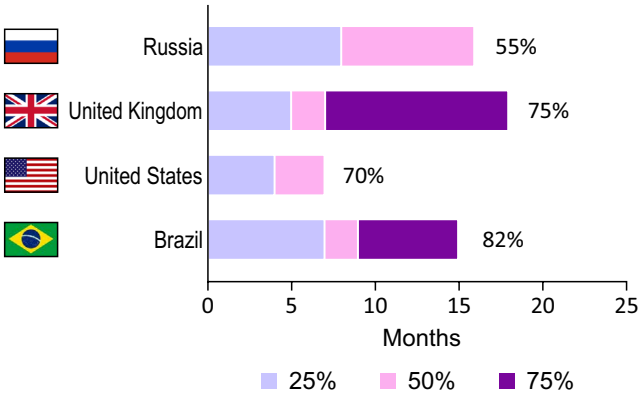

susceptible people and preventing infectious agent transmission. In this sense, the WHO advises countries to increase efforts to reach the goal of 70% vaccination coverage, prioritizing the vaccination of 100% of health professionals and 100% of the most vulnerable groups [17].

Final Considerations

Although Brazil has the most famous free healthcare system in the world, the SUS, as well as one of the most extensive mass immunization programs, the PNI, these resources were not used to their full potential at the beginning of the pandemic, mainly due to delays in vaccine purchase contracts by the Brazilian government, as well as planning and logistics problems in the acquisition and distribution of immunizations, diagnostic tests, and medical supplies. This fact may have contributed to the high number of cases and deaths at the beginning of the pandemic.

References

1. Umakanthan S et al. Origin, transmission, diagnosis and management of coronavirus disease 2019 (COVID-19). Postgrad Med J 2020;96(1142):753–758, Dec. 2020, doi: 10.1136/POSTGRADMEDJ-2020-138234.
2. Harrison A et al. Mechanisms of SARS-CoV-2 transmission and pathogenesis. Trends Immunol 2020;41(12):1100–1115, Dec. 2020, doi: 10.1016/J.IT.2020.10.004.

3. COVID-19 Data Explorer - Our World in Data. Available at https://ourworldindata.org/explorers/coronavirus-data-explorer?zoomToSelection=true&time=2020-03-01..latest&facet=none&pickerSort=asc&pickerMetric=location&Metric=Confirmed+deaths&Interval=Cumulative&Relative+to+Population=false&Color+by+test+positivity=f. Accessed on March 24, 2023.
4. The White House. National COVID-19 Preparedness Plan | The White House. Available at https://www.whitehouse.gov/covidplan/ Accessed on March 24, 2023.
5. Institute for Government. Coronavirus vaccine rollout | Institute for Government. Available at https://www.instituteforgovernment.org.uk/article/explainer/coronavirus-vaccine-rollout. Accessed on March 24, 2023.
6. Bigoni A et al., Brazil's health system functionality amidst of the COVID-19 pandemic: An analysis of resilience. Lancet Reg Heal Am 2022;10:100222, Jun. 2022, doi: 10.1016/j.lana.2022.100222.
7. Hallal P, Cesar V. Overcoming Brazil's monumental COVID-19 failure: an urgent call to action. Nat Med 2021;27(6):933–933. doi: 10.1038/s41591-021-01353-2.
8. Vandenberg O et al. Considerations for diagnostic COVID-19 tests. Nat Rev Microbiol 2020;:1–13, doi: 10.1038/s41579-020-00461-z.
9. Weissleder R et al. COVID-19 diagnostics in context. Sci Transl Med 2020;12(546):eabc1931. doi: 10.1126/scitranslmed.abc1931.
10. Laureano AF, Riboldi M. The different tests for the diagnosis of COVID-19 - A review in Brazil so far. JBRA Assist Reprod 2020;24(3):340–346. doi: 10.5935/1518-0557.20200046.
11. Neeraja R et al. Diagnostics for SARS-CoV-2 detection: A comprehensive review of the FDA-EUA COVID-19 testing landscape. Biosens Bioelectron 2020;165:112454. doi: 10.1016/j.bios.2020.112454.
12. Meng X et al. COVID-19 diagnostic testing: Technology perspective. Clin Transl Med2020;10(4):1–15. doi: 10.1002/ctm2.158.
13. Brasil. Anvisa. RESOLUÇÃO RDC No 348, DE 17 DE MARÇO DE 2020 - DOU - Imprensa Nacional. Disponível em: https://www.in.gov.br/en/web/dou/-/resolucao-rdc-n-348-de-17-de-marco-de-2020-248564332. Accessed on March 24, 2023.
14. Brasil. Anvisa. Vacinas. Disponível em: https://www.gov.br/anvisa/pt-br/assuntos/paf/coronavirus/vacinas. Accessed on March 24, 2023.
15. National Audit Office. Investigation into preparations for potential COVID-19 vaccines A picture of the National Audit Office. Dep. Business, Energy Ind. Strateg. Dep. Heal. Soc. Care, NHS Engl. NHS Improv. Public Heal Engl 2020:51.
16. Brasil. Ministério da Saúde. Plano Nacional de Operacionalização da Vacinação contra a COVID-19. Brasília, Dec. 2020.Accessed on March 24, 2023.
17. OMS. COVID-19 vaccines. Disponível em: https://www.who.int/emergencies/diseases/novel-coronavirus-2019/covid-19-vaccines. Accessed on March 24, 2023.

Technological Prospection and Flowchart for Production of Biogas Enriched with Hydrogen: A Proposal for Renewable Energy Sources

Larissa Sousa Cardeal de Miranda[1*], Fernando Luiz Pellegrini Pessoa[1], Ana Lucia Barbosa de Souza[1]
[1]SENAI CIMATEC University Center; Salvador, Bahia, Brazil

Over time, environmental issues have taken on significant proportions worldwide, making using renewable energy sources increasingly trivial, notorious, and indispensable. Projects focused on sustainability enable the expansion and diversification of current energy matrices, such as the potential use of biogas as an alternative source. Therefore, the project aimed to develop a flowchart proposal through technological prospection, given the production of biogas enriched with hydrogen through anaerobic digestion of solid waste. Thus, a technological prospecting of patents and quantitative analysis of scientific articles was carried out to show an overview of the production of biogas associated with hydrogen from 2012 to 2022, based on the studies that analyzed the viability and efficiency of the use of hydrogen for biogas production.
Keywords: Biogas. Biohydrogen. Anaerobic Digestion. Biofuel.

Introduction

The topic of energy is a significant issue in the world, as it is directly linked to the economy of countries. There is still a dependence on the oil industry as a source of energy production. Fossil fuels, oil, and natural gas are the primary raw materials for energy. However, this scenario has caused adverse environmental, social, and health impacts due to the high emission of greenhouse gases, promoting adverse effects, such as increased global warming and climate change. Faced with this, sanctions imposed at international conferences, such as the 1997 Kyoto Protocol, the 2015 Paris Agreement, and COP27, put pressure on reducing carbon and methane emissions and developing renewable energy sources [1,2].

According to Dorning (2015) [3], bioenergy production has become a viable and necessary alternative for energy production. The growth of renewable energies in Brazil's energy matrix has been evident, remaining among the highest in the world. In times of growing ecological problems, the need for sustainable technologies linked to bioenergy has been the subject of many studies worldwide [4,5].

Biogas is a renewable biofuel source composed of methane gas (CH_4) and carbon dioxide (CO_2). It is obtained through anaerobic digestion of solid or liquid waste. This process has 4 phases, where solid waste is digested and decomposed by bacteriological microorganisms following criteria of fermentation, temperature, humidity, and pH. The amount of gas produced depends on the organic matter used and may vary in composition [6].

Although the production of hydrogen-enriched biogas is a promising technology for generating energy from renewable sources, some gaps still need to be addressed to make it more efficient and viable. These gaps include Cost, Efficiency, Raw Material Availability, Infrastructure, and Regulation. The work aims to identify an optimal route to produce biogas enriched with hydrogen. Therefore, the objective is to evaluate the feasibility of producing biogas enriched with hydrogen through anaerobic digestion of solid waste.

Materials and Methods

In the project, a bibliographical review and technological prospecting of the biogas production scenario were developed, so patent searches and works were carried out to identify technologies

Received on 18 May 2023; revised 20 July 2023.
Address for correspondence: Larissa Sousa Cardeal de Miranda. Avenida Orlando Gomes,1845, Piatã. Salvador, Bahia, Brazil. Zipcode: 42701-310. E-mail: lariissacardeal@gmail.com.

J Bioeng. Tech. Health 2023;6(3):256-259

that addressed the production of biogas associated with hydrogen. To this end, data collection was carried out regarding technologies on a national and global scale, using the resources of the Derwent World Patents Index bases, which is a database that contains patent applications and concessions of 44 from the world's patent-issuing authorities and to publications in databases such as Google Scholar, SciELO, ACS publications, and Elsevier. Publication data

They were exported to Microsoft Excel® and transformed into graphs to better present and interpret the results. The terms biogas production, Biogas production, biogas and hydrogen, biogas production, Biomethane Production, Biomethane production, and Biomethane production are in the Title or abstract field. As a research strategy, 653 patent filings were found between 2012 and 2022. In addition, a preliminary flowchart of the biogas production process was created using the SUPERPRO Designer software.

Results and Discussion

As a result, we have carried out technological prospecting for biogas production, followed by the proposal of a preliminary flowchart of the production process using the SUPERPRO software.

In Figure 1, there was an increase in scientific production on the proposed topic. Through analysis of the selected patent documents, Figure 2 illustrates that several countries submitted patents on the topic, but the ones that stood out were China, Korea, and the United States.

China is in a prominent position as the largest applicant of patents related to researched technology, having almost all of the patent deposits protected in the country (267). This high number indicates that the technologies mentioned can be used in other countries that are not protected, leaving those who use them accessible from any sanctions. Concerning national participation, Brazil needs to present relevant quantified data regarding patents. They highlighted the need for more significant national scientific investments to develop patentable products and techniques. This technological prospection shows a strong trend towards growth in studies and research, demonstrating that the current scenario is quite dynamic and that there is a tendency for positive changes to occur in the short and medium term.

Anaerobic digestion is a process that has 4 phases: Hydrolysis, acidogenesis, acetogenesis, and methanogenesis, where solid waste is digested and decomposed by anaerobic microorganisms under controlled conditions to produce biogas.

In the acetogenesis phase, hydrogen will be produced to be consumed, stored, and consumed in the methanogenic stage along with the byproduct CO_2 to form CH_4. A preliminary flowchart of this biogas production process was created using the SUPERPRO DESIGNER software (Figure 2).

In Figure 3, there are two bioreactors in the series; the first in the fixed bed will be pre-treated without methanogenic microorganisms, in which the chosen substrate will enter, and hydrogen will be produced, and in the second bioreactor with the sludge without pre-treatment will produce the biogas from the substrate coming from the first bioreactor. Studies are underway to identify the best flowchart and, therefore, simulate the production process and analyze the economic viability of the process.

The production of a greater quantity of hydrogen in the acetogenesis phase allows the optimization of the result, as it will result in a more outstanding production of biogas in the methanogenesis phase and the possibility of storing hydrogen. Thus, although there are several processes to be applied to biogas, all of these processes require more time and additional costs to obtain biogas and do not generate a favorable amount of biogas.

Final Considerations

The study of the biogas production process with hydrogen shows promise in Brazil due to the opportunity to take advantage of the energy matrix

Figure 1. Number of article publications per year.

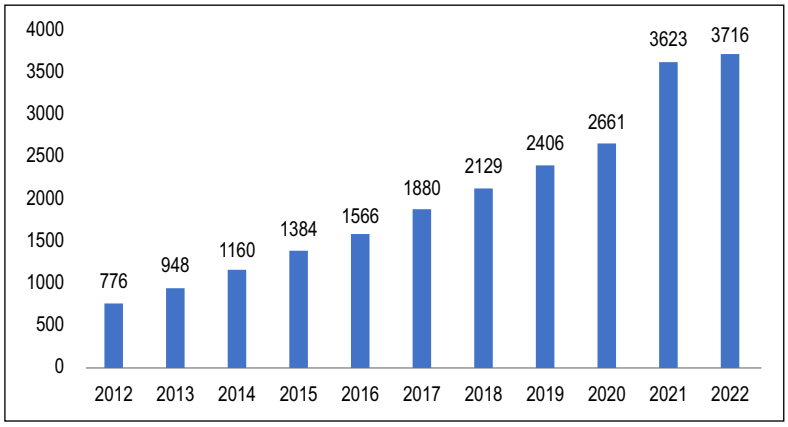

Figure 2. Number of patents by Country/Offices where they were filed.

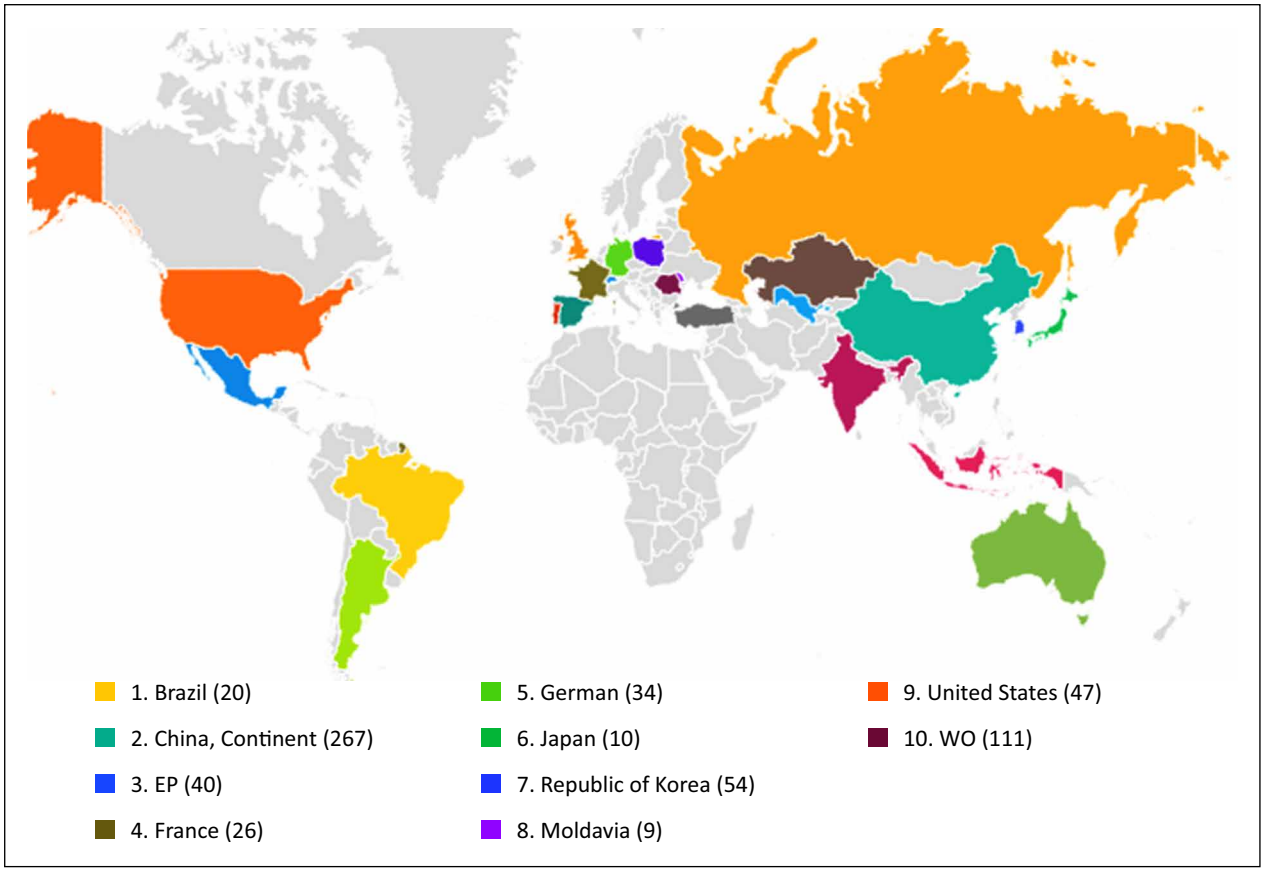

Source: Derwent, 2022.

Figure 3. Flowchart of the hydrogen-enriched biogas production process.

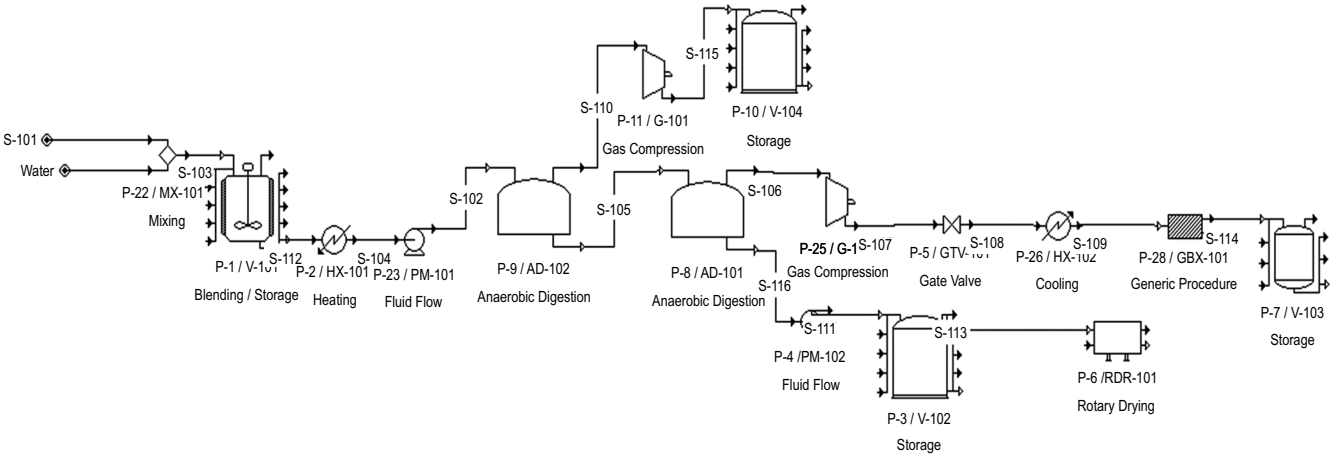

since we have different resources as a source for the biotransformation of this product.

Furthermore, the data collected during this essay objectively demonstrates the growing advancement in research. The increase in recent years in the development of scientific production and patents related to biogas was also highlighted, being a genuine alternative within the sustainable aspect and renewable energy on a global scale. Concerning national participation, it became clear during this work that Brazil needs to present relevant quantified data regarding patents.

Studies are underway to identify the optimal flowchart and simulate the process. In the following steps, the study will consider the technical-economic feasibility of producing more efficient biogas as it is enriched with hydrogen.

Acknowledgments

Fernando Pellegrini and Ana Lucia Barbosa for all their support throughout the project's development. We thank SENAI CIMATEC for the entire structure and the Human Resources Program 27.1 (PRH 27.1) of the National Petroleum, Gas and Biofuel Agency (ANP) - FINEP for the financial assistance.

References

1. Dos Santos CM et al. A indústria do petróleo e energia frente aos novos desafios de se inserir nos modelos da transição energética. Research, Society and Development 2022;11(9):e40711932000-e40711932000.
2. Vieira MA et al. CO_2: análise contemporânea no impacto do crescimento econômico e energia sobre a emissão de dióxido de carbono. 2023. Tese de Doutorado. Universidade Federal de Santa Maria.
3. Valencio MA. Evaluation of the efficiency of the addition of hydrogen in the combustion of biogas in industrial boilers. In: Electronic Proceedings of the XI EPCC - International Meeting of Scientific Production. Anais...Maringá(PR) UNICESUMAR, 2019. Available at: https//www.even3.com.br/anais/epcc2019/187550-AVALIACAO-DA-EFICIENCIA-DA-ADICAO-DO-HIDROGENIO-NA--COMBUSTAO -FROM-BIOGAS-IN-INDUSTRIAL-BOILER. Accessed on: 02/20/2023.
4. Dorning MA et al. Changing decisions in a changing landscape: How might forest owners in an urbanizing region respond to emerging bioenergy markets? Land Use Policy 2015;49:1-10.
5. Wang X, Zhang L, Zou J, Liu S. Optimizing net greenhouse gas balance of a bioenergy cropping system in southeast China with urease and nitrification inhibitors. Ecol Eng 2015;83:191–198. doi:10.1016/j.ecoleng.2015.05.047, 2015.
6. Salomon KR. Avaliação técnico-econômica e ambiental da utilização do biogás proveniente da biodigestão da vinhaça em tecnologias para geração de eletricidade. Tese de Doutorado, Universidade Federal de Itajubá – 2007.

Instructions for Authors

The Authors must indicate in a cover letter the address, telephone number and e-mail of the corresponding author. The corresponding author will be asked to make a statement confirming that the content of the manuscript represents the views of the co-authors, that neither the corresponding author nor the co-authors have submitted duplicate or overlapping manuscripts elsewhere, and that the items indicated as personal communications in the text are supported by the referenced person. Also, the protocol letter with the number should be included in the submission article, as well as the name of sponsors (if applicable).

Manuscripts may be submitted within designated categories of communication, including:

- Original basic or clinical investigation (original articles on topics of broad interest in the field of bioengineering and biotechnology applied to health). We particularly welcome papers that discuss epidemiological aspects of international health, clinical reports, clinical trials and reports of laboratory investigations.
- Case presentation and discussion (case reports must be carefully documented and must be of importance because they illustrate or describe unusual features or have important practice implications).
- Brief reports of new methods or observations (short communications brief reports of unusual or preliminary findings).
- State-of-the-art presentations (reviews on protocols of importance to readers in diverse geographic areas. These should be comprehensive and fully referenced).
- Review articles (reviews on topics of importance with a new approach in the discussion). However, review articles only will be accepted after an invitation of the Editors.
- Letters to the editor or editorials concerning previous publications (correspondence relating to papers recently published in the Journal, or containing brief reports of unusual or preliminary findings).
- Editor's corner, containing ideas, hypotheses and comments (papers that advance a hypothesis or represent an opinion relating to a topic of current interest).
- Innovative medical products (description of new biotechnology and innovative products applied to health).
- Health innovation initiatives articles (innovative articles of technological production in Brazil and worldwide, national policies and directives related to technology applied to health in our country and abroad).

The authors should checklist comparing the text with the template of the Journal.

Supplements to the JBTH include articles under a unifying theme, such as those summarizing presentations of symposia or focusing on a specific subject. These will be added to the regular publication of the Journal as appropriate, and will be peer reviewed in the same manner as submitted manuscripts.

Statement of Editorial Policy

The editors of the Journal reserve the right to edit manuscripts for clarity, grammar and style. Authors will have an opportunity to review these changes prior to creation of galley proofs. Changes in content after galley proofs will be sent for reviewing and could be required charges to the author. The JBTH does not accept articles which duplicate or overlap publications elsewhere.

Peer-Review Process

All manuscripts are assigned to an Associate Editor by the Editor-in-Chief and Deputy Editor, and sent to outside experts for peer review. The Associate Editor, aided by the reviewers' comments, makes a recommendation to the Editor-in-Chief regarding the merits of the manuscript. The Editor-in-Chief makes a final decision to accept, reject, or request revision of the manuscript. A request for revision does not guarantee ultimate acceptance of the revised manuscript.

Manuscripts may also be sent out for statistical review ou *ad hoc* reviewers. The average time from submission to first decision is three weeks.

Revisions

Manuscripts that are sent back to authors for revision must be returned to the editorial office by 15 days after the date of the revision request. Unless the decision letter specifically indicates otherwise, it is important not to increase the text length of the manuscript in responding to the comments. The cover letter must include a point-by-point response to the reviewers and Editors comments, and should indicate any additional changes made. Any alteration in authorship, including a change in order of authors, must be agreed upon by all authors, and a statement signed by all authors must be submitted to the editorial office.

Style

Manuscripts may be submitted only in electronic form by www.jbth.com.br. Each manuscript will be assigned a registration number, and the author notified that the manuscript is complete and appropriate to begin the review process. The submission file is in OpenOffice, Microsoft Word, or RTF document file format for texts and JPG (300dpi) for figures.

Authors must indicate in a cover letter the address, telephone number, fax number, and e-mail of the corresponding author. The corresponding author will be asked to make a statement confirming that the content of the manuscript represents the views of the co-authors, that neither the corresponding author nor the co-authors have submitted duplicate or overlapping manuscripts elsewhere, and that the items indicated as personal communications in the text are supported by the referenced person.

Manuscripts are to be typed as indicated in Guide for Authors, as well as text, tables, references, legends. All pages are to be numbered with the order of presentation as follows: title page, abstract, text, acknowledgements, references, tables, figure legends and figures. A running title of not more than 40 characters should be at the top of each page. References should be listed consecutively in the text and recorded as follows in the reference list, and must follow the format of the National Library of Medicine as in Index Medicus and "Uniform Requirements for Manuscripts Submitted to Biomedical Journals" or in "Vancouver Citation Style". Titles of journals not listed in Index Medicus should be spelled out in full.

Manuscript style will follow accepted standards. Please refer to the JBTH for guidance. The final style will be determined by the Editor-in-Chief as reviewed and accepted by the manuscript's corresponding author.

Approval of the Ethics Committee

The JBTH will only accept articles that are approved by the ethics committees of the respective institutions (protocol number and/or approval certification should be sent after the references). The protocol number should be included in the end of the Introduction section of the article.

Publication Ethics

Authors should observe high standards with respect to publication ethics as set out by the International Committee of Medical Journal Editors (ICMJE). Falsification or fabrication of data, plagiarism, including duplicate publication of the authors' own work without proper citation, and misappropriation of the work are all unacceptable practices. Any cases of ethical misconduct are treated very seriously and will be dealt with in accordance with the JBTH guidelines.

Conflicts of Interest

At the point of submission, each author should reveal any financial interests or connections, direct or indirect, or other situations that might raise the question of bias in the work reported or the conclusions, implications, or opinions stated - including pertinent commercial or other sources of funding for the individual author(s) or for the associated department(s) or organizations(s), and personal relationships. There is a potential conflict of interest when anyone involved in the publication process has a financial or other beneficial interest in

the products or concepts mentioned in a submitted manuscript or in competing products that might bias his or her judgment.

Material Disclaimer

The opinions expressed in JBTH are those of the authors and contributors, and do not necessarily reflect those of the SENAI CIMATEC, the editors, the editorial board, or the organization with which the authors are affiliated.

Privacy Statement

The names and email addresses entered in this Journal site will be used exclusively for the stated purposes of this journal and will not be made available for any other purpose or to any other party.

Brief Policies of Style

Manuscript	Original	Review	Birief Comunication	Case Report	Editorial ; Letter to the Editor; Editor' s Corner	Innovative Medical Products	State-of-the-Art	Health Innovation Initiatives
Font Type	Times or Arial	Times or Arial	Times or Arial	Times or Arial	Times or Arial	Times or Arial	Times or Arial	Times or Arial
Number of Words – Title	120	90	95	85	70	60	120	90
Font Size/Space-Title	12; double space	12; double space	12; double space	12; double space	12; double space	12; double space	12; double space	12; double space
Font Size/Space-Abstracts/Key Words and Abbreviations	10; single space	10; single space	10; single space	10; single space	-	-	10; single space	10; single space
Number of Words – Abstracts/Key Words	300/5	300/5	200/5	250/5	-	-	300/5	300/5
Font Size/Space-Text	12; Double space	12; Double space	12; Double space	12; Double space	12; Double space	12; Double space	12; Double space	12; Double space
Number of Words – Text	5,000 including spaces	5,500 including spaces	2,500 including spaces	1,000 including spaces	1,000 including spaces	550 including spaces	5,000 including spaces	5,500 including spaces
Number of Figures	8 (title font size 12, double space)	3 (title font size 12, double space)	2 (title font size 12, double space)	2 (title font size 12, double space)	-	2 (title font size 12, double space)	8 (title font size 12, double space)	8 (title font size 12, double space)
Number of Tables/Graphic	7 title font size 12, double space	2 title font size 12, double space	2(title font size 12, double space)	1(title font size 12, double space)	-	-	7 title font size 12, double space	4 title font size 12, double space
Number of Authors and Co-authors*	15	10	5	10	3	3	15	10
References	20 (font size 10,single space	30(font size 10,single space	15 (font size 10,single space)	10 (font size 10,single space)	10 (font size 10,single space	5(font size 10,single space	20 (font size 10,single space	20

*First and last name with a sequencing overwritten number. Corresponding author(s) should be identified with an asterisk; Type 10, Times or Arial, single space. Running title of not more than 40 characters should be at the top of each page. References should be listed consecutively in the text. References must be cited on (not above) the line of text and in brackets instead of parentheses, e.g., [7,8]. References must be numbered in the order in which they appear in the text. References not cited in the text cannot appear in the reference section. References only or first cited in a table or figures are numbered according to where the table or figure is cited in the text. For instance, if a table is placed after reference 8, a new reference cited in table 1 would be reference 9.1 would be reference 9.

Checklist for Submitted Manuscripts

❑1. Please provide a cover letter with your submission specifying the corresponding author as well as an address, telephone number and e-mail.

❑2. Submit your paper using our website www.jbth.com.br. Use Word Perfect/Word for Windows, each with a complete set of original illustrations.

❑3. The entire manuscript (including tables and references) must be typed according to the guidelines instructions.

❑4. The order of appearance of material in all manuscripts should be as follows: title page, abstract, text, acknowledgements, references, tables, figures/graphics/diagrams with the respective legends.

❑5. The title page must include a title of not more than three printed lines (please check the guidelines of each specific manuscript), authors (no titles or degrees), institutional affiliations, a running headline of not more than 40 letters with spaces.

❑6. Acknowledgements of persons who assisted the authors should be included on the page preceding the references.

❑7. References must begin on a separate page.

❑8. References must be cited on (not above) the line of text and in brackets instead of parentheses, e.g., [7,8].

❑9. References must be numbered in the order in which they appear in the text. References not cited in the text cannot appear in the reference section. References only or first cited in a table or figures are numbered according to where the table or figure is cited in the text. For instance, if a table is placed after reference 8, a new reference cited in table 1 would be reference 9.

❑10. Reference citations must follow the format established by the "Uniform Requirements for Manuscripts Submitted to Biomedical Journals" or in "Vancouver Citation Style".

❑11. If you reference your own unpublished work (i.e., an "in press" article) in the manuscript that you are submitting, you must attach a file of the "in press" article and an acceptance letter from the journal.

❑12. If you cite unpublished data that are not your own, you must provide a letter of permission from the author of that publication.

❑13. Please provide each figure in high quality (minimum 300 dpi: JPG or TIF). Figure must be on a separate file.

❑14. If the study received a financial support, the name of the sponsors must be included in the cover letter and in the text, after the author's affiliations.

❑15. Provide the number of the Ethics Committees (please check the guidelines for authors).